

CR 89.018

September 1989

NCEL

Contract Report

An Investigation Conducted by: Julius S. Bendat
J. S. Bendat Company
and
Paul A. Palo
Naval Civil Engineering Laboratory

Sponsored by: Office of the Chief of Naval
Research
Arlington, VA 22217-5000

AD-A216 760

NONLINEAR SYSTEM STOCHASTIC TECHNIQUES FOR OCEAN ENGINEERING APPLICATIONS

ABSTRACT This report discusses the analysis and identification of nonlinear system dynamic properties from measured data using a newly developed stochastic technique. This new technique replaces the original single-input/single-output nonlinear problem into an equivalent multiple-input/single-output linear problem that is much easier to analyze and interpret. Applications to ocean engineering such as nonlinear wave forces and nonsymmetrical restoring forces are included.

DTIC
ELECTE
JAN 10 1990
S B D

NAVAL CIVIL ENGINEERING LABORATORY PORT HUENEME CALIFORNIA 93043

Approved for public release; distribution is unlimited.

90 01 10 170

METRIC CONVERSION FACTORS

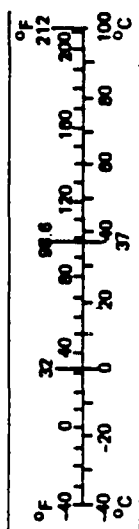
Approximate Conversions to Metric Measures

Symbol	When You Know	Multiply by	To Find	Symbol
LENGTH				
in	inches	2.5	centimeters	cm
ft	feet	30	centimeters	cm
yd	yards	0.9	meters	m
mi	miles	1.6	kilometers	km
AREA				
in ²	square inches	6.5	square centimeters	cm ²
ft ²	square feet	0.09	square meters	m ²
yd ²	square yards	0.8	square meters	m ²
mi ²	square miles	2.6	square kilometers	km ²
	acres	0.4	hectares	ha
MASS (weight)				
oz	ounces	28	grams	g
lb	pounds	0.45	kilograms	kg
	short tons (2,000 lb)	0.9	tonnes	t
VOLUME				
tsp	teaspoons	5	milliliters	ml
Tbsp	tablespoons	15	milliliters	ml
fl oz	fluid ounces	30	milliliters	ml
c	cups	0.24	liters	l
pt	pints	0.47	liters	l
qt	quarts	0.95	liters	l
gal	gallons	3.8	liters	l
ft ³	cubic feet	0.03	cubic meters	m ³
yd ³	cubic yards	0.76	cubic meters	m ³
TEMPERATURE (exact)				
°F	Fahrenheit temperature	5/9 (after subtracting 32)	Celsius temperature	°C

*1 in = 2.54 (exact). For other exact conversions and more detailed tables, see NBS Misc. Publ. 286, Units of Weights and Measures, Price \$2.25, SD Catalog No. C13.10-286.

Approximate Conversions from Metric Measures

When You Know	Multiply by	To Find	Symbol
LENGTH			
millimeters	0.04	inches	in
centimeters	0.4	inches	in
meters	3.3	feet	ft
meters	1.1	yards	yd
kilometers	0.6	miles	mi
AREA			
square centimeters	0.16	square inches	in ²
square meters	1.2	square yards	yd ²
square kilometers	0.4	square miles	mi ²
hectares (10,000 m ²)	2.5	acres	
MASS (weight)			
grams	0.035	ounces	oz
kilograms	2.2	pounds	lb
tonnes (1,000 kg)	1.1	short tons	
VOLUME			
milliliters	0.03	fluid ounces	fl oz
liters	2.1	pints	pt
liters	1.06	quarts	qt
liters	0.26	gallons	gal
cubic meters	35	cubic feet	ft ³
cubic meters	1.3	cubic yards	yd ³
TEMPERATURE (exact)			
Celsius temperature	9/5 (then add 32)	Fahrenheit temperature	°F



REPORT DOCUMENTATION PAGE			Form Approved OMB No. 0704-0188	
<small>Public reporting burden for this collection of information is estimated to average 1 hour per response, including the time for reviewing instructions, searching existing data sources, gathering and maintaining the data needed, and completing and reviewing the collection of information. Send comments regarding this burden estimate or any other aspect of this collection of information, including suggestions for reducing this burden, to Washington Headquarters Services, Directorate for Information Operations and Reports, 1215 Jefferson Davis Highway, Suite 1204, Arlington, VA 22202-4302, and to the Office of Management and Budget, Paperwork Reduction Project (0704-0188), Washington, DC 20503.</small>				
1. AGENCY USE ONLY (Leave blank)	2. REPORT DATE September 1989	3. REPORT TYPE AND DATES COVERED Final — Oct 1988 to Sep 1989		
4. TITLE AND SUBTITLE Nonlinear System Stochastic Techniques for Ocean Engineering Applications		5. FUNDING NUMBERS C - N62474-86-7275 WU - RR000-01-201		
6. AUTHOR(S) Julius S. Bendat and Paul A. Palo*				
7. PERFORMING ORGANIZATION NAME(S) AND ADDRESS(ES) J. S. Bendat 833 Moraga Drive Los Angeles, CA 90049		8. PERFORMING ORGANIZATION REPORT NUMBER CR 89.018		
9. SPONSORING/MONITORING AGENCY NAME(S) AND ADDRESS(ES) Office of the Chief of Naval Research Arlington, VA 22217-5000		10. SPONSORING/MONITORING AGENCY REPORT NUMBER CR 89.018		
11. SUPPLEMENTARY NOTES				
12a. DISTRIBUTION/AVAILABILITY STATEMENT Approved for public release; distribution unlimited.			12b. DISTRIBUTION CODE	
13. ABSTRACT (Maximum 200 words) This report discusses the analysis and identification of nonlinear system dynamic properties from measured data using a newly developed stochastic technique. This new technique replaces the original single-input/single-output nonlinear problem into an equivalent multiple-input/single-output linear problem that is much easier to analyze and interpret. Applications to ocean engineering such as nonlinear wave forces and nonsymmetrical restoring forces are included.				
14. SUBJECT TERMS Nonlinear stochastic analysis, nonlinear wave forces, wave drift forces, nonlinear systems identification			15. NUMBER OF PAGES 134	
			16. PRICE CODE	
17. SECURITY CLASSIFICATION OF REPORT Unclassified	18. SECURITY CLASSIFICATION OF THIS PAGE Unclassified	19. SECURITY CLASSIFICATION OF ABSTRACT Unclassified	20. LIMITATION OF ABSTRACT UL	

NONLINEAR SYSTEM STOCHASTIC TECHNIQUES FOR OCEAN ENGINEERING APPLICATIONS

Abstract

This report discusses the analysis and identification of nonlinear system dynamic properties by stochastic techniques on measured experimental data. Two ocean engineering applications of this material are developed of concern to NCEL representing: (a) nonlinear wave force problems, and (b) nonlinear drift force problems. General models are formulated consisting of parallel linear and nonlinear systems where the input data can be Gaussian or non-Gaussian. Formulas are stated for statistical errors in estimates from measured random data to help design experiments and to evaluate results. The last section of this report derives various useful input/output relationships when stationary random data pass through three types of nonlinear nonsymmetrical systems of physical interest. /

Acknowledgment

This nonlinear system research work was sponsored by the Naval Civil Engineering Laboratory (NCEL) in Port Hueneme, California under the supervision of Paul Palo from the Ocean Structures Division. The author expresses his great appreciation to Paul Palo for reviewing and guiding many parts of this work to help advance new ocean engineering applications of this material.

CONTENTS

	Page
INTRODUCTION	1
1. PARALLEL LINEAR AND NONLINEAR SYSTEMS	3
1.1 Zero-Memory Nonlinear Systems	3
1.2 Optimum Third-Order Polynomial Approximation	7
1.3 Finite-Memory Nonlinear Systems	12
1.4 Non-Gaussian Input Data	15
1.5 Gaussian Input Data	27
2. NONLINEAR WAVE FORCE MODELS	31
2.1 Formulation of Wave Force Model	32
2.2 Spectral Decomposition Problem	35
2.3 System Identification Problem	43
2.4 Nonzero Mean Value Input	50
2.5 Statistical Errors in Estimates	58
3. NONLINEAR DRIFT FORCE MODELS	59
3.1 Formulation of Drift Force Model	60
3.2 Basic Formulas for Nonlinear Drift Force Model	63
3.3 Previous Drift Force Models	69
3.4 Spectral Decomposition Problem	72
3.5 System Identification Problem	77
3.6 Nonzero Mean Value Input	80
3.7 Statistical Errors in Estimates	86
3.8 Derivations of Theoretical Formulas	89
4. NONLINEAR NONSYMMETRICAL SYSTEMS	100
4.1 Three-Slope Systems	101
4.2 Catenary Systems	109
4.3 Smooth-Limiter Systems	120
REFERENCES	130

FIGURES

- 1.1 Zero-memory nonlinear system.
- 1.2 Least-squares approximation of $x|x|$.
- 1.3 Finite-memory nonlinear system.
- 1.4 Parallel linear and finite-memory nonlinear systems.
- 1.5 General single-input/single-output nonlinear model.
- 1.6 Equivalent three-input/single-output linear model to Figure 1.5.
- 1.7 Revised three-input/single output linear model to Figure 1.5.
- 1.8 Case 1 single-input/single-output nonlinear model.
- 1.9 Revised three-input/single-output model to Figure 1.8.

- 2.1 Illustration of wave force problem.
- 2.2 Nonlinear wave force model.
- 2.3 Third-order polynomial for $x(t)|x(t)|$.
- 2.4 Nonlinear wave force model with correlated outputs.
- 2.5 Two-input/single-output linear model with correlated inputs.
- 2.6 Nonlinear wave force model with uncorrelated outputs.
- 2.7 Two-input/single-output linear model with uncorrelated inputs.
- 2.8 Nonlinear system for $x^3(t)$ when $\mu_x \neq 0$.
- 2.9 Nonlinear system approximating $x(t)|x(t)|$ when $\mu_x \neq 0$.
- 2.10 Extension of model in Figure 2.4 when $\mu_x \neq 0$.
- 2.11 Extension of model in Figure 2.6 when $\mu_x \neq 0$.

- 3.1 Illustration of drift force problem.
- 3.2 Nonlinear drift force model.
- 3.3 Parallel linear and bilinear systems.
- 3.4 Nonlinear system when $\mu_x \neq 0$.
- 3.5 Nonlinear drift force model when $\mu_x \neq 0$.
- 3.6 Equivalent model to Figure 3.5.

- 4.1 Three-slope system.
- 4.2 Gaussian input PDF.
- 4.3 Output PDF for three-slope system.
- 4.4 Hard-limited three-slope system.
- 4.5 Output PDF for hard-limited three-slope system.
- 4.6 Catenary system.
- 4.7 Gaussian input PDF.
- 4.8 Output PDF for catenary system.
- 4.9 Catenary system model.
- 4.10 Smooth-limiter system.
- 4.11 Output PDF for smooth-limiter system.

Accession For	
DTIS GRA&I	<input checked="checked" type="checkbox"/>
DTIC TAB	<input type="checkbox"/>
Unannounced	<input type="checkbox"/>
Justification	
Distribution/	
Availability Codes	
Dist	Avail and/or Special
A-1	

NONLINEAR SYSTEM STOCHASTIC TECHNIQUES FOR OCEAN ENGINEERING APPLICATIONS

INTRODUCTION

The Naval Civil Engineering Laboratory (NCEL) has sponsored development of a new approach for random data analysis and identification of nonlinear systems under NCEL Contract N62474-86-7275 with J. S. Bendat Company, the contractor. This research has been conducted in a series of tasks, each of which resulted in an informal report. During this period, work on related matters was performed by the J. S. Bendat Company for other sponsors, and much work was also done as independent research and development. The basic mathematical aspects of these new results is now being published in book form by J. S. Bendat with John Wiley & Sons, New York. However, some of the material that relates specifically to ocean engineering will not be included. This present NCEL contractor report complements the book by emphasizing certain matters that represent important new practical ways to analyze and identify nonlinear system dynamic properties from measured data, and by focusing on ocean engineering problems of concern to NCEL.

This report discusses the following topics:

- Section 1. Parallel Linear and Nonlinear Systems.
- Section 2. Nonlinear Wave Force Models.
- Section 3. Nonlinear Drift Force Models.
- Section 4. Nonlinear Nonsymmetrical Systems.

Techniques are explained in Section 1 on how to replace a large class of single-input/single-output nonlinear models by equivalent multiple-input/single-output linear models. This is a significant achievement because it permits complicated nonlinear problems to be solved by known linear procedures. Input data to the nonlinear systems can be Gaussian or non-Gaussian; the data can be stationary random data or transient random data. Formulas for non-Gaussian input data require the computation of conditioned spectral density functions. Formulas for Gaussian input data require only ordinary auto-spectral and cross-spectral density functions when the parallel nonlinear systems are square-law and cubic systems. Square-law and cubic nonlinear systems are the nonlinear systems that occur when one obtains an optimum third-order polynomial least-squares approximation to an arbitrary zero-memory nonlinear transformation. Thus, linear systems in parallel with square-law systems and cubic systems are of major importance in modeling many physical problems.

Sections 2 and 3 discuss nonlinear wave force problems and nonlinear drift force problems. Appropriate models are formulated for each problem where zero-memory nonlinear systems are followed by linear systems. Two types of problems are solved: (a) the spectral decomposition problem, and (b) the system identification problem. Statistical errors in estimates are given to help design experiments and to evaluate measured results. Section 4 develops input/output relationships for stationary random data through three zero-memory nonlinear nonsymmetrical systems: (a) three-slope systems, (b) catenary systems and (c) smooth-limiter systems. Formulas are stated for input/output probability density functions, correlation functions and spectral density functions.

1. PARALLEL LINEAR AND NONLINEAR SYSTEMS

Before discussing techniques for analyzing and identifying system properties in parallel linear and nonlinear systems, three topics need to be covered that will occur in later material. These topics are

1. zero-memory nonlinear systems,
2. optimum third-order polynomial least-squares approximations to zero-memory nonlinear systems, and
3. finite-memory nonlinear systems.

1.1 ZERO-MEMORY NONLINEAR SYSTEMS

A "zero-memory" nonlinear system is a system that acts instantaneously on present inputs in some nonlinear fashion. It does not weight past inputs due to "memory" operations as in convolution integrals for constant parameter linear systems, where the present value of the output is a function of both present and past values of the input. For zero-memory nonlinear systems, the output $y(t)$ at any time t is a single-valued nonlinear function $g[x(t)]$ of the input $x(t)$ at the same instant of time. Thus, as shown in Figure 1.1,

$$y(t) = g[x(t)] \tag{1.1}$$

where $g(x)$ is a single-valued nonlinear function of x . Note that $g(x)$ is not a function of t .

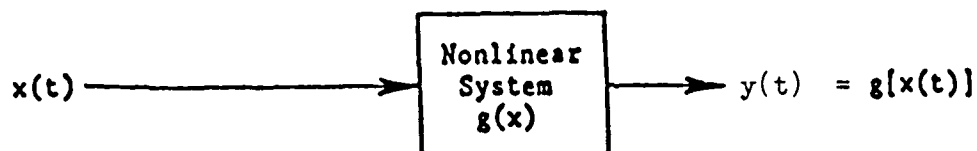


Figure 1.1 Zero memory nonlinear system.

The system $g(x)$ is nonlinear means that for any constants a_1, a_2 and any inputs x_1, x_2

$$g(a_1x_1 + a_2x_2) \neq a_1 g(x_1) + a_2 g(x_2) \quad (1.2)$$

either because $g(x)$ is not additive or because $g(x)$ is not homogenous, or both. The system is a constant parameter nonlinear system if the response of the system is independent of the particular time of use, namely, if an input $x(t)$ is translated to an input $x(t + \tau)$, then the output $y(t)$ is translated to an output $y(t + \tau)$. If the system is a constant parameter nonlinear system, and if the input $x(t)$ represents a stationary random process, then the output $y(t)$ will also be a stationary random process. For these cases $y(t) = g[x(t)]$ gives $y(t + \tau) = g[x(t + \tau)]$ and the correlation functions

$$R_{xy}(\tau) = E[x(t)y(t + \tau)] = E[x(t)g[x(t + \tau)]] \quad (1.3)$$

$$R_{yy}(\tau) = E[y(t)y(t + \tau)] = E[g[x(t)]g[x(t + \tau)]] \quad (1.4)$$

are functions only of τ as required for stationary random data.

Many examples of zero-memory nonlinear symmetrical systems are discussed in References [1, 2]. They include two-slope systems, dead-zone systems, clipped systems, square-law systems, cubic systems, hardening spring systems and softening spring systems. Three examples of zero-memory nonlinear nonsymmetrical systems are treated here in Section 4.

Three theorems are proved in References [1, 2] that are useful for determining input/output relations when stationary random data pass through a zero-memory nonlinear system. Theorem 1 applies to arbitrary stationary random input data. Theorems 2 and 3 apply only to Gaussian stationary random input data. These theorems will be used in Section 4.

Theorem 1.

For any input data $x(t)$ with probability density function $p(x)$ where $x(t)$ passes through a zero-memory nonlinear system to produce $y = g(x)$ which is single-valued and one-to-one, the output probability density function $p_2(y)$ for the output $y(t)$ satisfies the relation

$$p_2(y) = \frac{p(x)}{|dy/dx|} \quad (1.5)$$

This theorem assumes that $(dy/dx) = g'(x)$ exists and is not equal to zero. When solving for $p_2(y)$, the variable x on the right-hand side should be replaced by its equivalent y from $x = g^{-1}(y)$.

Theorem 2. (Price)

For Gaussian input data $x(t)$ with known autocorrelation function $R_{xx}(\tau)$, where $x(t)$ passes through any zero-memory nonlinear system to produce $y = g(x)$, the output autocorrelation function $R_{yy}(\tau)$ for $y(t)$ satisfies the relation

$$\frac{\partial R_{yy}(\tau)}{\partial R_{xx}(\tau)} = E[g'(x_1)g'(x_2)] \quad (1.6)$$

whenever $g'(x) = [dg(x)/dx]$ exists at $x_1 = x(t)$ and $x_2 = x(t + \tau)$.

Theorem 3. (Busgang)

For Gaussian input data $x(t)$ with known autocorrelation function $R_{xx}(\tau)$, where $x(t)$ passes through any zero memory nonlinear system to produce $y = g(x)$, the input/output cross-correlation function $R_{xy}(\tau)$ satisfies the relation

$$R_{xy}(\tau) = \frac{R_{xx}(\tau)}{\sigma_x^2} \int_{-\infty}^{\infty} x g(x) p(x) dx = \frac{R_{xx}(\tau)}{\sigma_x^2} E[x g(x)] \quad (1.7)$$

In Theorems 2 and 3, the first-order probability density function for x is given by the Gaussian form

$$p(x) = (1/\sigma_x \sqrt{2\pi}) \exp(-x^2/2\sigma_x^2) \quad (1.8)$$

where the mean value is assumed to be zero and the variance $\sigma_x^2 = E[x^2(t)]$. In Equation 1.7, the quantity

$$E[xg(x)] = \int_{-\infty}^{\infty} xg(x)p(x) dx \quad (1.9)$$

Identification of Zero-Memory Nonlinear Systems

When $y = g(x)$ is single-valued and one-to-one, it can be identified from measurements of $x(t)$ and $y(t)$ by using the relation

$$P_2(y_0) = \int_{-\infty}^{y_0} p_2(y) dy = \int_{-\infty}^{x_0} p(x) dx = P(x_0) \quad (1.10)$$

where $P(x_0)$ and $P_2(y_0)$ are the probability distribution functions of $x(t)$ at x_0 and of $y(t)$ at $y_0 = g(x_0)$, respectively. To determine the zero-memory nonlinear function $y = g(x)$, one should select various values of x_0 , calculate $P(x_0)$ and then determine the associated values of y_0 such that $P_2(y_0) = P(x_0)$.

1.2 OPTIMUM THIRD-ORDER POLYNOMIAL APPROXIMATION

Suppose $y = g(x)$ represents any zero-memory nonlinear system where $y = y(t)$ and $x = x(t)$. What is the optimum least-squares approximation to $y = g(x)$ by the third-order polynomial $\tilde{y} = \tilde{y}(t)$ where

$$\tilde{y} = a_1 x + a_2 x^2 + a_3 x^3 \quad (1.11)$$

under the assumption that x follows a zero mean value Gaussian distribution? To be specific, what should be the choices of the coefficients a_1 , a_2 and a_3 so as to minimize the quantity

$$Q = E[y - \tilde{y}]^2 = E[(y - a_1 x - a_2 x^2 - a_3 x^3)^2] \quad (1.12)$$

over all possible choices of these coefficients?

For any y , the Gaussian assumption on x gives

$$Q = E[y^2] - 2a_1E[xy] - 2a_2E[x^2y] - 2a_3E[x^3y] \\ + a_1^2E[x^2] + 2a_1a_3E[x^4] + a_2^2E[x^4] + a_3^2E[x^6] \quad (1.13)$$

using the fact that $E[x] = E[x^3] = E[x^5] = 0$ for the $p(x)$ of Equation 1.8. Then setting partial derivatives of Q with respect to a_1 , a_2 , and a_3 equal to zero shows

$$\frac{\partial Q}{\partial a_1} = -2E[xy] + 2a_1E[x^2] + 2a_3E[x^4] = 0 \quad (1.14)$$

$$\frac{\partial Q}{\partial a_2} = -2E[x^2y] + 2a_2E[x^4] = 0 \quad (1.15)$$

$$\frac{\partial Q}{\partial a_3} = -2E[x^3y] + 2a_1E[x^4] + 2a_3E[x^6] = 0 \quad (1.16)$$

Now, using the fact that $E[x^2] = \sigma_x^2$, $E[x^4] = 3\sigma_x^4$, and $E[x^6] = 15\sigma_x^6$ for the Gaussian $p(x)$ of Equation 1.8 shows

$$a_1\sigma_x^2 + 3a_3\sigma_x^4 = E[xy] \quad (1.17)$$

$$3a_2\sigma_x^4 = E[x^2y] \quad (1.18)$$

$$3a_1\sigma_x^4 + 15a_3\sigma_x^6 = E[x^3y] \quad (1.19)$$

Hence, for any y , one obtains the \tilde{y} of Equation 1.11 from the special coefficients

$$a_1 = \frac{15\sigma_x^6 E[xy] - 3\sigma_x^4 E[x^3y]}{6\sigma_x^8} \quad (1.20)$$

$$a_2 = \frac{E[x^2y]}{3\sigma_x^4} \quad (1.21)$$

$$a_3 = \frac{\sigma_x^2 E[x^3y] - 3\sigma_x^4 E[xy]}{6\sigma_x^8} \quad (1.22)$$

Example. Square-Law System with Sign

Consider application of these matters to a square-law system with sign where

$$y = x|x| \quad (1.23)$$

For this particular y , the Gaussian assumption on x yield

$$E[xy] = E[x^2|x|] = 2E[x^3]_{x>0} = 2\sigma_x^3 \sqrt{(2/\pi)} \quad (1.24)$$

$$E[x^2y] = E[x^3|x|] = 0 \quad (1.25)$$

$$E[x^3y] = E[x^4|x|] = 2E[x^5]_{x>0} = 8\sigma_x^5 \sqrt{(2/\pi)} \quad (1.26)$$

From Equations (1.20) to (1.22), one obtains

$$a_1 = \sigma_x \sqrt{(2/\pi)} \quad (1.27)$$

$$a_2 = 0 \quad (1.28)$$

$$a_3 = \sqrt{(2/\pi)}/3\sigma_x \quad (1.29)$$

Hence, the optimum third-order polynomial least-squares approximation to $x|x|$ by Equation 1.11 is

$$\begin{aligned} \tilde{y} &= a_1 x + a_3 x^3 \\ &= \left[\sigma_x \sqrt{(2/\pi)} \right] x + \left[\sqrt{(2/\pi)}/3\sigma_x \right] x^3 \end{aligned} \quad (1.30)$$

Thus $x|x|$ can be treated as a combination of a linear system in parallel with a cubic system. Figure 1.2 shows $x|x|$ compared to the \tilde{y} of Equation 1.30.

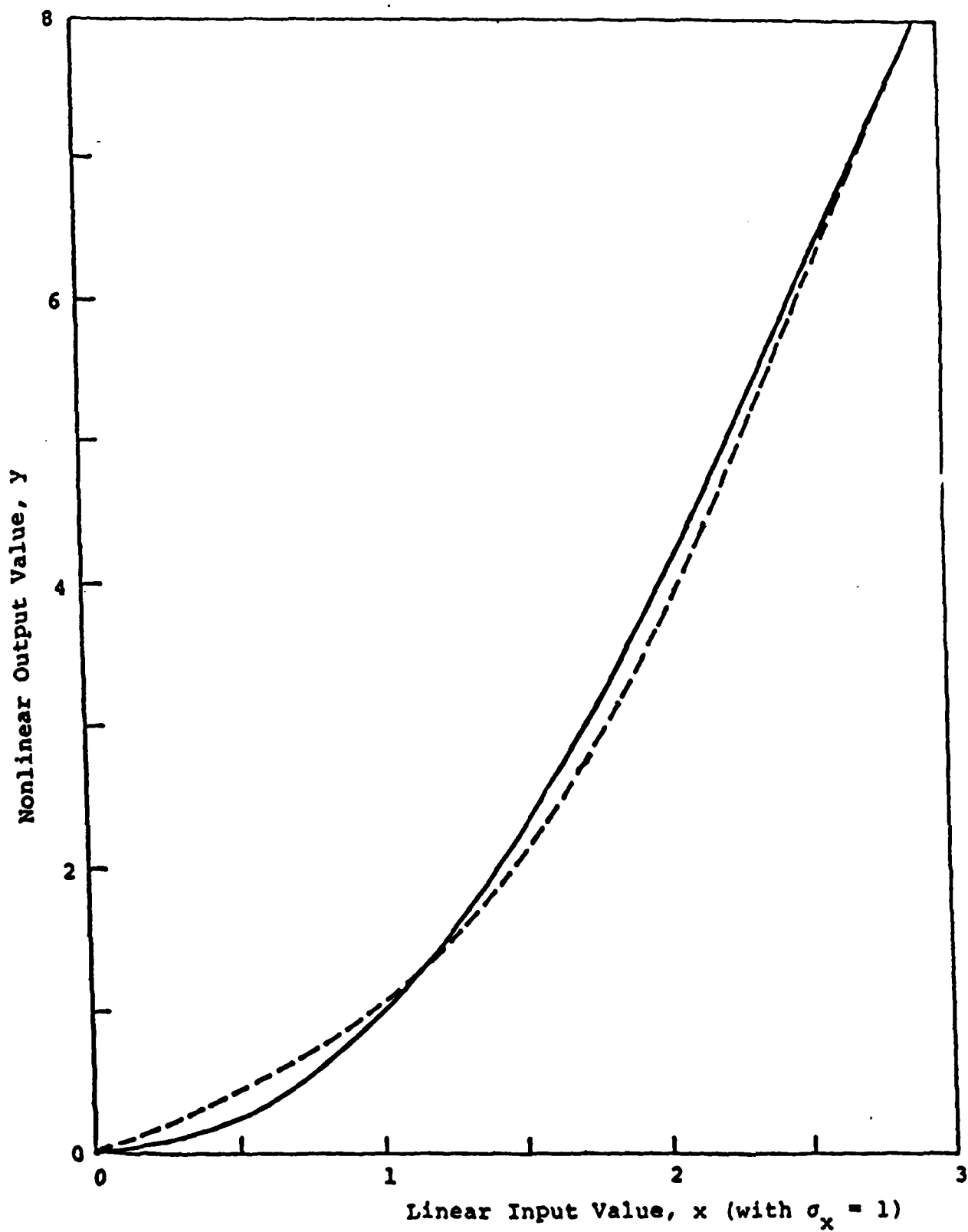


Figure 1.2 Least squares approximation of $x|x|$.
 — is $x|x|$; - - - is Equation (1.30).

1.3 FINITE-MEMORY NONLINEAR SYSTEMS

When finite-memory operations are desired in connection with zero-memory nonlinear systems, they can often be obtained by inserting a constant-parameter linear system before and/or after the zero-memory nonlinear system. Cases where the linear system is after the zero-memory nonlinear system represent the cases of greatest interest and are the only cases discussed in this report. Other cases where the linear system precedes the zero-memory nonlinear system are discussed in References [1, 2]. Figure 1.3 shows a finite-memory nonlinear system with a linear system $A(f)$ that is after the zero-memory nonlinear system defined by $g(x)$.

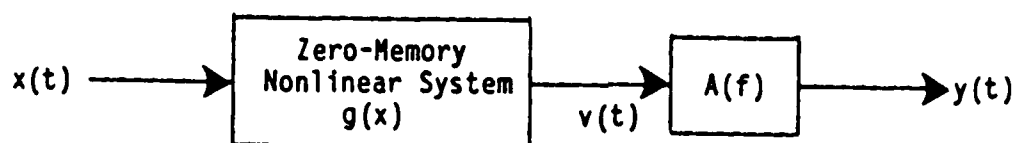


Figure 1.3 Finite-memory nonlinear system.

An extension of Figure 1.3 that is applicable to many physical problems occurs when the input data $x(t)$ passes through parallel linear and finite-memory nonlinear systems as shown in Figure 1.4, where $H(f)$ and $A(f)$ are two arbitrary constant-parameter linear systems and where $g(x)$ is any specified zero-memory nonlinear system. The output noise data $n(t)$ is assumed to be uncorrelated with both $x(t)$ and $y(t)$.

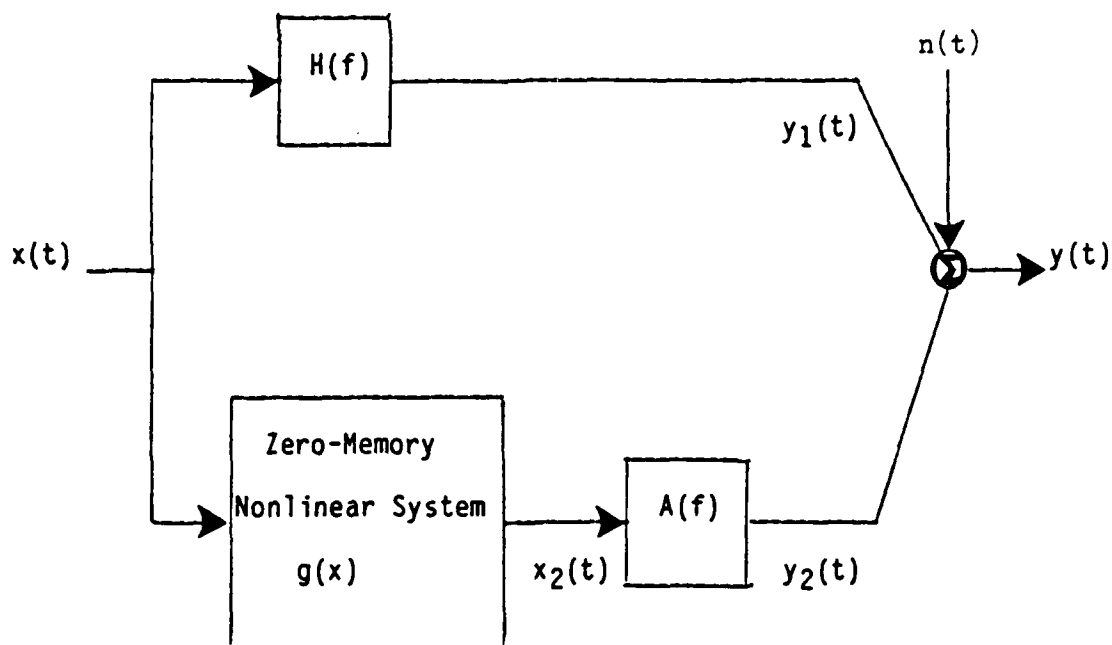


Figure 1.4 Parallel linear and finite-memory nonlinear systems.

Two problems are associated with the nonlinear model in Figure 1.4.

- (1) Spectral Decomposition Problem. Given $H(f)$, $A(f)$ and $g(x)$, plus measurements only of $x(t)$, determine the spectral properties of $y_1(t)$ and $y_2(t)$. If $y(t)$ is measured as well as $x(t)$, determine also the spectral properties of $n(t)$.
- (2) System Identification Problem. From simultaneous measurements of both $x(t)$ and $y(t)$, identify the optimum frequency response functions $H(f)$ and $A(f)$ to minimize the autospectrum of $n(t)$.

Sections 1.4 and 1.5 outline practical techniques that can solve these two problems. In Section 1.4, input data can be non-Gaussian, whereas in Section 1.5, input data are assumed to be Gaussian. Thus, these techniques are applicable to physical situations of widespread importance without restricting the probability density function of the measured input data. More general models than Figure 1.4 are considered involving one linear path and two parallel nonlinear paths as shown in Figure 1.5. Sections 2 and 3 apply these techniques to wave force problems and drift force problems.

1.4 NON-GAUSSIAN INPUT DATA

Consider the general single-input/single-output nonlinear model of Figure 1.5 with three parallel paths where the input data $x(t)$ can be non-Gaussian. Let $g_2[x(t)]$ be an arbitrary known zero-memory nonlinear transformation of $x(t)$ and let $g_3[x(t)]$ be a different arbitrary known zero-memory nonlinear transformation of $x(t)$. Let

$$x_1(t) = x(t), \quad x_2(t) = g_2[x(t)], \quad x_3(t) = g_3[x(t)] \quad (1.31)$$

represent the three usually correlated input records to the three linear systems $A_1(f)$, $A_2(f)$ and $A_3(f)$, respectively. The three associated usually correlated output records from these systems are denoted by $y_1(t)$, $y_2(t)$ and $y_3(t)$, respectively. To complete the model, let $n(t)$ represent extraneous uncorrelated output noise and let $y(t)$ represent the total output from the system. A special important case of Figure 1.5 is when $g_2[x(t)] = x^2(t)$ and $g_3[x(t)] = x^3(t)$. This case is treated in Section 1.5.

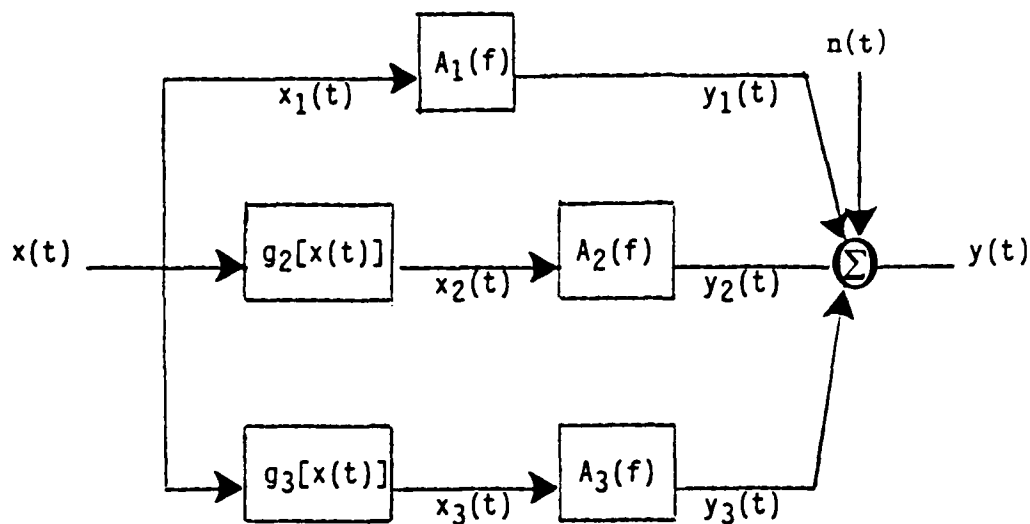


Figure 1.5 General single-input/single-output nonlinear model for non-Gaussian input data that passes through a linear system in parallel with two finite-memory nonlinear systems.

Note that Figure 1.5 simplifies to Figure 1.4 when $g_3[x(t)] = 0$ so that all results obtained here apply to the model in Figure 1.4 by merely setting $x_3(t)$ and all subsequent terms computed from $x_3(t)$ to zero.

Figure 1.5 can be replaced by the equivalent three-input/single-output linear model of Figure 1.6 where the capital letter quantities are Fourier transforms of associated small letter quantities. To be specific, let

$$X_1(f) = \mathcal{F}[x_1(t)], \quad Y_1(f) = \mathcal{F}[y_1(t)] \quad (1.32)$$

$$X_2(f) = \mathcal{F}[x_2(t)], \quad Y_2(f) = \mathcal{F}[y_2(t)] \quad (1.33)$$

$$X_3(f) = \mathcal{F}[x_3(t)], \quad Y_3(f) = \mathcal{F}[y_3(t)] \quad (1.34)$$

$$N(f) = \mathcal{F}[n(t)], \quad Y(f) = \mathcal{F}[y(t)] \quad (1.35)$$

Measurement of $x(t)$ and $y(t)$ enables one to compute the quantities $X_1(f)$, $X_2(f)$, $X_3(f)$ and $Y(f)$ when $x_2(t)$ and $x_3(t)$ are known.

Recognition of the equivalence between Figures 1.5 and 1.6 is a significant achievement because Figure 1.6 can be solved by well-known multiple-input/single-output techniques that are derived and discussed fully in References [3, 4]. These procedures are applicable for input data that can be Gaussian or non-Gaussian. Independent research on these matters based on References [5-7] is in Reference [8].

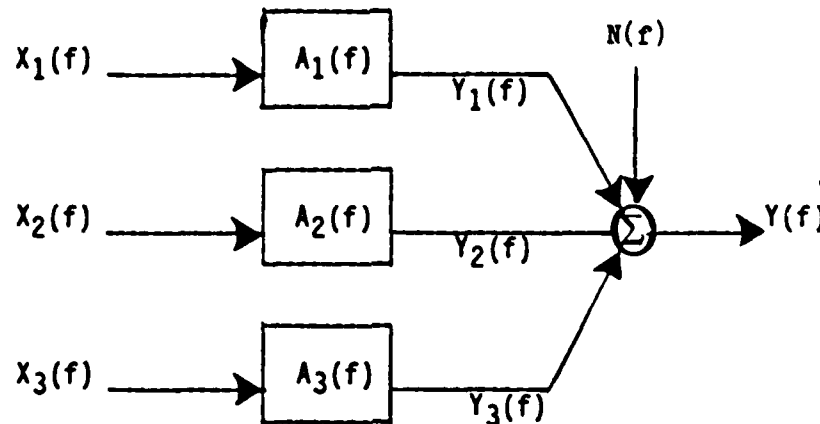


Figure 1.6 Equivalent three-input/single-output linear model to Figure 1.5 where the three input records can be correlated.

The basis of multiple-input/single-output procedures for solving Figure 1.6 is to change the input records by conditioned spectral density techniques so that $X_1(f)$ is left alone, $X_2(f)$ is changed to $X_{2.1}(f)$ where the linear effects of $X_1(f)$ are removed from $X_2(f)$, and $X_3(f)$ is changed to $X_{3.2!}(f)$ where the linear effects of both $X_1(f)$ and $X_2(f)$ are removed from $X_3(f)$. These new input records, $X_1(f)$, $X_{2.1}(f)$ and $X_{3.2!}(f)$ will then be mutually uncorrelated and become the inputs to the revised three-input/single-output linear model shown in Figure 1.7. The noise output record $N(f)$ and the total signal output record $Y(f)$ are the same as before. However, the three previous separate output records $Y_1(f)$, $Y_2(f)$ and $Y_3(f)$ are now replaced by three new separate output records $Y_a(f)$, $Y_b(f)$ and $Y_c(f)$ that will be mutually uncorrelated. Also the three previous linear systems $A_1(f)$, $A_2(f)$ and $A_3(f)$ are now replaced by three new linear systems $L_1(f)$, $L_2(f)$ and $L_3(f)$.

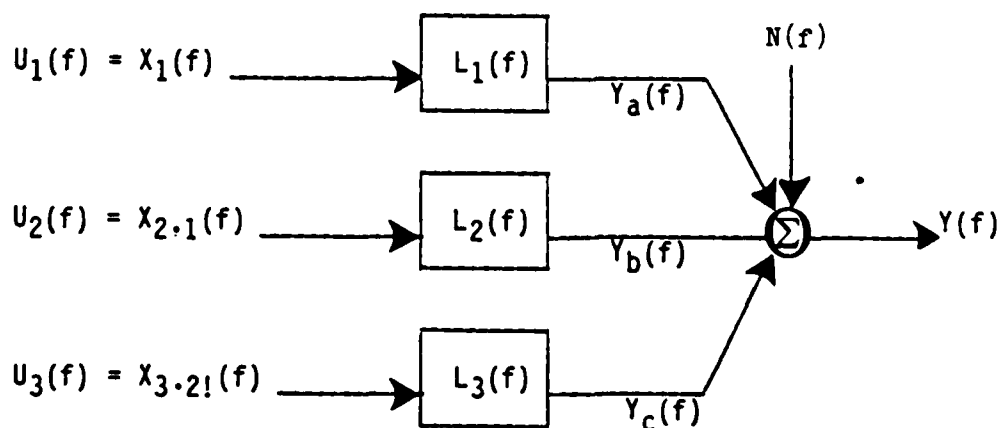


Figure 1.7 Revised three-input/single-output linear model equivalent to Figure 1.5 where the input records are mutually uncorrelated.

To simplify the notation, the three mutually uncorrelated input records in Figure 1.7 will be denoted by $U_1(f)$, $U_2(f)$ and $U_3(f)$ where

$$U_1(f) = X_1(f) = X(f) \quad (1.36)$$

$$U_2(f) = X_{2.1}(f) \quad (1.37)$$

$$U_3(f) = X_{3.2}(f) \quad (1.38)$$

Figure 1.7 is now essentially three separate single-input/single-output linear models where the linear systems $L_1(f)$, $L_2(f)$ and $L_3(f)$ can be computed by the usual spectral relations

$$L_1(f) = \frac{G_{u_1 y}(f)}{G_{u_1 u_1}(f)} \quad (1.39)$$

$$L_2(f) = \frac{G_{u_2 y}(f)}{G_{u_2 u_2}(f)} \quad (1.40)$$

$$L_3(f) = \frac{G_{u_3 y}(f)}{G_{u_3 u_3}(f)} \quad (1.41)$$

The $G(f)$ quantities are one-sided spectral density functions that can be computed easily using formulas in References [3, 4].

Note that the linear system $L_1(f)$ is the same as the overall optimum linear system $H_0(f)$ between the input $x(t)$ and the total output $y(t)$ as computed by

$$H_0(f) = \frac{G_{xy}(f)}{G_{xx}(f)} \quad (1.42)$$

where $G_{xy}(f)$ is the cross-spectral density function between $x(t)$ and $y(t)$, and $G_{xx}(f)$ is the autospectral density function of $x(t)$.

Other relations for Figure 1.7 are as follows.

$$Y(f) = Y_a(f) + Y_b(f) + Y_c(f) + N(f) \quad (1.43)$$

$$G_{yy}(f) = G_{y_a y_a}(f) + G_{y_b y_b}(f) + G_{y_c y_c}(f) + G_{nn}(f) \quad (1.44)$$

$$G_{y_a y_a}(f) = |L_1(f)|^2 G_{u_1 u_1}(f) = \gamma_{u_1 y}^2(f) G_{yy}(f) \quad (1.45)$$

$$G_{y_b y_b}(f) = |L_2(f)|^2 G_{u_2 u_2}(f) = \gamma_{u_2 y}^2(f) G_{yy}(f) \quad (1.46)$$

$$G_{y_c y_c}(f) = |L_3(f)|^2 G_{u_3 u_3}(f) = \gamma_{u_3 y}^2(f) G_{yy}(f) \quad (1.47)$$

$$G_{nn}(f) = [1 - \gamma_{u_1 y}^2(f) - \gamma_{u_2 y}^2(f) - \gamma_{u_3 y}^2(f)] G_{yy}(f) \quad (1.48)$$

The quantities $\gamma_{u_1 y}^2(f)$, $\gamma_{u_2 y}^2(f)$ and $\gamma_{u_3 y}^2(f)$ are the ordinary coherence functions between $y(t)$ and the three inputs $u_1(t)$, $u_2(t)$ and $u_3(t)$, respectively.

The quantities $U_2(f)$ and $U_3(f)$ in Figure 1.7 are given by

$$U_2(f) = X_2(f) - L_{12}(f)X_1(f) \quad (1.49)$$

$$U_3(f) = X_3(f) - L_{13}(f)X_1(f) - L_{23}(f)U_2(f) \quad (1.50)$$

where

$$L_{12}(f) = \frac{G_{12}(f)}{G_{11}(f)} \quad (1.51)$$

$$L_{13}(f) = \frac{G_{13}(f)}{G_{11}(f)} \quad (1.52)$$

$$L_{23}(f) = \frac{G_{23}(f) - L_{13}(f)G_{21}(f)}{G_{22}(f) - L_{12}(f)G_{21}(f)} \quad (1.53)$$

From knowledge of $L_1(f)$, $L_2(f)$ and $L_3(f)$, the linear systems $A_1(f)$, $A_2(f)$ and $A_3(f)$ can be computed by the algebraic relations

$$A_3(f) = L_3(f) \quad (1.54)$$

$$A_2(f) = L_2(f) - L_{23}(f)A_3(f) \quad (1.55)$$

$$A_1(f) = L_1(f) - L_{12}(f)A_2(f) - L_{13}(f)A_3(f) \quad (1.56)$$

In terms of more basic spectral quantities, the terms used in Equations 1.39 to 1.41 to compute $L_1(f)$ $L_2(f)$ and $L_3(f)$ are

$$G_{u_1y}(f) = G_{1y}(f) \quad (1.57)$$

$$G_{u_1u_1}(f) = G_{11}(f) \quad (1.58)$$

$$G_{u_2y}(f) = G_{2y}(f) - L_1(f)G_{21}(f) \quad (1.59)$$

$$G_{u_2u_2}(f) = G_{22}(f) - L_{12}(f)G_{21}(f) \quad (1.60)$$

$$G_{u_3y}(f) = G_{3y}(f) - L_1(f)G_{31}(f) - L_2(f)G_{3u_2}(f) \quad (1.61)$$

$$G_{u_3u_3}(f) = G_{33}(f) - L_{13}(f)G_{31}(f) - L_{23}(f)G_{3u_2}(f) \quad (1.62)$$

where

$$G_{3u_2}(f) = G_{32}(f) - L_{12}(f)G_{31}(f) \quad (1.63)$$

All of these terms are generally required when dealing with non-Gaussian input data. Note that $G_{u_2u_2}(f) \neq G_{22}(f)$ and $G_{u_3u_3}(f) \neq G_{33}(f)$ except for special cases.

Some further points are worthy of note. The relation

$$L_1(f) = A_1(f) + L_{12}(f)A_2(f) + L_{13}(f)A_3(f) \quad (1.64)$$

shows that, in general, $L_1(f) \neq A_1(f)$. Thus determination of $L_1(f)$, representing the overall optimum linear system $H_0(f)$ between $X_1(f)$ and $Y(f)$, is not the same as the actual linear system $A_1(f)$ that exists between $X_1(f)$ and $Y_1(f)$. The spectral output of $y_1(t)$ given by

$$G_{y_1 y_1}(f) = |A_1(f)|^2 G_{11}(f) \quad (1.65)$$

will generally differ from the spectral output of $y_a(t)$ given by

$$G_{y_a y_a}(f) = |L_1(f)|^2 G_{11}(f) \quad (1.66)$$

Note also that the relation

$$L_2(f) = A_2(f) + L_{23}(f)A_3(f) \quad (1.67)$$

shows that in general that $L_2(f) \neq A_2(f)$. The system $L_2(f)$ represents the overall optimum linear system between $U_2(f)$ and $Y(f)$. This is not the same as the actual linear system $A_2(f)$ that exists between $X_2(f)$ and $Y_2(f)$. Also, the spectral output of $y_2(t)$ given by

$$G_{y_2 y_2}(f) = |A_2(f)|^2 G_{22}(f) \quad (1.68)$$

will generally differ from the spectral output of $y_b(t)$ given by

$$G_{y_b y_b}(f) = |L_2(f)|^2 G_{u_2 u_2}(f) \quad (1.69)$$

However, note the equality relation that

$$L_3(f) = A_3(f) \quad (1.70)$$

where $L_3(f)$ represents the overall optimum linear system between $U_3(f)$ and $Y(f)$, while $A_3(f)$ is the actual linear system between $X_3(f)$ and $Y_3(f)$. In general, since $G_{u_3 u_3}(f) \neq G_{33}(f)$, the spectral output of $y_3(t)$ given by

$$G_{y_3 y_3}(f) = |A_3(f)|^2 G_{33}(f) \quad (1.71)$$

will differ from the spectral output of $y_c(t)$ given by

$$G_{y_c y_c}(f) = |L_3(f)|^2 G_{u_3 u_3}(f) \quad (1.72)$$

Example of Figure 1.4

Consider the example of Figure 1.4 where a linear system is in parallel with only one finite-memory nonlinear system. This example corresponds to Figure 1.5 where $H(f) = A_1(f)$, $g(x) = g_2(x)$, $A(f) = A_2(f)$ and $g_3(x) = 0$. Appropriate formulas for this example are as follows.

$$U_1(f) = X_1(f) \quad (1.73)$$

$$U_2(f) = X_2(f) - L_{12}(f)X_1(f) \quad (1.74)$$

$$L_{12}(f) = [G_{12}(f)/G_{11}(f)] \quad (1.75)$$

$$L_1(f) = [G_{1y}(f)/G_{11}(f)] \quad (1.76)$$

$$L_2(f) = [G_{u_2y}(f)/G_{u_2u_2}(f)] \quad (1.77)$$

where

$$G_{u_2y}(f) = G_{2y}(f) - L_{12}^*(f)G_{1y}(f) \quad (1.78)$$

$$G_{u_2u_2}(f) = G_{22}(f) - L_{12}(f)G_{21}(f) \quad (1.79)$$

Finally, for the systems in Figure 1.3,

$$A(f) = A_2(f) = L_2(f) \quad (1.80)$$

$$H(f) = A_1(f) = L_1(f) - L_{12}(f)A(f) \quad (1.81)$$

Note that $H(f) \neq L_1(f)$ unless $A(f) = 0$. Individual spectral outputs are

$$G_{y_1y_1}(f) = |H(f)|^2 G_{11}(f) \quad (1.82)$$

$$G_{y_2y_2}(f) = |A(f)|^2 G_{22}(f) \quad (1.83)$$

$$G_{y_ay_a}(f) = |L_1(f)|^2 G_{11}(f) \quad (1.84)$$

$$G_{y_by_b}(f) = |L_2(f)|^2 G_{u_2u_2}(f) \quad (1.85)$$

The total output spectral density function is given by

$$G_{yy}(f) = G_{y_a y_a}(f) + G_{y_b y_b}(f) + G_{nn}(f) \quad (1.86)$$

where

$$G_{y_a y_a}(f) = \gamma_{u_1 y}^2(f) G_{yy}(f) \quad (1.87)$$

$$G_{y_b y_b}(f) = \gamma_{u_2 y}^2(f) G_{yy}(f) \quad (1.88)$$

$$G_{nn}(f) = [1 - \gamma_{u_1 y}^2(f) - \gamma_{u_2 y}^2(f)] G_{yy}(f) \quad (1.89)$$

These formulas are general results for Figure 1.4 where the input data can be non-Gaussian and where $X_2(f)$ represents the Fourier transform of any zero-memory nonlinear system output $x_2(t) = g[x(t)]$.

This concludes the example of Figure 1.4.

1.5 GAUSSIAN INPUT DATA

A special case of great interest is the case where input data are Gaussian and where the zero-memory nonlinear systems in Figure 1.4 are

$$g_2[x(t)] = x^2(t), \quad g_3[x(t)] = x^3(t) \quad (1.90)$$

This case, shown in Figure 1.8, is the Case 1 single-input/single-output nonlinear model in References [1, 2].

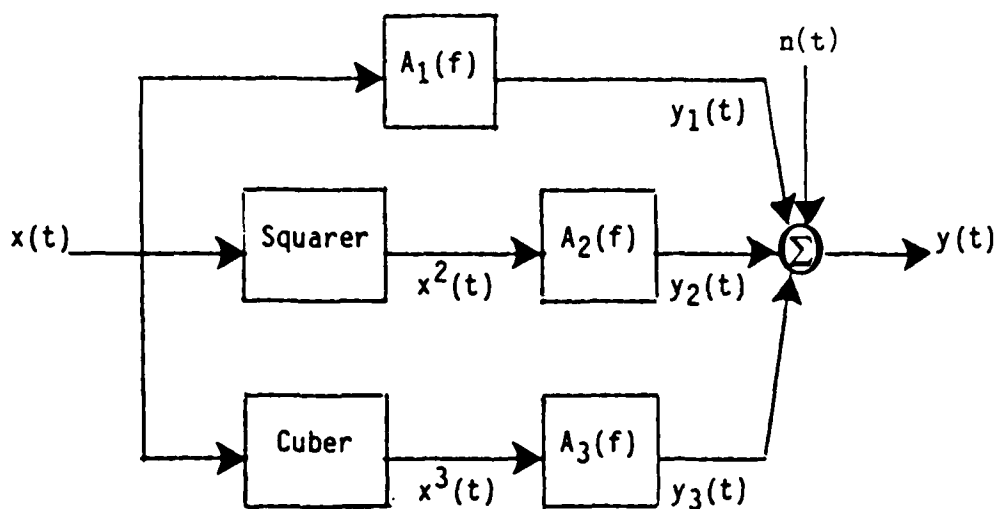


Figure 1.8 Case 1 single-input/single-output nonlinear model with Gaussian input data.

The Fourier transforms $X_2(f)$ and $X_3(f)$ on the related three-input/single-output linear model of Figure 1.6 have a very special meaning for this Case 1 nonlinear model. Specifically, $X_2(f)$ is the Fourier transform of $x^2(t)$ and $X_3(f)$ is the Fourier transform of $x^3(t)$ as denoted by

$$X_2(f) = \mathcal{F}[x^2(t)] \quad (1.91)$$

$$X_3(f) = \mathcal{F}[x^3(t)] \quad (1.92)$$

For Gaussian input data, $x(t)$ will be uncorrelated with $x^2(t)$ but $x(t)$ will be correlated with $x^3(t)$. It follows that the cross-spectral density functions $G_{12}(f) = 0$ and $G_{23}(f) = 0$. Also, as shown in Reference [1], the cross-spectral density function

$$G_{13}(f) = 3\sigma_x^2 G_{11}(f) \quad (1.93)$$

where the variance $\sigma_x^2 = E[x^2(t)]$ when $E[x(t)] = 0$. Here, $L_{12}(f) = 0$ and $L_{23}(f) = 0$ but

$$L_{13}(f) = 3\sigma_x^2 \quad (1.94)$$

The three mutually uncorrelated input records $U_1(f)$, $U_2(f)$ and $U_3(f)$ in Figure 1.7 are given now by the simple relations

$$U_1(f) = X_1(f) \quad (1.95)$$

$$U_2(f) = X_2(f) \quad (1.96)$$

$$U_3(f) = X_3(f) - 3\sigma_x^2 X_1(f) \quad (1.97)$$

Thus, Figure 1.7 becomes Figure 1.9 for the model of Figure 1.8, and the L-systems can be computed easily by Equations 1.39 to 1.41.

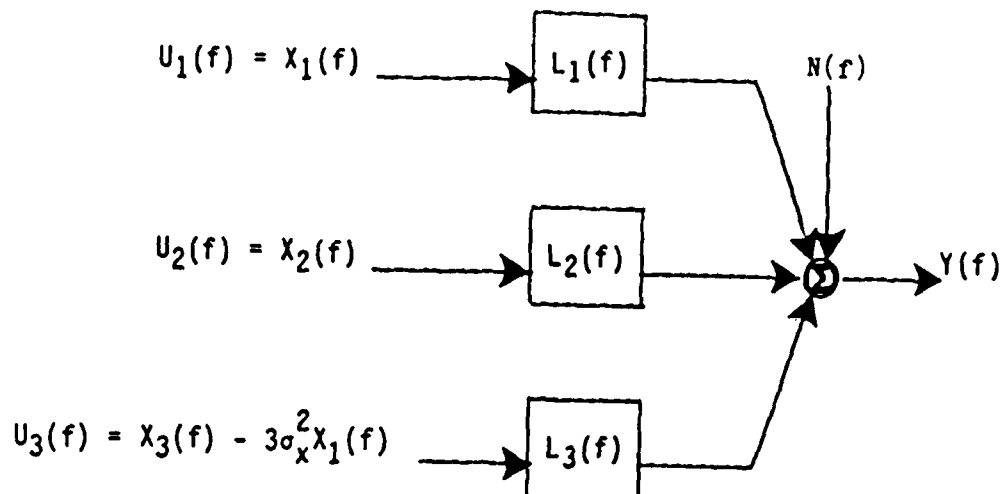


Figure 1.9 Revised three-input/single-output linear model equivalent to Figure 1.8 where the input records are mutually uncorrelated.

Specifically for the model of Figure 1.9, the L-systems are given by the formulas

$$L_1(f) = \frac{G_{1y}(f)}{G_{11}(f)} \quad (1.98)$$

$$L_2(f) = \frac{G_{2y}(f)}{G_{22}(f)} \quad (1.99)$$

$$L_3(f) = \frac{G_{u_3y}(f)}{G_{u_3u_3}(f)} \quad (1.100)$$

where

$$G_{u_3y}(f) = G_{3y}(f) - 3\sigma_x^2 G_{1y}(f) \quad (1.101)$$

$$G_{u_3u_3}(f) = G_{33}(f) - 9\sigma_x^4 G_{11}(f) \quad (1.102)$$

In place of Equations 1.54 to 1.56, simpler relations between the linear systems in Figures 1.8 and 1.9 are now

$$A_3(f) = L_3(f) \quad (1.103)$$

$$A_2(f) = L_2(f) \quad (1.104)$$

$$A_1(f) = L_1(f) - 3\sigma_x^2 A_3(f) \quad (1.105)$$

Note that computation of $A_1(f)$ requires knowledge of $A_3(f)$, and that $A_1(f) \neq L_1(f)$ when $A_3(f) \neq 0$. Also the relation

$$L_1(f) = A_1(f) + 3\sigma_x^2 A_3(f) \quad (1.106)$$

shows that $L_1(f)$ is a function of the input variance σ_x^2 and so will change with different input records. However, the systems $A_1(f)$, $A_2(f)$ and $A_3(f)$ in Figure 1.8 are independent of the input variance when Figure 1.8 is a valid nonlinear model. Thus, conventional linear system identification techniques where only $L_1(f)$ is computed give erroneous estimates of $A_1(f)$.

This concludes Section 1.

2. NONLINEAR WAVE FORCE MODELS

Section 2 details a methodology for analyzing parallel linear and nonlinear systems involving a square-law operation with sign. The analysis is applied specifically to the problem of decomposing random wave forces on a structure into linear (inertial force) and nonlinear (drag force) components. A procedure is presented for identifying the individual initial and drag force parameters based solely upon measurements of the input wave velocity and the output wave force. The input wave velocity is assumed to be a Gaussian stationary random process with arbitrary autospectral density function. Formulas are stated for random errors in estimates. These formulas are also useful in the design of experiments.

2.1 FORMULATION OF WAVE FORCE MODEL

Morison's Equation is widely used to study wave forces on structures, References [7, 9-11], where a wave force output $y(t)$ due to a wave velocity input $x(t)$ consists of two main components:

- (1) an inertial force $m(t)$ that is proportional to the derivative $\dot{x}(t)$ of the wave velocity $x(t)$,
- (2) a drag force $d(t)$ that is proportional to $x(t)|x(t)|$.

Morison's Equation is thus of the form

$$y(t) = m(t) + d(t) = C_1 \dot{x}(t) + C_2 x(t)|x(t)| \quad (2.1)$$

where the exact nature of the constants C_1 and C_2 would either be known or to be determined. In Morison's work, C_1 and C_2 are not functions of frequency. It is clear that Figure 1.4 can represent Equation 2.1 by setting

$$\begin{aligned} H(f) &= C_1(j2\pi f) \\ A(f) &= C_2 \end{aligned} \quad (2.2)$$

Equation 2.1 can apply to more general situations by allowing C_1 and C_2 to be functions of frequency. Figure 2.1 illustrates this wave force problem for a tall structure in the ocean.

The problem of concern is to determine the spectral properties of the inertial component $m(t)$ and the drag component $d(t)$ from measurements of the wave velocity $x(t)$ and the net force $y(t)$. This determination is difficult for two reasons:

- (a) the drag force $d(t)$ has a nonlinear relationship of the type $x(t)|x(t)|$, namely, a square-law operation with sign, and
- (b) the inertial force $m(t)$ and the drag force $d(t)$ are correlated.

The specific model to be evaluated here is shown in Figure 2.2 where $n(t)$ is extraneous noise, and $H(f)$ and $A(f)$ are the frequency response functions of constant parameter linear systems given by the Fourier transforms of weighting functions $h(\tau)$ and $a(\tau)$, namely,

$$\begin{aligned} H(f) &= \mathcal{F}[h(\tau)] = \int_0^{\infty} h(\tau) e^{-j2\pi f\tau} d\tau \\ A(f) &= \mathcal{F}[a(\tau)] = \int_0^{\infty} a(\tau) e^{-j2\pi f\tau} d\tau \end{aligned} \tag{2.3}$$

The system $x|x|$ is a zero memory nonlinear system with an instantaneous output $w(t) = x(t)|x(t)|$. Note that unlike Morison's relationship in Equation 2.1, the systems $H(f)$ and $A(f)$ are not assumed to be constants or even real numbers.

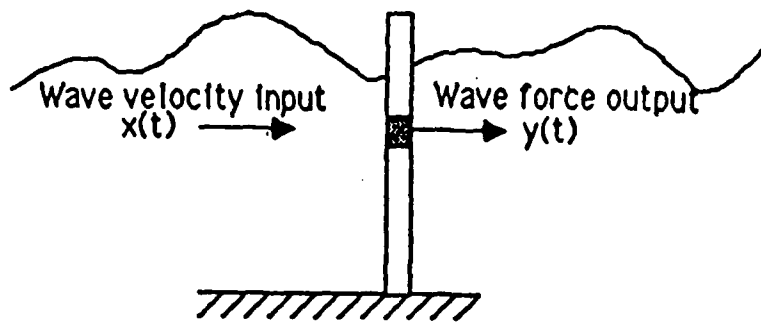


Figure 2.1 Illustration of wave force problem.

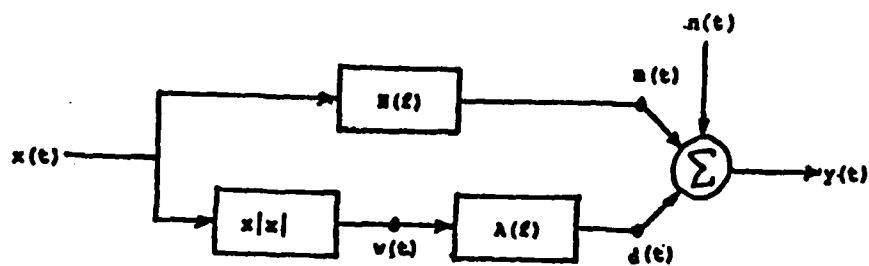


Figure 2.2 Nonlinear wave force model.

Two problems will be treated for the model of Figure 2.2.

- (1) Spectral Decomposition Problem. Given $H(f)$ and $A(f)$ plus measurement of $x(t)$ only, determine the spectral properties of $m(t)$ and $d(t)$. If $y(t)$ is measured as well as $x(t)$, determine also the spectral properties of $n(t)$.
- (2) System Identification Problem. From measurements of $x(t)$ and $y(t)$, identify the optimum frequency properties of $H(f)$ and $A(f)$ to minimize the autospectrum of $n(t)$.

2.2 SPECTRAL DECOMPOSITION PROBLEM

Referring to Figure 2.2, assume the input record $x(t)$ is a sample time history of a stationary (ergodic) Gaussian random process with mean value $\mu_x = E[x(t)] = 0$. Nonzero mean value inputs are treated later in Section 2.4. To solve the Decomposition Problem for the model in Figure 2.2, an approximation is required for the nonlinear operation $x|x|$. The third-order polynomial least-squares approximation is given by using Equation 1.30, namely,

$$\begin{aligned} x|x| &= \left(\sigma_x \sqrt{\frac{2}{\pi}}\right)x + \left(\frac{1}{3\sigma_x} \sqrt{\frac{2}{\pi}}\right)x^3 \\ &= k(3\sigma_x^2 x + x^3) \quad k = \frac{1}{3\sigma_x} \sqrt{\frac{2}{\pi}} \end{aligned} \tag{2.4}$$

where k is the same as a_3 in Equation 1.29 and σ_x is the standard deviation of $x(t)$ defined by

$$\sigma_x = \left\{ E \left[(x(t) - \mu_x)^2 \right] \right\}^{1/2} \tag{2.5}$$

In words, $x|x|$ can be replaced by the sum of a linear operation plus a cubic operation. For an input $x(t)$ with a zero mean value, this nonlinear system approximation is Figure 2.3. Substitution of

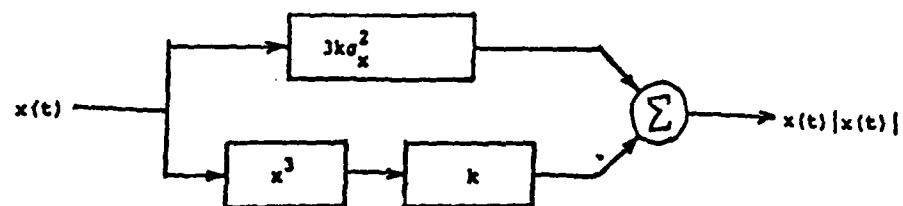


Figure 2.3 Third-order polynomial for $x(t) | x(t) |$.

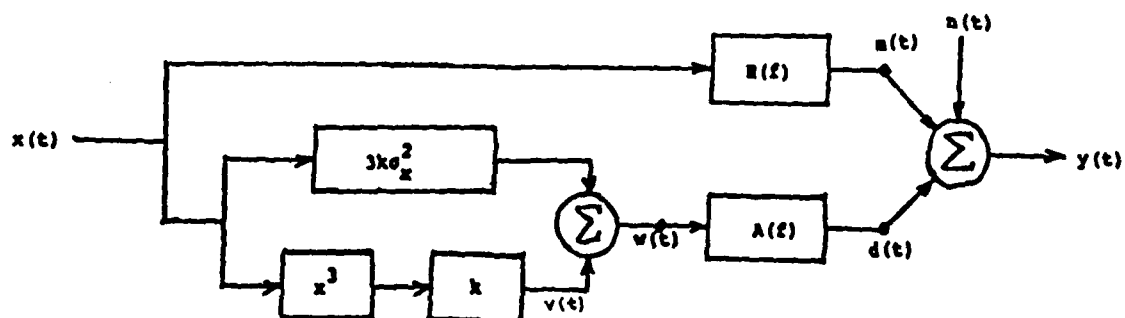


Figure 2.4 Nonlinear wave force model with correlated outputs representing Figure 2.2.

Figure 2.3 for the $x|x|$ operator into Figure 2.2 yields the model shown in Figure 2.4 which, henceforth, is used to approximate the model in Figure 2.2. Formulas will now be derived to compute the autospectral density functions of $m(t)$ and $d(t)$ from knowledge of $H(f)$ and $A(f)$, using measurements of $x(t)$ and $y(t)$.

It should be noted here that Figure 2.4 is a special case of Figures 1.5 and 1.8 that can be analyzed by formulas in Sections 1.4 and 1.5. However, it is more instructive to directly develop here the desired formulas for this special problem. In agreement with physically measurable results, one-sided spectral density functions will be used instead of theoretical two-sided spectral density functions.

In Figure 2.4, for a Gaussian input $x(t)$ with zero mean value and standard deviation σ_x , the terms $m(t)$, $d(t)$, $n(t)$ and $y(t)$ will also have zero mean values. Formulas for the Fourier transforms of such records with long, but finite length T are given by

$$\begin{aligned} X(f) &= \mathcal{F}[x(t)] = \int_0^T x(t) e^{-j2\pi ft} dt \\ Y(f) &= \mathcal{F}[y(t)] = \int_0^T y(t) e^{-j2\pi ft} dt \end{aligned} \quad (2.6)$$

It is assumed that $x(t)$ and $y(t)$ can be divided into n_d associated sub-records, each of length T , to compute desired averages. Autospectral and cross-spectral density functions of $x(t)$ and $y(t)$ are then computed for one-sided spectra by

$$\begin{aligned} G_{xx}(f) &= \frac{2}{T} E[X^*(f)X(f)] \\ G_{yy}(f) &= \frac{2}{T} E[Y^*(f)Y(f)] \\ G_{xy}(f) &= \frac{2}{T} E[X^*(f)Y(f)] \end{aligned} \quad (2.7)$$

where the asterisk (*) denotes complex conjugate and $E[]$ is approximated in practice by an ensemble average over n_d quantities.

In terms of the functions $H(f)$ and $A(f)$, Fourier transforms of the output quantities over long, but finite length records yield

$$Y(f) = M(f) + D(f) + N(f) \quad (2.8)$$

$$M(f) = H(f)X(f) \quad (2.9)$$

$$D(f) = A(f)W(f)$$

where $W(f)$ is the Fourier transform of $w(t)$ defined by

$$W(f) = k \left[3\sigma_x^2 X(f) + X_3(f) \right] \quad (2.10)$$

Here, $w(t) = k[3\sigma_x^2 x(t) + x^3(t)]$ and

$$X_3(f) = \mathcal{F}[x^3(t)] = \int_0^T x^3(t) e^{-j2\pi ft} dt \quad (2.11)$$

The quantity $N(f)$ is the Fourier transform of the unmeasured extraneous output noise $n(t)$ that is assumed to be uncorrelated with both $m(t)$ and $d(t)$.

Figure 2.4 is equivalent to the two-input/single-output linear model shown in Figure 2.5 where the inputs $x(t)$ and $v(t)$ are correlated. Figure 2.5 is a special case of Figure 1.6.

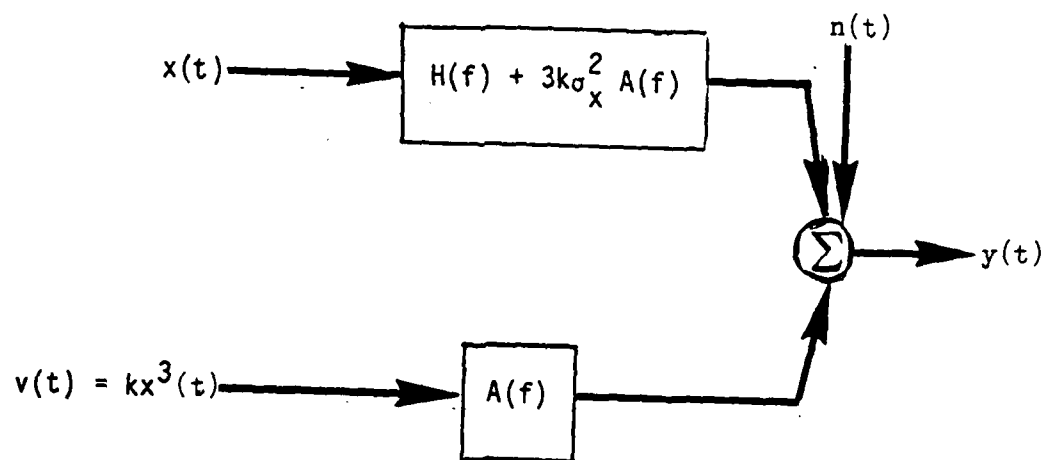


Figure 2.5 Two-input/single-output linear model with correlated inputs that is equivalent to Figure 2.4.

Let $y(t) = x_3(t) = x^3(t)$ with $E[x(t)] = 0$. The cross-correlation function

$$\begin{aligned} R_{xy}(\tau) &= E[x(t)y(t+\tau)] = E[x(t)x^3(t+\tau)] \\ &= E[x(t)x(t+\tau)x(t+\tau)x(t+\tau)] \end{aligned}$$

For zero mean value Gaussian data, $E[y(t)] = 0$ and a fourth-order moment breaks up into the product of all possible pairs of second-order moments. Specifically,

$$E[a_1 a_2 a_3 a_4] = E[a_1 a_2] E[a_3 a_4] + E[a_1 a_3] E[a_2 a_4] + E[a_1 a_4] E[a_2 a_3]$$

Hence, $R_{xy}(\tau)$ becomes

$$R_{xy}(\tau) = 3E[x(t+\tau)x(t+\tau)] E[x(t)x(t+\tau)] = 3\sigma_x^2 R_{xx}(\tau)$$

The corresponding cross-spectrum relationship is

$$G_{xy}(f) = 3\sigma_x^2 G_{xx}(f)$$

This proves by letting $y(t) = x_3(t) = x^3(t)$ that

$$G_{xx_3}(f) = 3\sigma_x^2 G_{xx}(f) \quad (2.12)$$

Note that

$$G_{xx_3}^*(f) = G_{xx_3}(f) = G_{x_3x}(f)$$

The one-sided autospectral density function of $x_3(t) = x^3(t)$ is

$$G_{x_3 x_3}(f) = \frac{2}{T} E[X_3^*(f) X_3(f)] \quad (2.13)$$

This computation can be done directly. The one-sided autospectral density function of $w(t)$ is defined by

$$G_{ww}(f) = \frac{2}{T} E[W^*(f) W(f)] \quad (2.14)$$

This computation requires some extra work.

A formula will now be derived for $G_{ww}(f)$ in terms of $G_{xx}(f)$ and $G_{x_3 x_3}(f)$. Equation 2.12 proves that $x(t)$ and $x_3(t)$ are correlated with

$$G_{xx_3}(f) = 3\sigma_x^2 G_{xx}(f) \quad (2.15)$$

Hence,

$$\begin{aligned} G_{ww}(f) &= k^2 \left[9\sigma_x^4 G_{xx}(f) + 3\sigma_x^2 G_{xx_3}(f) + 3\sigma_x^2 G_{xx_3}^*(f) + G_{x_3 x_3}(f) \right] \\ &= k^2 \left[27\sigma_x^4 G_{xx}(f) + G_{x_3 x_3}(f) \right] \end{aligned} \quad (2.16)$$

It follows also that

$$G_{xw}(f) = k \left[3\sigma_x^2 G_{xx}(f) + G_{xx_3}(f) \right] = 6k\sigma_x^2 G_{xx}(f) \quad (2.17)$$

This shows that $x(t)$ and $w(t)$ are correlated.

It is now simple to compute the desired autospectral density functions of $m(t)$ and $d(t)$. From Equation 2.9,

$$G_{mm}(f) = |H(f)|^2 G_{xx}(f) \quad (2.18)$$

This represents the inertial term in Equation 2.1. Also

$$G_{dd}(f) = |A(f)|^2 G_{ww}(f) \quad (2.19)$$

where $G_{ww}(f)$ should be computed using Equation 2.16. This represents the drag term in Equation 2.1. The cross-spectral density function between $m(t)$ and $d(t)$ is obtained using Equation 2.17 as follows.

$$\begin{aligned} G_{md}(f) &= \frac{2}{T} E \left[y_m^*(f) y_d(f) \right] = H^*(f) A(f) G_{xw}(f) \\ &= 6k\sigma_x^2 H^*(f) A(f) G_{xx}(f) \end{aligned} \quad (2.20)$$

Thus, $m(t)$ and $d(t)$ are correlated and from Equation 2.8

$$G_{yy}(f) = G_{mm}(f) + G_{dd}(f) + G_{md}(f) + G_{md}^*(f) + G_{nn}(f) \quad (2.21)$$

Note that computation of Equations 2.18 and 2.19 involves measurement only of $x(t)$, whereas Equation 2.21 requires measurement also of $y(t)$. When both $x(t)$ and $y(t)$ are measured, Equation 2.21 can compute the autospectrum of the unmeasured $n(t)$. Good models occur when $G_{nn}(f)$ is small compared to $G_{yy}(f)$.

From Equations 2.16 and 2.19 the drag term can be written as

$$G_{dd}(f) = k^2 |A(f)|^2 \left[27\sigma_x^4 G_{xx}(f) + G_{x_3 x_3}(f) \right] \quad (2.22)$$

This $G_{dd}(f)$ is the sum of two parts obtained by using the correlated terms $x(t)$ and $x_3(t)$. An alternative formula for $G_{dd}(f)$ is derived later in Equation 2.44 where $G_{dd}(f)$ is based upon two terms that are uncorrelated. From Equation 2.21, note that

$$G_{yy}(f) = G_{nn}(f) + G_{dd}(f) + G_{nn}(f) \quad (2.23)$$

To obtain $G_{nn}(f)$, Equation 2.21 shows that

$$G_{nn}(f) = G_{yy}(f) - \left[G_{nn}(f) + G_{dd}(f) + G_{md}(f) + G_{md}^*(f) \right] \quad (2.24)$$

A more informative formula for $G_{nn}(f)$ will be derived later in Equation 2.49.

2.3 SYSTEM IDENTIFICATION PROBLEM

The starting point for this problem is the model in Figure 2.4 where it is now assumed the properties of $H(f)$ and $A(f)$ are not known. These properties will be determined from $x(t)$ and $y(t)$ based upon minimizing the spectral density function $G_{nn}(f)$ of $n(t)$ over all possible choices of linear systems to predict $y(t)$

from $x(t)$. It is assumed here that the mean value $\mu_x = E[x(t)] = 0$. Nonzero mean value inputs are treated in Section 2.3.

In Figure 2.4, it follows that

$$Y(f) = H(f)X(f) + kA(f)\left[3\sigma_x^2 X(f) + X_3(f)\right] + N(f) \quad (2.25)$$

and using Equation 2.15,

$$\begin{aligned} G_{xy}(f) &= H(f)G_{xx}(f) + 3k\sigma_x^2 A(f)G_{xx}(f) + kA(f)G_{xx_3}(f) \\ &= \left[H(f) + 6k\sigma_x^2 A(f)\right] G_{xx}(f) \end{aligned} \quad (2.26)$$

Hence, as proved in Reference [2], the optimum linear system is given by

$$H_o(f) = \frac{G_{xy}(f)}{G_{xx}(f)} = H(f) + 6k\sigma_x^2 A(f) \quad (2.27)$$

This system $H_o(f)$ computed from $x(t)$ and $y(t)$ only, gives the minimum $G_{nn}(f)$ over all possible linear systems. It also automatically makes $n(t)$ uncorrelated with $x(t)$.

Note that $H_o(f) \neq H(f)$ and that $H_o(f)$ is a function of the input variance σ_x^2 . Thus $H_o(f)$ will change with different inputs while $H(f)$ will be the same.

Note also that determination of $H(f)$ requires knowledge of $A(f)$ as well as $H_o(f)$. By using $H_o(f)$ instead of $H(f)$, Figure 2.4 can be redrawn as Figure 2.6. This is then equivalent to the two-input/single-output linear model of Figure 2.7 where $x(t)$ and $u(t)$ are uncorrelated. Figure 2.7 is a special case of Figure 1.9. Figure 2.7 can also be derived directly from Figure 2.5.

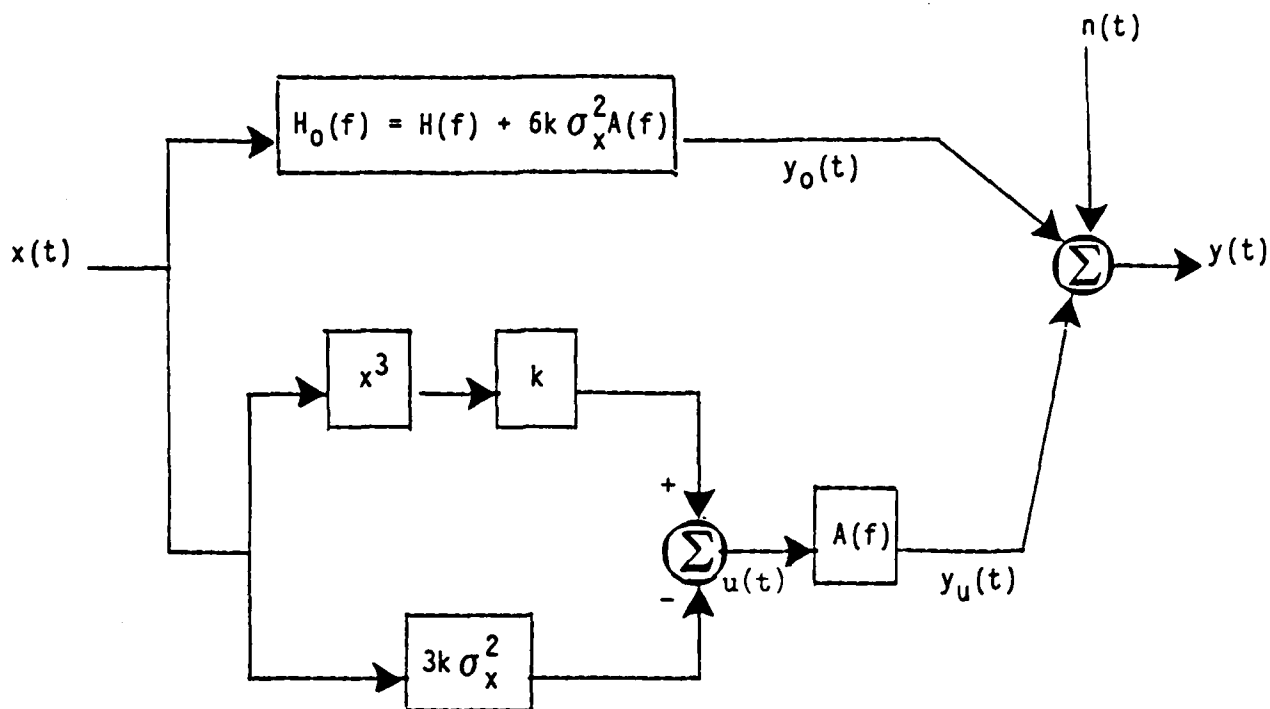


Figure 2.6 Nonlinear wave force model with uncorrelated outputs that is equivalent to Figure 2.4.

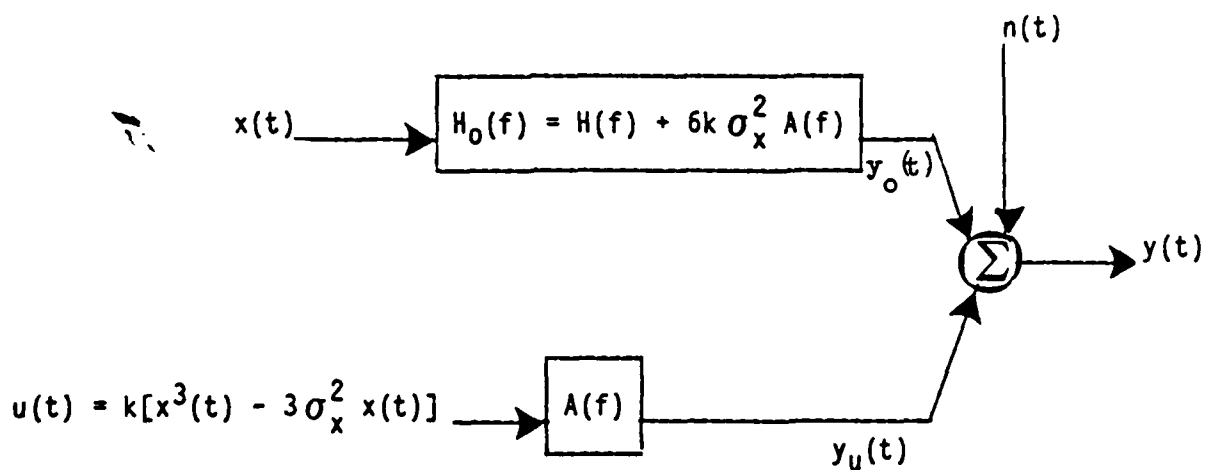


Figure 2.7 Two-input/single-output linear model with uncorrelated inputs that is equivalent to Figure 2.5.

Fourier transform relations for Figures 2.6 and 2.7 show that $Y(f)$ is the sum of a linear term $Y_o(f)$, an uncorrelated nonlinear term $Y_u(f)$, and an uncorrelated noise term $N(f)$ where

$$Y_o(f) = H_o(f)X(f) = [H(f) + 6k\sigma_x^2 A(f)] X(f) \quad (2.28)$$

$$Y_u(f) = A(f)U(f) = kA(f) [X_3(f) - 3\sigma_x^2 X(f)] \quad (2.29)$$

Here, the cross-spectral density function

$$G_{Y_o Y_u}(f) = 0 \quad (2.30)$$

Now, noting that the total force is given by

$$Y(f) = Y_o(f) + Y_u(f) + N(f) \quad (2.31)$$

it follows from Equation 2.30 that the autospectrum of the total force decomposes into three additive terms, as follows.

$$G_{YY}(f) = G_{Y_o Y_o}(f) + G_{Y_u Y_u}(f) + G_{nn}(f) \quad (2.32)$$

This gives the model in Figure 2.6 that is equivalent to Figure 2.4.

The quantity $u(t)$ in Figure 2.6 is not the same as the quantity $w(t)$ in Figure 2.4 and $U(f) \neq W(f)$. In this case,

$$u(t) = k[x^3(t) - 3\sigma_x^2 x(t)] \quad (2.33)$$

which has a Fourier transform from a long but finite record given by

$$U(f) = k[X_3(f) - 3\sigma_x^2 X(f)] \quad (2.34)$$

Here, $x(t)$ and $u(t)$ are uncorrelated. Using Equation 2.15, the autospectrum of $u(t)$ is given by

$$\begin{aligned} G_{uu}(f) &= k^2 \left[G_{x_3 x_3}(f) - 3\sigma_x^2 G_{xx_3}(f) - 3\sigma_x^2 G_{xx_3}^*(f) + 9\sigma_x^4 G_{xx}(f) \right] \\ &= k^2 \left[G_{x_3 x_3}(f) - 9\sigma_x^4 G_{xx}(f) \right] \end{aligned} \quad (2.35)$$

Also, from Equation 2.34,

$$G_{uy}(f) = k \left[G_{x_3 y}(f) - 3\sigma_x^2 G_{xy}(f) \right] \quad (2.36)$$

However,

$$G_{uy}(f) = A(f) G_{uu}(f) \quad (2.37)$$

Hence, it follows that

$$A(f) = \frac{G_{uy}(f)}{G_{uu}(f)} = \frac{G_{x_3 y}(f) - 3\sigma_x^2 G_{xy}(f)}{k \left[G_{x_3 x_3}(f) - 9\sigma_x^4 G_{xx}(f) \right]} \quad (2.38)$$

where computations for $G_{x_3 x_3}(f)$ and $G_{x_3 y}(f)$ can be done directly from $X_3(f)$ and $Y(f)$, similar to direct computations of $G_{xx}(f)$ and $G_{xy}(f)$ from $X(f)$ and $Y(f)$. Equation 2.38 is the desired result to identify the system $A(f)$.

The system $H(f)$ can now be determined. From Equation 2.27, using the just computed $A(f)$,

$$H(f) = H_0(f) - 6k\sigma_x^2 A(f) \quad (2.39)$$

This is the desired result to identify the system $H(f)$.

After $A(f)$ and $H(f)$ are computed, then all formulas in Section 2.2 follow. In particular, one obtains desired inertial and drag results by using Equations 2.18 and 2.19. From Equations 2.16 and 2.35,

$$G_{ww}(f) = 36k^2\sigma_x^4 G_{xx}(f) + G_{uu}(f) \quad (2.40)$$

Hence, in place of Equation 2.19, one can write

$$G_{dd}(f) = G_{d_l d_l}(f) + G_{d_n d_n}(f) \quad (2.41)$$

where $G_{d_l d_l}(f)$ represents the linear part of the drag term given by

$$G_{d_l d_l}(f) = 36k^2\sigma_x^4 |A(f)|^2 G_{xx}(f) \quad (2.42)$$

and $G_{d_n d_n}(f)$ represents the uncorrelated nonlinear part of the drag term given by

$$G_{d_n d_n}(f) = |A(f)|^2 G_{uu}(f) \quad (2.43)$$

Here, $G_{uu}(f)$ should be computed using Equation 2.35. Thus,

$G_{dd}(f)$ is the sum of two parts obtained from the uncorrelated terms $x(t)$ and $u(t)$, namely,

$$G_{dd}(f) = |A(f)|^2 \left[36k^2\sigma_x^4 G_{xx}(f) + G_{uu}(f) \right] \quad (2.44)$$

Equation 2.44 is more instructive than Equation 2.22. Further new results for the autospectral density functions of $y_o(t)$ and $y_u(t)$ in Figures 2.6 and 2.7 are

$$G_{y_o y_o}(f) = |H_o(f)|^2 G_{xx}(f) \quad (2.45)$$

using $H_o(f)$ from equation 2.67, and

$$G_{y_u y_u}(f) = |A(f)|^2 G_{uu}(f) \quad (2.46)$$

using $A(f)$ from Equation 2.38 and $G_{uu}(f)$ from Equation 2.35. Note that Equation 2.46 is the same as Equation 2.43.

The linear coherence function $\gamma_{xy}^2(f)$ between the input $x(t)$ and the total output $y(t)$ is defined by

$$\gamma_{xy}^2(f) = \frac{G_{y_o y_o}(f)}{G_{yy}(f)} = \frac{|G_{xy}(f)|^2}{G_{xx}(f) G_{yy}(f)} \quad (2.47)$$

where the $G_{y_o y_o}(f)$ is given by Equation 2.45. The nonlinear coherence function $q_{xy}^2(f)$ is defined here by

$$q_{xy}^2(f) = \frac{G_{y_u y_u}(f)}{G_{yy}(f)} \quad (2.48)$$

where the $G_{y_u y_u}(f)$ is given by Equation 2.46. Equation 2.48 is the same as the linear coherence function between the uncorrelated input $u(t)$ and the total output $y(t)$.

In terms of these coherence functions, the output noise autospectral density function is given by the simple formula

$$G_{nn}(f) = [1 - \gamma_{xy}^2(f) - q_{xy}^2(f)] G_{yy}(f) \quad (2.49)$$

Clearly, this model will be valid at frequencies where the sum $[\gamma_{xy}^2(f) + q_{xy}^2(f)]$ is close to unity.

2.4 NONZERO MEAN VALUE INPUT

Suppose that the input $x(t)$ has a nonzero mean value $\mu_x = E[x(t)] \neq 0$. For the case where $x(t)$ represents the velocity of an ocean wave, μ_x would be the underlying current. When $\mu_x \neq 0$, the input $x(t)$ should be expressed as

$$x(t) = [x(t) - \mu_x] + \mu_x \quad (2.50)$$

consisting of a variable input term $[x(t) - \mu_x]$ with zero mean value, plus a constant term μ_x . Now the cubing operation $x^3(t)$ becomes

$$\begin{aligned} x^3(t) &= \left\{ [x(t) - \mu_x] + \mu_x \right\}^3 \\ &= [x(t) - \mu_x]^3 + 3(\mu_x)[x(t) - \mu_x]^2 + 3(\mu_x)^2[x(t) - \mu_x] + (\mu_x)^3 \end{aligned} \quad (2.51)$$

where the final constant term μ^3 produces an effect in the spectrum of $x^3(t)$ only at $f = 0$. For $f \neq 0$, Equation 2.51. shows that the diagram in Figure 2.8 should represent the nonlinear operation $x^3(t)$ for the input $[x(t) - \mu_x]$. Note that Figure 2.8 simplifies to the cubic operator by itself when $\mu_x = 0$.

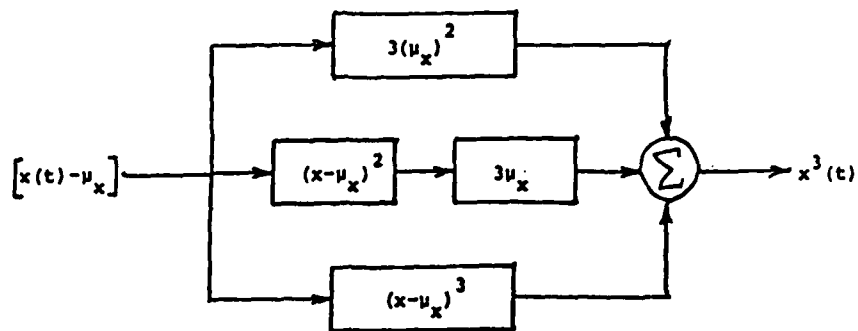


Figure 2.8 Nonlinear system for $x^3(t)$ when $\mu_x \neq 0$.

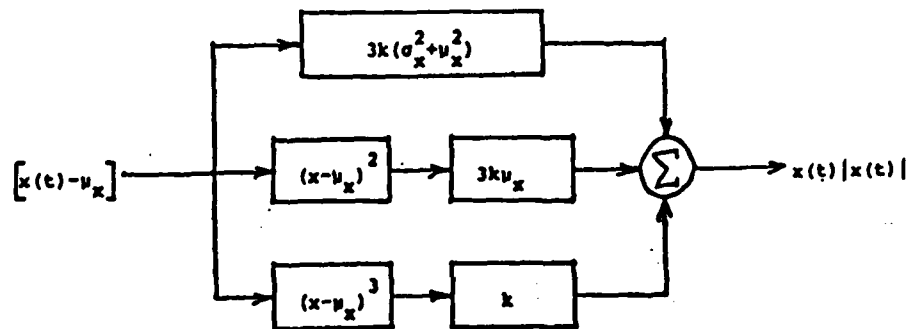


Figure 2.9 Nonlinear system approximating $x(t)|x(t)|$ when $\mu_x \neq 0$.

Consider next the nonlinear operation $x(t)|x(t)|$ of a square-law system with sign which is represented by the least-squares approximation of Equation 2.4, namely

$$x(t)|x(t)| = 3k\sigma_x^2 x(t) + kx^3(t) \quad (2.52)$$

$$k = \frac{1}{3\sigma_x} \sqrt{\frac{2}{\pi}}$$

Here from Equation 2.50,

$$\begin{aligned} x(t)|x(t)| &= 3k\sigma_x^2 \left\{ [x(t) - \mu_x] + \mu_x \right\} + k \left\{ [x(t) - \mu_x] + \mu_x \right\}^3 \\ &= k [x(t) - \mu_x]^3 + 3k\mu_x [x(t) - \mu_x]^2 \\ &\quad + 3k(\sigma_x^2 + \mu_x^2) [x(t) - \mu_x] + k(3\sigma_x^2\mu_x + \mu_x^3) \end{aligned} \quad (2.53)$$

where the final constant term $k(3\sigma_x^2\mu_x + \mu_x^3)$ produces an effect in the spectrum only at $f = 0$. For $f \neq 0$, Equation 2.52 shows that the diagram of Figure 2.9 should represent the nonlinear operation $x(t)|x(t)|$ for the input $[x(t) - \mu_x]$. Note that Figure 2.9 simplifies to Figure 2.3 when $\mu_x = 0$.

Return now to the original problem covered by Figure 2.4. For situations where the input changes to $[x(t) - \mu_x]$ with $\mu_x \neq 0$, Figure 2.4 becomes the new extended Figure 2.10. For Gaussian data, a linear output is uncorrelated with the output from a square-law operation but is correlated with the output from a cubic-law operation. Hence, in place of Figure 2.6, when the input changes to $[x(t) - \mu_x]$ with $\mu_x \neq 0$, Figure 2.6 becomes the new extended Figure 2.11.

The optimum linear system $H_o(f)$ in Figure 2.11 is computed as before by the equation

$$H_o(f) = \frac{G_{xy}(f)}{G_{xx}(f)} \quad (2.54)$$

In terms of $H(f)$ and $A(f)$, one finds that

$$H_o(f) = H(f) + 6k\sigma_x^2 A(f) + 3k\mu_x^2 A(f) \quad (2.55)$$

Note this reduces to Equation 2.27 when $\mu_x = 0$. In Figure 2.11, the Fourier transform $U(f)$ of $u(t)$ is given in place of Equation 2.34 by

$$U(f) = k[X_3(f) + 3\mu_x X_2(f) - 3\sigma_x^2 X(f)] \quad (2.56)$$

where

$$X(f) = \mathcal{F}\{[x(t) - \mu_x]\} \quad (2.57)$$

$$X_2(f) = \mathcal{F}\{[x(t) - \mu_x]^2\} \quad (2.58)$$

$$X_3(f) = \mathcal{F}\{[x(t) - \mu_x]^3\} \quad (2.59)$$

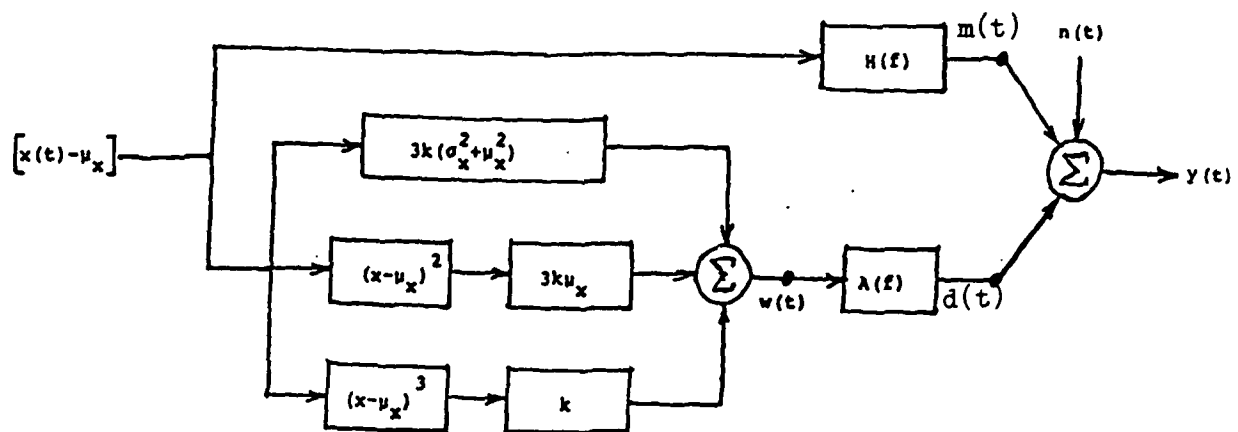


Figure 2.10 Extention of model in figure 2.4
when $\mu_x \neq 0$.

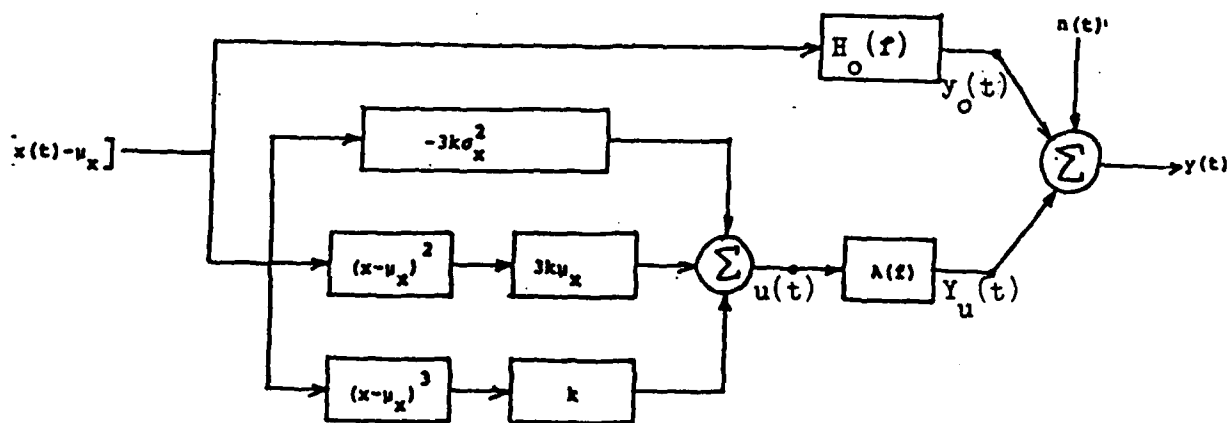


Figure 2.11 Extention of model in figure 2.6
when $\mu_x \neq 0$.

One should now proceed as was done previously to compute $G_{uu}(f)$ and $G_{uy}(f)$ where

$$G_{uu}(f) = \frac{2}{T} E [U(f)U(f)] \quad (2.60)$$

$$G_{uy}(f) = \frac{2}{T} E [U(f)Y(f)] \quad (2.61)$$

Then, the system $A(f)$ is computed by

$$A(f) = \frac{G_{uy}(f)}{G_{uu}(f)} \quad (2.62)$$

and from Equation 2.55, the system $H(f)$ is computed by

$$H(f) = H_o(f) - 6k\sigma_x^2 A(f) - 3k\mu_x^2 A(f) \quad (2.63)$$

The inertial component $m(t)$ in Figure 2.10 has the autospectrum

$$G_{mm}(f) = |H(f)|^2 G_{xx}(f) \quad (2.64)$$

The drag component $d(t)$ in Figure 2.10 has the autospectrum

$$G_{dd}(f) = |A(f)|^2 G_{ww}(f) \quad (2.65)$$

where $G_{ww}(f)$ in Figure 2.10 should not be confused with $G_{uu}(f)$ in Figure 2.11. The output $w(t)$ in Figure 2.10 is quite different from the output $u(t)$ in Figure 2.11. Also, the output $m(t)$ in Figure 2.10 is quite different from the output $y_o(t)$ in Figure 2.11.

The quantity $G_{ww}(f)$ is computed by the usual formula

$$G_{ww}(f) = \frac{2}{T} E[W^*(f)W(f)] \quad (2.66)$$

where $W(f)$ is given by

$$W(f) = k[X_3(f) + 3\mu_x X_2(f) + 3(\sigma_x^2 + \mu_x^2)X(f)] \quad (2.67)$$

Note that Equation 2.67 reduces to Equation 2.10 when $\mu_x = 0$.

The relationship between $U(f)$ and $W(f)$ is given by

$$W(f) = U(f) + 3k(2\sigma_x^2 + \mu_x^2)X(f) \quad (2.68)$$

which leads to the autospectral density function

$$G_{ww}(f) = G_{uu}(f) + 9k^2(2\sigma_x^2 + \mu_x^2)^2 G_{xx}(f) \quad (2.69)$$

This result extends Equation 2.40 for $\mu_x \neq 0$ and occurs because

$$G_{xx_2}(f) = 0 \quad (2.70)$$

$$G_{xx_3}(f) = 3\sigma_x^2 G_{xx}(f) \quad (2.71)$$

Thus, in place of Equation 2.65, one can write

$$G_{dd}(f) = |A(f)|^2 G_{uu}(f) + 9k^2(2\sigma_x^2 + \mu_x^2)^2 |A(f)|^2 G_{xx}(f) \quad (2.72)$$

These two parts of $G_{dd}(f)$ represent uncorrelated nonlinear and linear parts of the drag term. Equation 2.72 reduces to Equation 2.44 when $\mu_x = 0$.

Formulas derived in Section 2.4 for $\mu_x \neq 0$ have been shown to be extensions of corresponding formulas in Section 2.2 and 2.3 where $\mu_x = 0$. In place of Equations 2.45 and 2.46, when $\mu_x \neq 0$,

$$G_{y_o y_o}(f) = |H_o(f)|^2 G_{xx}(f) \quad (2.73)$$

using $H_o(f)$ from Equation 2.54, and

$$G_{y_u y_u}(f) = |A(f)|^2 G_{uu}(f) \quad (2.74)$$

using $A(f)$ from Equation 2.62 and $G_{uu}(f)$ from Equation 2.60. The linear coherence function $\gamma_{xy}^2(f)$ is here

$$\gamma_{xy}^2(f) = \frac{G_{y_o y_o}(f)}{G_{yy}(f)} \quad (2.75)$$

using the $G_{y_o y_o}(f)$ from Equation 2.73, and the nonlinear coherence function $q_{xy}^2(f)$ is

$$q_{xy}^2(f) = \frac{G_{y_u y_u}(f)}{G_{yy}(f)} \quad (2.76)$$

using the $G_{y_u y_u}(f)$ from Equation 2.74. In terms of the coherence functions from Equations 2.75 and 2.76, the output noise autospectral density function is now

$$G_{nn}(f) = [1 - \gamma_{xy}^2(f) - q_{xy}^2(f)] G_{yy}(f) \quad (2.77)$$

2.5 RANDOM ERRORS IN ESTIMATES

Referring back to Figure 2.5 and Equations 2.68 through 2.32, one can view the model in Figure 2.5 as a two-input system with uncorrelated inputs as shown in Figure 2.7. In this form, the random errors to be expected in the computation of certain critical parameter values are given directly from Reference [1]. In terms of the normalized random error (coefficient of variation) of an estimate $\hat{\phi}$ defined by

$$\epsilon[\hat{\phi}] = \frac{\sigma[\hat{\phi}]}{\hat{\phi}} \quad (2.78)$$

the random errors for four important parameter values may be approximated as follows:

$$\epsilon[\hat{\gamma}_{xy}^2(f)] = \frac{\sqrt{2}[1 - \hat{\gamma}_{xy}^2(f)]}{\sqrt{n_d} |\hat{\gamma}_{xy}(f)|} \quad (2.79)$$

$$\epsilon[|\hat{H}_0(f)|] = \frac{[1 - \hat{\gamma}_{xy}^2(f)]^{1/2}}{\sqrt{2n_d} |\hat{\gamma}_{xy}(f)|} \quad (2.80)$$

$$\epsilon[\hat{q}_{xy}^2(f)] = \frac{\sqrt{2}[1 - \hat{q}_{xy}^2(f)]}{\sqrt{(n_d - 1)} |\hat{q}_{xy}(f)|} \quad (2.81)$$

$$\epsilon[|\hat{A}(f)|] = \frac{[1 - \hat{q}_{xy}^2(f)]^{1/2}}{\sqrt{(n_d - 1)} |\hat{q}_{xy}(f)|} \quad (2.82)$$

These formulas can also be used to determine the required values for n_d to achieve acceptable random errors for these four parameter values under assumed conditions for the coherence functions.

This concludes Section 2.

3. NONLINEAR DRIFT FORCE MODELS

Section 2 details a mathematical procedure to determine the spectral decomposition of nonlinear drift forces due to random ocean waves hitting a floating structure such as a ship. More generally, it shows how to determine the spectral decomposition of random data passing through parallel linear and nonlinear systems, where the nonlinear system involves a square-law envelope detector. Different linear operations that may be present in the parallel linear and nonlinear paths can be identified based solely upon measurements of the input data and total output data. The input is assumed to be a Gaussian stationary random process with arbitrary autospectral density function. Formulas are stated to evaluate statistical errors in various estimates made from measured data. These formulas can also be used to design experiments that will achieve desired statistical errors.

3.1 FORMULATION OF DRIFT FORCE MODEL

The general problem to be analyzed for slowly varying drift forces on floating structures is shown in Figure 3.1. A ship is assumed to be subjected to random ocean waves represented by the wave elevation input $x(t)$. This produces a force $F(t)$ on the ship that results in the ship motion output $y(t)$. The spectral decomposition of $y(t)$ is desired that is due to $x(t)$. Random data analysis techniques from References [3,4] will be applied to obtain desired results.

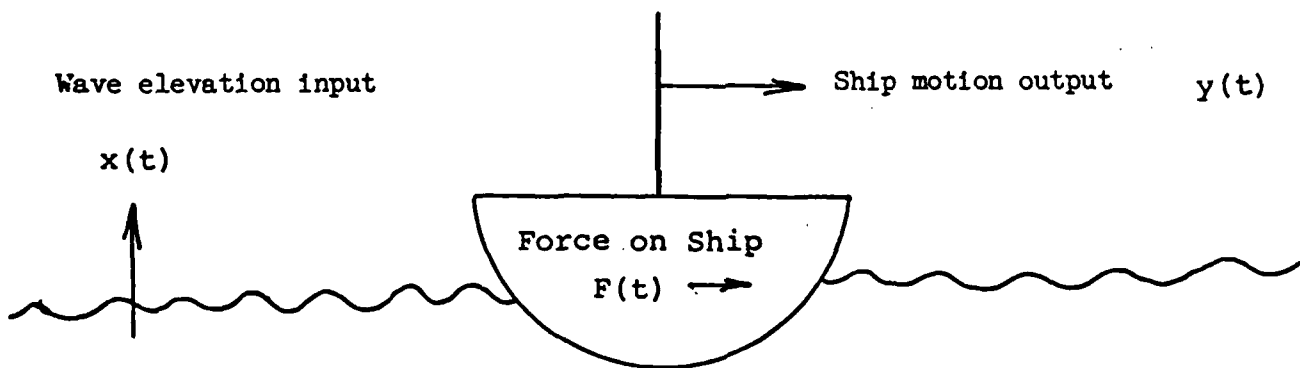


Figure 3.1 Illustration of drift force problem.

The force $F(t)$ acting on the ship in Figure 3.1 is assumed to consist of two components:

- (1) a linear term that is proportional to $x(t)$,
- (2) a nonlinear term that is proportional to the squared envelope signal of $x(t)$.

This nonlinear term is called the slowly varying drift force, References [13-14]. Thus the force $F(t)$ acting on the ship can be expressed as

$$F(t) = k_1 x(t) + k_2 u(t) \quad (3.1)$$

where

$$x(t) = \text{wave elevation input} \quad (3.2)$$

$$u(t) = \text{squared envelope signal of } x(t) \quad (3.3)$$

$$k_1, k_2 = \text{proportionality constants} \quad (3.4)$$

Equation 3.1 can be made to apply to more general situations by letting k_1 and k_2 be functions of frequency. This will be done in the following development.

The ship motion output $y(t)$ in Figure 3.1 will be represented by the nonlinear drift force model in Figure 3.2 such that the total output record

$$y(t) = y_1(t) + y_2(t) + n(t) \quad (3.5)$$

where

$$y_1(t) = \text{linear output due to } x(t) \quad (3.6)$$

$$y_2(t) = \text{uncorrelated nonlinear output due to } u(t) \quad (3.7)$$

$$n(t) = \text{uncorrelated zero mean Gaussian output noise} \quad (3.8)$$

In Figure 3.2, the quantities $H_1(f)$ and $H_2(f)$ are frequency response functions of constant parameter linear systems that incorporate the constants k_1 and k_2 from Equation 3.1.

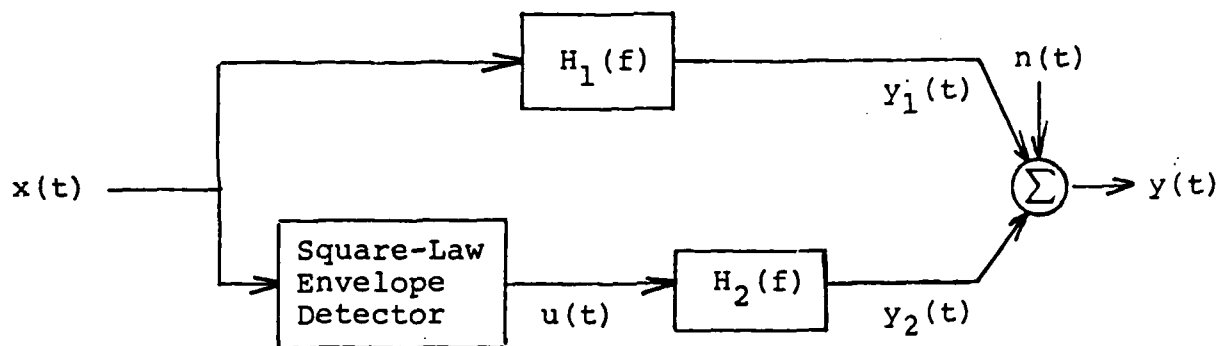


Figure 3.2 Nonlinear drift force model.

Two problems will be treated using the model of Figure 3.2.

- (1) Spectral Decomposition Problem. Given $H_1(f)$ and $H_2(f)$ plus measurement of $x(t)$ only, determine the spectral properties of $y_1(t)$ and $y_2(t)$. If $y(t)$ is measured as well as $x(t)$, determine also the spectral properties of $n(t)$.
- (2) System Identification Problem. From measurements of $x(t)$ and $y(t)$, identify the optimum frequency response functions $H_1(f)$ and $H_2(f)$ to minimize the autospectrum of $n(t)$.

A similar analysis was previously carried out in Section 2 for the nonlinear wave force model of Figure 2.4 that represents Figure 2.2. Note that Figure 3.2 is a special case of Figure 1.4 and can be replaced by an equivalent two-input/single-output linear model using the inputs $x(t)$ and $u(t)$.

3.2 BASIC FORMULAS FOR NONLINEAR DRIFT FORCE MODEL

In the nonlinear model of Figure 3.2, the linear output term $y_1(t)$ is due to $x(t)$ passing through a constant parameter linear system defined by the frequency response function $H_1(f)$. The function $H_1(f)$ is the Fourier transform of a linear weighting function $h_1(\tau)$ such that in the time domain

$$y_1(t) = \int_{-\infty}^{\infty} h_1(\tau) x(t - \tau) d\tau \quad (3.9)$$

and in the frequency domain

$$Y_1(f) = H_1(f) X(f) \quad (3.10)$$

where $X(f)$ and $Y_1(f)$ are Fourier transforms of $x(t)$ and $y_1(t)$, respectively. Theoretically,

$$H_1(f) = \int_{-\infty}^{\infty} h_1(\tau) e^{-j2\pi f\tau} d\tau \quad (3.11)$$

$$X(f) = \int_{-\infty}^{\infty} x(t) e^{-j2\pi ft} dt \quad (3.12)$$

$$Y_1(f) = \int_{-\infty}^{\infty} y_1(t) e^{-j2\pi ft} dt \quad (3.13)$$

It is assumed here and in following formulas that mean values are always removed prior to computing Fourier transforms.

The nonlinear output term $y_2(t)$ in Figure 3.2 is due to $x(t)$ passing through a square-law envelope detector to produce $u(t)$, followed by $u(t)$ passing through a constant parameter linear system described by a frequency response function $H_2(f)$. The

function $H_2(f)$ is the Fourier transform of a linear weighting function $h_2(\tau)$ where, in general, $h_2(\tau) \neq h_1(\tau)$ and $H_2(f) \neq H_1(f)$. In the time domain

$$y_2(t) = \int_{-\infty}^{\infty} h_2(\tau) u(t - \tau) d\tau \quad (3.14)$$

and in the frequency domain

$$Y_2(f) = H_2(f) U(f) \quad (3.15)$$

where $U(f)$ and $Y_2(f)$ are Fourier transforms of $u(t)$ and $y_2(t)$, respectively. Theoretically,

$$H_2(f) = \int_{-\infty}^{\infty} h_2(\tau) e^{-j2\pi f\tau} d\tau \quad (3.16)$$

$$U(f) = \int_{-\infty}^{\infty} u(t) e^{-j2\pi ft} dt \quad (3.17)$$

$$Y_2(f) = \int_{-\infty}^{\infty} y_2(t) e^{-j2\pi ft} dt \quad (3.18)$$

As proved in Reference [3], the output $u(t)$ of the square-law envelope detector is given by

$$u(t) = x^2(t) + \tilde{x}^2(t) \quad (3.19)$$

where

$$\tilde{x}(t) = \text{Hilbert transform of } x(t) \quad (3.20)$$

When $x(t)$ has a zero mean value, then $\tilde{x}(t)$ will also have a zero mean value. However, the mean value of $u(t)$, denoted by $E[u(t)]$, is

$$\mu_u = E[u(t)] = 2\sigma_x^2 \quad (3.21)$$

from Equation 3.19 and the fact that

$$E[x^2(t)] = E[\tilde{x}^2(t)] = \sigma_x^2 \quad (3.22)$$

As usual, the notation $E[]$ denotes the expected value of the quantity inside the brackets. The Fourier transform of $\tilde{x}(t)$, denoted by $\tilde{X}(f)$, is

$$\tilde{X}(f) = \int_{-\infty}^{\infty} \tilde{x}(t) e^{-j2\pi ft} dt \quad (3.23)$$

Now, Fourier transforms of both sides of Equation 3.19 yield

$$U(f) = \int_{-\infty}^{\infty} [X(\alpha)X(f - \alpha) + \tilde{X}(\alpha)\tilde{X}(f - \alpha)] d\alpha \quad (3.24)$$

Reference [3] also proves that

$$\tilde{X}(f) = B(f)X(f) \quad (3.25)$$

where

$$B(f) = -j \operatorname{sgn} f = \begin{cases} -j & f > 0 \\ 0 & f = 0 \\ j & f < 0 \end{cases} \quad (3.26)$$

Hence

$$U(f) = \int_{-\infty}^{\infty} [1 + B(\alpha)B(f - \alpha)] X(\alpha)X(f - \alpha) d\alpha \quad (3.27)$$

and Equation 3.15 becomes

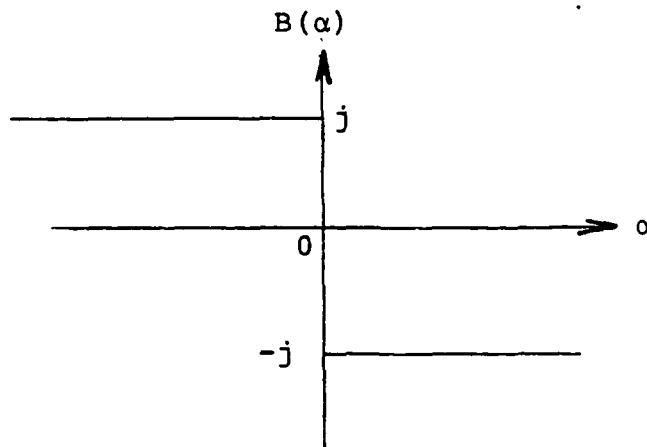
$$Y_2(f) = H_2(f) \int_{-\infty}^{\infty} [1 + B(\alpha)B(f - \alpha)]X(\alpha)X(f - \alpha)d\alpha \quad (3.28)$$

Equations 3.10 and 3.28 show how to compute $Y_1(f)$ and $Y_2(f)$ from knowledge of $X(f)$, $H_1(f)$ and $H_2(f)$. Equations 3.24 to 3.27 show how to compute $\tilde{X}(f)$ and $U(f)$ from knowledge of $X(f)$.

The factor $B(\alpha)B(f - \alpha)$ in Equations 3.27 and 3.28 can be determined as follows. From Equation 3.26, the quantity

$$B(\alpha) = \begin{cases} -j & \alpha > 0 \\ 0 & \alpha = 0 \\ j & \alpha < 0 \end{cases} \quad (3.29)$$

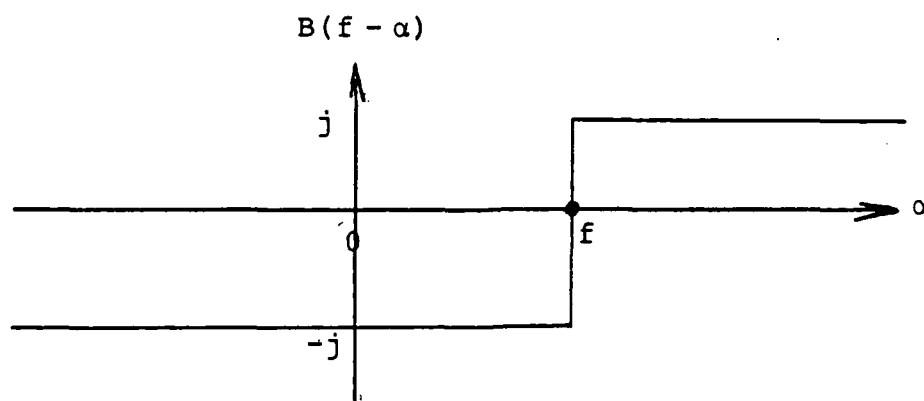
An appropriate plot for $B(\alpha)$ is



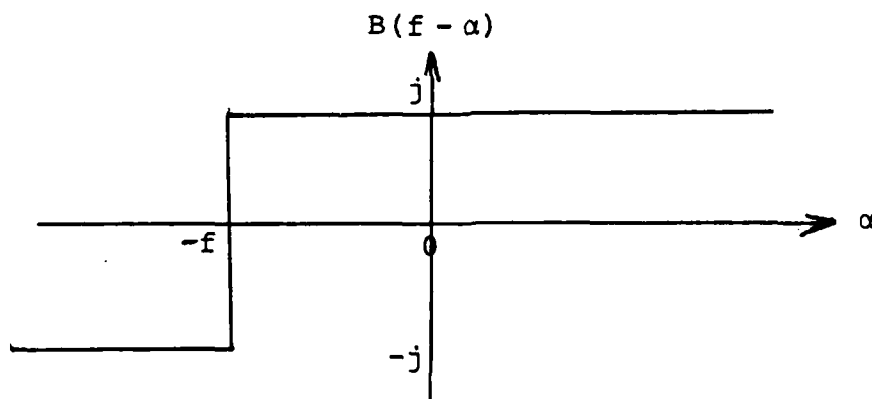
From Equation 3.26, the quantity

$$B(f - \alpha) = \begin{cases} -j & \alpha < f \\ 0 & \alpha = f \\ j & \alpha > f \end{cases} \quad (3.30)$$

Hence, for any $f > 0$, an appropriate plot for $B(f - \alpha)$ is



while for any $f < 0$, an appropriate plot is



Thus, for any $f > 0$, the product

$$B(\alpha)B(f - \alpha) = \begin{cases} 1 & \alpha < 0 \\ -1 & 0 < \alpha < f \\ 1 & \alpha > f \end{cases} \quad (3.31)$$

while for any $f < 0$, the product

$$B(\alpha)B(f - \alpha) = \begin{cases} 1 & \alpha < f \\ -1 & f < \alpha < 0 \\ 1 & \alpha > 0 \end{cases} \quad (3.32)$$

At values of $\alpha = 0$ and $\alpha = f$, note that

$$B(\alpha)B(f - \alpha) = B(0)B(f) = 0 \quad (3.33)$$

Before applying these formulas, a brief discussion will be given on previous drift force models.

3.3 PREVIOUS DRIFT FORCE MODELS

Previous drift force models, such as those assumed in References [12-14] are considerably more complicated because of employing a bilinear (quadratic) weighting function $h_2(\tau_1, \tau_2)$ and bilinear (quadratic) frequency response $H_2(f, g)$ function to represent the nonlinear path. Specifically, Figure 3.2 is extended to a more general Figure 3.3 where $y_1(t)$ is the same but $y_2(t)$ is replaced in the time domain by

$$y_2(t) = \int_{-\infty}^{\infty} h_2(\tau_1, \tau_2) x(t - \tau_1) x(t - \tau_2) d\tau_1 d\tau_2 \quad (3.34)$$

and in the frequency domain by

$$Y_2(f) = \int_{-\infty}^{\infty} H_2(\alpha, f - \alpha) X(\alpha) X(f - \alpha) d\alpha \quad (3.35)$$

Here, $X(f)$ and $Y_2(f)$ are Fourier transforms of $x(t)$ and $y_2(t)$, respectively, while the bilinear frequency response function $H_2(f, g)$ is the double Fourier transform of the bilinear weighting function $h_2(\tau_1, \tau_2)$, namely,

$$H_2(f, g) = \int_{-\infty}^{\infty} h_2(\tau_1, \tau_2) e^{-j2\pi(f\tau_1 + g\tau_2)} d\tau_1 d\tau_2 \quad (3.36)$$

This bilinear frequency response function $H_2(f, g)$ in two frequency variables f and g is much more difficult to compute and interpret than the alternative $H_2(f)$ in Figure 3.2. Mathematical developments of bilinear functions are contained in References [1,2]. Some books that discuss these matters are References [14,15,16].

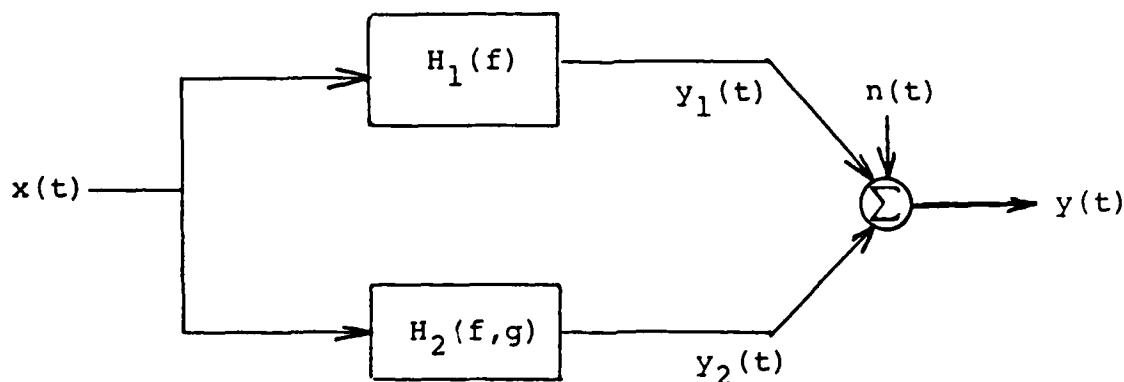


Figure 3.3 Parallel linear and bilinear systems.

Comparison of Equation 3.35 for $Y_2(f)$ in Figure 3.3 with Equation 3.28 for $Y_2(f)$ in Figure 3.2 shows that the same $Y_2(f)$ will occur if

$$H_2(\alpha, f - \alpha) = H_2(f) [1 + B(\alpha)B(f - \alpha)] \quad (3.37)$$

Thus, knowledge of the linear frequency response function $H_2(f)$ in Figure 3.2 can yield an equivalent bilinear frequency response $H_2(\alpha, f - \alpha)$ for Figure 3.3. However, knowledge of the bilinear frequency response function $H_2(\alpha, f - \alpha)$ will not yield an equivalent linear frequency response function $H_2(f)$ for Figure 3.2

To explain this matter, note from Equations 3.31 and 3.32 that the function $[1 + B(\alpha)B(f - \alpha)]$ will be zero for $0 < \alpha < f$ when $f > 0$, and will be zero for $f < \alpha < 0$ when $f < 0$. For these values of α and f , one cannot solve Equation 3.37 for $H_2(f)$ to satisfy an arbitrary $H_2(\alpha, f - \alpha) \neq 0$. Even when the factor $[1 + B(\alpha)B(f - \alpha)] \neq 0$, from Equation 3.37, $H_2(f)$ must satisfy

$$H_2(f) = \frac{H_2(\alpha, f - \alpha)}{[1 + B(\alpha)B(f - \alpha)]} \quad (3.38)$$

This requires the right-hand side to be independent of α , a situation that is highly unlikely to occur in practice for an arbitrary $H_2(\alpha, f - \alpha)$. The conclusion is that one cannot use past results about $H_2(\alpha, f - \alpha)$ to determine an equivalent $H_2(f)$ for Figure 3.2. Instead, future work should be based on new results obtained by following the procedures described in this report.

3.4 SPECTRAL DECOMPOSITION PROBLEM

For Figure 3.2, the Fourier transform of Equation 3.5 proves that

$$Y(f) = Y_1(f) + Y_2(f) + N(f) \quad (3.39)$$

where

$$Y_1(f) = H_1(f)X(f) \quad (3.40)$$

$$Y_2(f) = H_2(f)U(f) \quad (3.41)$$

$$N(f) = \text{Fourier transform of } n(t) \quad (3.42)$$

Equation 3.39 will be used henceforth in place of Equation 3.5 and all further analysis will be done with frequency domain quantities.

As derived and illustrated in References [3,4], from knowledge of $X(f)$ and $Y(f)$ for a number of different stationary random records of length T , their one-sided ($f \geq 0$) autospectral and cross-spectral density functions can be computed by the direct formulas

$$G_{xx}(f) = \frac{2}{T} E[X^*(f)X(f)] \quad (3.43)$$

$$G_{yy}(f) = \frac{2}{T} E[Y^*(f)Y(f)] \quad (3.44)$$

$$G_{xy}(f) = \frac{2}{T} E[X^*(f)Y(f)] \quad (3.45)$$

This procedure does not require the computation of any associated autocorrelation or cross-correlation functions.

From Equations 3.39 to 3.42, the total output autospectral density function is given by the formula

$$G_{yy}(f) = G_{y_1y_1}(f) + G_{y_2y_2}(f) + G_{nn}(f) \quad (3.46)$$

where

$$G_{y_1y_1}(f) = |H_1(f)|^2 G_{xx}(f) \quad (3.47)$$

$$G_{y_2y_2}(f) = |H_2(f)|^2 G_{uu}(f) \quad (3.48)$$

$$G_{nn}(f) = \text{autospectrum of } n(t) \quad (3.49)$$

The cross-spectral density function between $y_1(t)$ and $y_2(t)$, namely,

$$G_{y_1y_2}(f) = H_1^*(f)H_2(f)G_{xu}(f) = 0 \quad (3.50)$$

because $x(t)$ being Gaussian makes

$$G_{xu}(f) = 0 \quad (3.51)$$

Also, assumptions about $n(t)$ make

$$G_{y_1n}(f) = G_{y_2n}(f) = 0 \quad (3.52)$$

The spectral quantity $G_{uu}(f)$ in Equation 3.48 can be computed knowledge of $U(f)$ for a number of different stationary random records of length T by the direct formula

$$G_{uu}(f) = \frac{2}{T} E[U^*(f)U(f)] \quad (3.53)$$

Since $U(f)$ is known from $\bar{X}(f)$, Equation 3.53 actually shows that $G_{uu}(f)$ is a function of $X(f)$.

A useful theoretical formula is derived in Section 3.8.1 to compute $G_{uu}(f)$ from knowledge of the input autospectral density function $G_{xx}(f)$. For any $f > 0$, the formula is

$$G_{uu}(f) = 4 \int_0^{\infty} G_{xx}(\alpha) G_{xx}(f + \alpha) d\alpha + 4 \int_f^{\infty} G_{xx}(\alpha) G_{xx}(\alpha - f) d\alpha \quad (3.54)$$

Another theoretical formula is derived in Section 3.8.2 that shows how to compute $G_{uy}(f)$ from knowledge of the input/output cross-bispectrum $G_{xxy}(f, g)$ where

$$G_{xxy}(f, g) = E[X^*(f)X^*(g)Y(f + g)] \quad (3.55)$$

For any $f > 0$, this formula is

$$G_{uy}(f) = 2 \int_0^{\infty} G_{xxy}(-\alpha, f + \alpha) d\alpha + 2 \int_f^{\infty} G_{xxy}(\alpha, f - \alpha) d\alpha \quad (3.56)$$

Equation 3.54 is applicable to both the spectral decomposition problem and the system identification problem, while Equation 3.56 is applicable only to the system identification problem.

The spectral decomposition problem has now been solved. From measurement only of $x(t)$, one can compute $G_{xx}(f)$ and $G_{uu}(f)$. Then from knowledge of $H_1(f)$ and $H_2(f)$, one can compute the linear part of the output autospectrum $G_{y_1y_1}(f)$ due to the wave elevation force by Equation 3.47, and the nonlinear part of the output autospectrum $G_{y_2y_2}(f)$ due to the nonlinear drift force by Equation 3.48.

If $y(t)$ is measured as well as $x(t)$, then one can compute $G_{yy}(f)$. It is now possible to obtain the output noise autospectrum $G_{nn}(f)$ from Equation 3.46 by the formula

$$G_{nn}(f) = G_{yy}(f) - G_{y_1y_1}(f) - G_{y_2y_2}(f) \quad (3.57)$$

Note also that if $G_{nn}(f)$ is zero, then $G_{yy}(f)$ can be predicted without measuring $y(t)$ by the formula

$$G_{yy}(f) = G_{y_1y_1}(f) + G_{y_2y_2}(f) \quad (3.58)$$

Coherece functions are required to evaluate statistical errors in estimates to be given in Section 3.7. The linear coherence function $\gamma_{xy}^2(f)$ between the input $x(t)$ and the total output $y(t)$ is defined by

$$\gamma_{xy}^2(f) = \frac{|G_{xy}(f)|^2}{G_{xx}(f)G_{yy}(f)} = \frac{G_{y_1y_1}(f)}{G_{yy}(f)} \quad (3.59)$$

This gives the percentage of the total output autospectrum due to the linear operations on $x(t)$. A nonlinear coherence function $q_{xy}^2(f)$ can be defined here by

$$q_{xy}^2(f) = \frac{G_{y_2y_2}(f)}{G_{yy}(f)} \quad (3.60)$$

This gives the percentage of the total output autospectrum due to the nonlinear operations on $x(t)$. In terms of these two coherence functions, the output noise autospectrum of Equation 3.57 becomes

$$G_{nn}(f) = \left[1 - \gamma_{xy}^2(f) - q_{xy}^2(f) \right] G_{yy}(f) \quad (3.61)$$

Figure 3.2 will be a good nonlinear drift force model at those frequencies where $G_{nn}(f)$ is close to zero, namely, where the sum $[\gamma_{xy}^2(f) + c_{xy}^2(f)]$ is close to unity. Otherwise, Figure 3.2 is a poor model.

3.5 SYSTEM IDENTIFICATION PROBLEM

Assume now that the system properties of $H_1(f)$ and $H_2(f)$ are not known in Figure 3.2. Optimum properties are to be identified from measurements of $x(t)$ and $y(t)$ based upon minimizing the autospectrum $G_{nn}(f)$ of $n(t)$ over all possible choices of linear systems to predict $y(t)$ from $x(t)$. It is assumed as before that $x(t)$ follows a Gaussian distribution with zero mean value. Nonzero mean value inputs are treated in Section 3.6.

In Figure 3.2, from Equations 3.39 to 3.42, the basic Fourier transform relation is

$$Y(f) = H_1(f)X(f) + H_2(f)U(f) + N(f) \quad (3.62)$$

where $X(f)$, $U(f)$ and $Y(f)$ can be calculated from the given $x(t)$ and $y(t)$. From Equation 3.62, the cross-spectral density function $G_{xy}(f)$ between $x(t)$ and $y(t)$ satisfies

$$G_{xy}(f) = H_1(f)G_{xx}(f) \quad (3.63)$$

provided that

$$G_{xu}(f) = 0 \quad (3.64)$$

$$G_{xn}(f) = 0 \quad (3.65)$$

Equation 3.64 occurs because $x(t)$ and $u(t)$ will be uncorrelated when $x(t)$ is Gaussian data. Equation 3.65 occurs by assuming $x(t)$ and $n(t)$ are uncorrelated.

From References [3,4], the optimum linear system $H_o(f)$ between $x(t)$ and $y(t)$ is given by the formula

$$H_o(f) = \frac{G_{xy}(f)}{G_{xx}(f)} \quad (3.66)$$

For Figure 3.2, from Equation 3.63,

$$H_1(f) = \frac{G_{xy}(f)}{G_{xx}(f)} = |H_1(f)| e^{-j\phi_1(f)} \quad (3.67)$$

Thus $H_1(f)$ is the same here as the optimum linear system $H_o(f)$ that produces the minimum $G_{nn}(f)$ at all f over all possible linear systems. The optimum system automatically makes $n(t)$ uncorrelated with $x(t)$ so that Equation 3.65 applies without the necessity to assume in advance that $x(t)$ and $n(t)$ will be uncorrelated. Equation 3.67 shows that the complete $H_1(f)$ in both gain and phase can be identified using only $x(t)$ and $y(t)$.

From Equation 3.62, the cross-spectral density function $G_{uy}(f)$ between $u(t)$ and $y(t)$ satisfies

$$G_{uy}(f) = H_2(f) G_{uu}(f) \quad (3.68)$$

provided

$$G_{ux}(f) = 0 \quad (3.69)$$

$$G_{un}(f) = 0 \quad (3.70)$$

These two results follow from Equations 3.64 and 3.65. They also occur because $x(t)$ and $u(t)$ will be uncorrelated when $x(t)$ is Gaussian data, and because $n(t)$ and $u(t)$ will be automatically uncorrelated when $H_1(f)$ satisfies Equation 3.67. For Figure 3.2, from Equation 3.68 ,

$$H_2(f) = \frac{G_{uy}(f)}{G_{uu}(f)} = |H_2(f)| e^{-j\phi_2(f)} \quad (3.71)$$

In practice, $G_{uu}(f)$ can be computed directly by Equation 3.53 and $G_{uy}(f)$ can be computed directly by

$$G_{uy}(f) = \frac{2}{T} E[U^*(f)Y(f)] \quad (3.72)$$

Since $u(t)$ is known from $x(t)$, Equations 3.53, 3.71 and 3.72 show that the complete $H_2(f)$ in both gain and phase can be identified using only $x(t)$ and $y(t)$. Alternate theoretical ways to compute $G_{uu}(f)$ and $G_{uy}(f)$ are given in Equations 3.54 and 3.56, based upon derivations in Sections 3.8.1 and 3.8.2. A different new theoretical way to identify $H_2(f)$ is derived in Section 3.8.3.

After $H_1(f)$ and $H_2(f)$ have been computed by Equations 3.67 and 3.71, respectively, the spectral decomposition problem can then be solved using Equations 3.47, 3.48, and 3.57. To evaluate statistical errors in estimates, one should also compute the linear coherence function $\gamma_{xy}^2(f)$ by Equation 3.59 and the nonlinear coherence function $q_{xy}^2(f)$ by Equation 3.60.

3.6 NONZERO MEAN VALUE INPUT

Suppose that the Gaussian input $x(t)$ has a nonzero mean value given by

$$\mu_x = E[x(t)] \neq 0 \quad (3.73)$$

Then $x(t)$ can be expressed as

$$x(t) = [x(t) - \mu_x] + \mu_x \quad (3.74)$$

consisting of a variable input term $[x(t) - \mu_x]$ with zero mean value, plus a constant term μ_x . Here $\tilde{x}(t)$, the Hilbert transform of $x(t)$, will still have a zero mean value since

$$\mu_{\tilde{x}} = E[\tilde{x}(t)] = B(0)\mu_x = 0 \quad (3.75)$$

and $B(0) = 0$ from Equation 3.26. In place of Equation 3.19, the output of the square-law envelope detector is now given by $w(t)$ where $w(t)$ is

$$\begin{aligned} w(t) &= \{[x(t) - \mu_x] + \mu_x\}^2 + \tilde{x}^2(t) \\ &= [x(t) - \mu_x]^2 + \tilde{x}^2(t) + 2\mu_x[x(t) - \mu_x] + \mu_x^2 \\ &= u(t) + 2\mu_x[x(t) - \mu_x] + \mu_x^2 \end{aligned} \quad (3.76)$$

The last term μ_x^2 produces an effect in the spectrum of $w(t)$ only at $f = 0$. For $f \neq 0$, Equation 3.76 consists of a nonlinear square-law envelope detector in parallel with a linear operation $2\mu_x$ as shown in Figure 3.4. Note that Figure 3.4 simplifies to the square-law envelope detector by itself when $\mu_x = 0$.

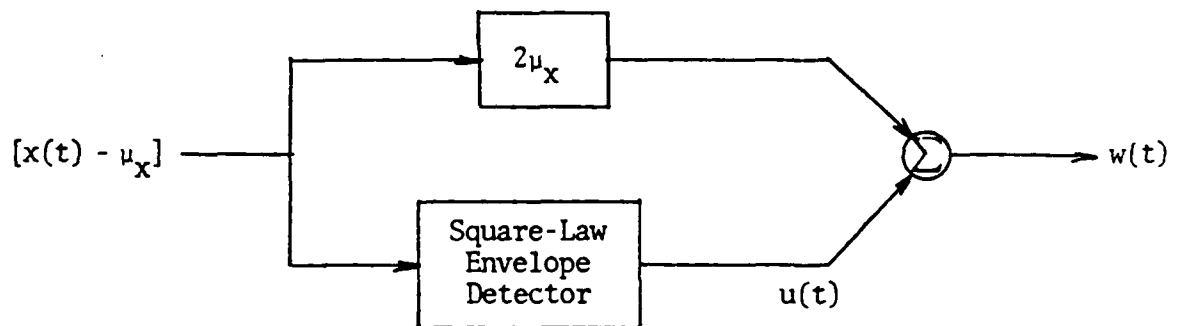
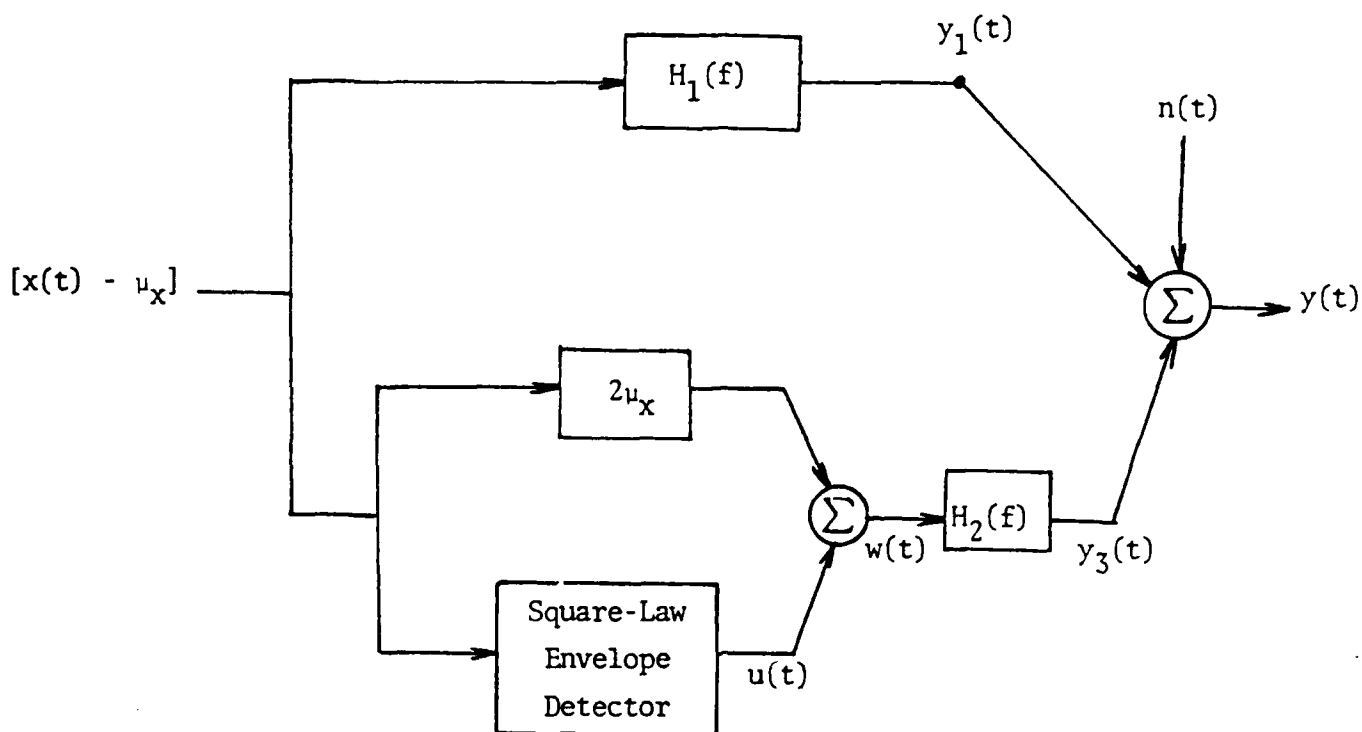


Figure 3.4 Nonlinear system when $\mu_x \neq 0$.

Return now to the original problem covered by Figure 3.2. For situations where the input changes to $[x(t) - \mu_x]$ with $\mu_x \neq 0$, Figure 3.2 becomes the new extended Figure 3.5. In Figure 3.5, the two outputs $y_1(t)$ and $y_3(t)$ will be correlated because of the linear operation in the nonlinear path.



3.5 Nonlinear drift force model when $u_x \neq 0$.

The optimum linear system $H_o(f)$ in Figure 3.5 is computed as before by the equation

$$H_o(f) = \frac{G_{xy}(f)}{G_{xx}(f)} = H_1(f) + 2u_x H_2(f) \quad (3.77)$$

Note that $H_o(f)$ is now a function of both $H_1(f)$ and $H_2(f)$. Figure 3.5 should now be revised so that $H_1(f)$ is replaced by $H_o(f)$ to produce a new output $y_4(t)$ in place of $y_1(t)$. The output $y_3(t)$ in Figure 3.5 will then become the previous output $y_2(t)$ in Figure 3.2 and will preserve the sum

$$y_1(t) + y_3(t) = y_4(t) + y_2(t) \quad (3.78)$$

This will give Figure 3.6 where the two outputs $y_4(t)$ and $y_2(t)$ will be uncorrelated because of the properties of $H_0(f)$ and the Gaussian nature of the input $[x(t) - \mu_x]$.

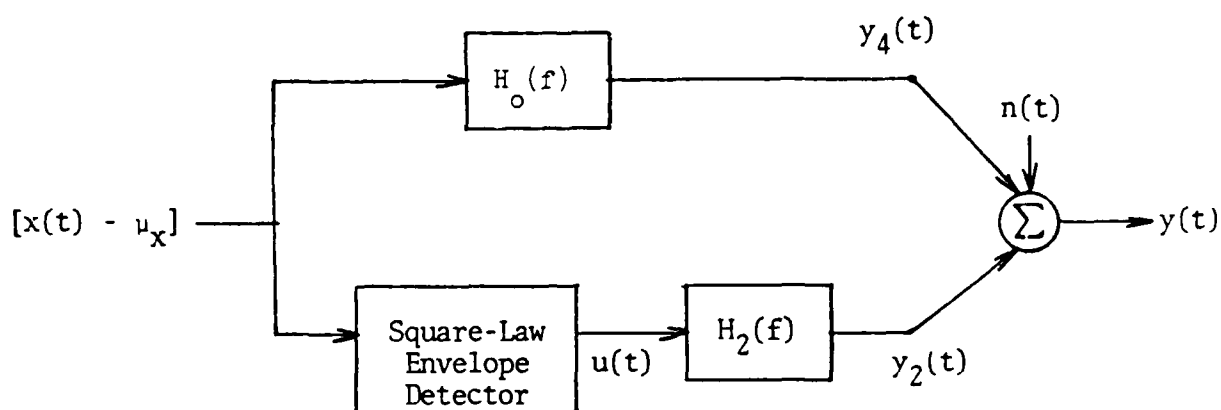


Figure 3.6 Equivalent model to Figure 3.5.

The following Fourier transform relations are satisfied by the quantities shown in Figure 3.5 and 3.6. Various applications are feasible depending upon what is known and what can be measured.

$$X(f) = \mathcal{F}[x(t) - \mu_x] \quad (3.79)$$

$$U(f) = \mathcal{F}[u(t) - \mu_u] \quad (3.80)$$

$$W(f) = \mathcal{F}[w(t) - \mu_w] \quad (3.81)$$

$$Y(f) = \mathcal{F}[y(t) - \mu_y] \quad (3.82)$$

Also, for $f \neq 0$,

$$W(f) = U(f) + 2\mu_x X(f) \quad (3.83)$$

$$Y_1(f) = \mathcal{F}[y_1(t) - \mu_{y_1}] = H_1(f)X(f) \quad (3.84)$$

$$Y_2(f) = \mathcal{F}[y_2(t) - \mu_{y_2}] = H_2(f)U(f) \quad (3.85)$$

$$Y_3(f) = \mathcal{F}[y_3(t) - \mu_{y_3}] = H_2(f)W(f) \quad (3.86)$$

$$Y_4(f) = \mathcal{F}[y_4(t) - \mu_{y_4}] = H_o(f)X(f) \quad (3.87)$$

where $H_o(f)$ is given by Equation 3.77. The output term

$$Y(f) = Y_4(f) + Y_2(f) + N(f) \quad (3.88)$$

From Equation 3.88, the output autospectral density function is

$$G_{yy}(f) = G_{y_4y_4}(f) + G_{y_2y_2}(f) + G_{nn}(f) \quad (3.89)$$

where

$$G_{y_4y_4}(f) = |H_o(f)|^2 G_{xx}(f) \quad (3.90)$$

$$G_{y_2y_2}(f) = |H_2(f)|^2 G_{uu}(f) \quad (3.91)$$

$$G_{nn}(f) = \text{autospectrum of unmeasured extraneous output noise}$$

From knowledge of $H_1(f)$, $H_2(f)$ and $x(t)$, one can compute $H_o(f)$, $G_{xx}(f)$ and $G_{uu}(f)$ so as to be able to predict $G_{y_4y_4}(f)$ and $G_{y_2y_2}(f)$. When $G_{nn}(f) = 0$, this will predict the total output spectrum $G_{yy}(f)$.

To identify the optimum system properties of $H_o(f)$, $H_1(f)$ and $H_2(f)$ from measured input/output data, the appropriate equations to use are

$$G_{xy}(f) = H_o(f)G_{xx}(f) \quad (3.92)$$

$$G_{uy}(f) = H_2(f)G_{uu}(f) \quad (3.93)$$

As in Section 3.5, from measurements of $x(t)$ and $y(t)$, one can compute the spectral quantities shown in Equations 3.92 and 3.93. This gives

$$H_o(f) = \frac{G_{xy}(f)}{G_{xx}(f)} \quad (3.94)$$

$$H_2(f) = \frac{G_{uy}(f)}{G_{uu}(f)} \quad (3.95)$$

Then, from Equation 3.77

$$H_1(f) = H_o(f) - 2\mu_x H_2(f) \quad (3.96)$$

Other spectral relations of possible interest for special applications when $\mu_x \neq 0$ are

$$G_{y_1 y_1}(f) = |H_1(f)|^2 G_{xx}(f) \quad (3.97)$$

$$G_{y_3 y_3}(f) = |H_2(f)|^2 G_{ww}(f) \quad (3.98)$$

$$G_{ww}(f) = G_{uu}(f) + 4\mu_x^2 G_{xx}(f) \quad (3.99)$$

$$G_{y_1 y_3}(f) = 2\mu_x H_1^*(f) H_2(f) G_{xx}(f) \quad (3.100)$$

$$G_{y_2 y_4}(f) = 0 \quad (3.101)$$

This completes the analysis for nonzero mean value inputs.

3.7 STATISTICAL ERRORS IN ESTIMATES

Return back to Figure 3.2 and the equations in Sections 3.4 and 3.5. For this error analysis, replace Figure 3.2 by a two-input/single-output linear model with uncorrelated inputs $x(t)$ and $u(t)$ as shown in Figure 3.7.

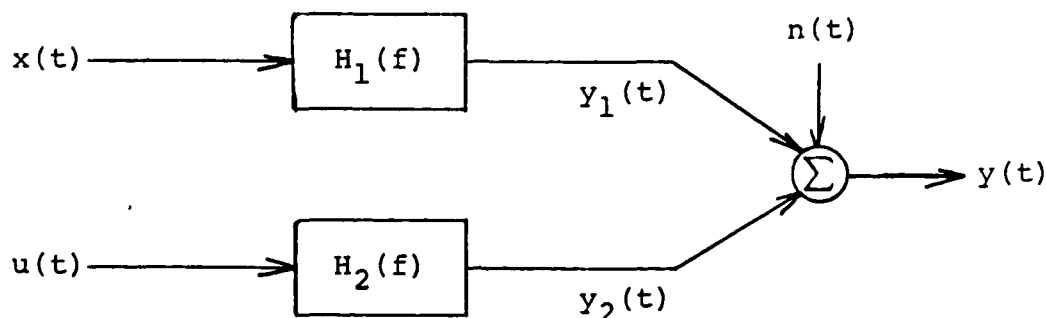


Figure 3.7 Two-input/single-output linear model for Figure 3.2.

Statistical random error formulas will now be stated for estimates of the following six quantities. These formulas are derived in Reference [3] and summarized in Reference [4].

- (1) $\hat{G}_{y_1 y_1}(f)$ computed by Equation 3.47
- (2) $\hat{G}_{y_2 y_2}(f)$ computed by Equation 3.48
- (3) $\hat{\gamma}_{xy}^2(f)$ computed by Equation 3.59
- (4) $\hat{q}_{xy}^2(f)$ computed by Equation 3.60
- (5) $\hat{H}_1(f)$ computed by Equation 3.67
- (6) $\hat{H}_2(f)$ computed by Equation 3.71

The normalized random errors for the two output spectra estimates $\hat{G}_{Y_1Y_1}(f)$ and $\hat{G}_{Y_2Y_2}(f)$ are approximated by

$$\epsilon[\hat{G}_{Y_1Y_1}(f)] \approx \frac{[2 - \hat{\gamma}_{xy}^2(f)]^{1/2}}{|\hat{\gamma}_{xy}(f)| \sqrt{n_d}} \quad (3.102)$$

$$\epsilon[\hat{G}_{Y_2Y_2}(f)] \approx \frac{[2 - \hat{q}_{xy}^2(f)]^{1/2}}{|\hat{q}_{xy}(f)| \sqrt{n_d - 1}} \quad (3.103)$$

where n_d is the number of independent averages used to compute the original spectral density quantities. Required values of n_d to achieve desired values of $\epsilon[\hat{G}_{Y_1Y_1}(f)]$ or $\epsilon[\hat{G}_{Y_2Y_2}(f)]$ are obtained by solving Equations (73) and (74) for n_d .

The normalized random errors for the two coherence function estimates $\hat{\gamma}_{xy}^2(f)$ and $\hat{c}_{xy}^2(f)$ are approximated by

$$\epsilon[\hat{\gamma}_{xy}^2(f)] \approx \frac{\sqrt{2} [1 - \hat{\gamma}_{xy}^2(f)]}{|\hat{\gamma}_{xy}(f)| \sqrt{n_d}} \quad (3.104)$$

$$\epsilon[\hat{c}_{xy}^2(f)] \approx \frac{\sqrt{2} [1 - \hat{q}_{xy}^2(f)]}{|\hat{q}_{xy}(f)| \sqrt{n_d - 1}} \quad (3.105)$$

Bias errors for these estimates are

$$b[\hat{\gamma}_{xy}^2(f)] \approx \frac{[1 - \hat{\gamma}_{xy}^2(f)]^2}{\sqrt{n_d}} \quad (3.106)$$

$$b[\hat{q}_{xy}(f)] \approx \frac{[1 - \hat{q}_{xy}^2(f)]^2}{\sqrt{n_d} - 1} \quad (3.107)$$

These bias errors are over and above the random errors.

Normalized random errors for the frequency response function estimates $\hat{H}_1(f)$ and $\hat{H}_2(f)$ are required for both gain factor estimates and phase factor estimates. For gain factor estimates $|\hat{H}_1(f)|$ and $|\hat{H}_2(f)|$, the normalized random errors are approximated by

$$\epsilon[|\hat{H}_1(f)|] \approx \frac{[1 - \hat{\gamma}_{xy}^2(f)]^{1/2}}{|\hat{\gamma}_{xy}(f)| \sqrt{2n_d}} \quad (3.108)$$

$$\epsilon[|\hat{H}_2(f)|] \approx \frac{[1 - \hat{q}_{xy}^2(f)]^{1/2}}{|\hat{q}_{xy}(f)| \sqrt{2(n_d - 1)}} \quad (3.109)$$

The standard deviations (in radians) of the two associated phase factor estimates $\hat{\phi}_1(f)$ and $\hat{\phi}_2(f)$ (in radians) are approximated by

$$\sigma[\hat{\phi}_1(f)] \approx \sin^{-1} \left\{ \epsilon[|\hat{H}_1(f)|] \right\} \quad (3.110)$$

$$\sigma[\hat{\phi}_2(f)] \approx \sin^{-1} \left\{ \epsilon[|\hat{H}_2(f)|] \right\} \quad (3.111)$$

For small values of $\epsilon[|\hat{H}_1(f)|]$ and $\epsilon[|\hat{H}_2(f)|]$, Equations 3.110 and 3.111 can be further simplified to

$$\sigma[\hat{\phi}_1(f)] \approx \epsilon[|\hat{H}_1(f)|] \quad (3.112)$$

$$\sigma[\hat{\phi}_2(f)] \approx \epsilon[|\hat{H}_2(f)|] \quad (3.113)$$

Various bias error in frequency response function estimates are discussed also in Reference [3] that should be minimized as much as possible in practice.

3.8 DERIVATIONS OF THEORETICAL FORMULAS

To make this report more self-contained, some special theoretical formulas are derived here that supplement material discussed in earlier sections. These formulas deal with quantities $G_{uu}(f)$, $G_{uy}(f)$ and $H_2(f)$ that are involved in the nonlinear drift force models of Figures 3.2 and 3.6. Readers not interested in these matters should proceed to Section 4.

3.8.1 Theoretical Formula for $G_{uu}(f)$

A useful theoretical formula will now be derived to determine $G_{uu}(f)$ from knowledge of $G_{xx}(f)$. From Equation 3.24,

$$u(f) = \int_{-\infty}^{\infty} [X(\alpha)X(f - \alpha) + \tilde{X}(\alpha)\tilde{X}(f - \alpha)]d\alpha \quad (3.114)$$

$$u^*(f) = \int_{-\infty}^{\infty} [X^*(\beta)X^*(f - \beta) + \tilde{X}^*(\beta)\tilde{X}^*(f - \beta)]d\beta \quad (3.115)$$

The two-sided autospectral density function $S_{uu}(f)$ of $u(t)$ is defined by

$$\begin{aligned} S_{uu}(f) &= \frac{1}{T} E[u^*(f)u(f)] \\ &= \frac{1}{T} \int_{-\infty}^{\infty} \int_{-\infty}^{\infty} E[\{X^*(\beta)X^*(f - \beta) + X^*(\beta)X^*(f - \beta)\}\{X(\alpha)X(f - \alpha) \\ &\quad + X(\beta)X(f - \beta)\}]d\alpha d\beta \end{aligned} \quad (3.116)$$

In Equation 3.116 the integrand involves a total of four different fourth-order moments of Gaussian data that breaks down into products of pairs of second-order moments. A typical fourth-order moment can be replaced by the three product pairs

$$\begin{aligned} E[X^*(\beta)X^*(f - \beta)X(\alpha)X(f - \alpha)] &= E[X^*(\beta)X^*(f - \beta)]E[X(\alpha)X(f - \alpha)] \\ &+ E[X^*(\beta)X(\alpha)]E[X^*(f - \beta)X(f - \alpha)] + E[X^*(\beta)X(f - \alpha)]E[X^*(f - \beta)X(\alpha)] \end{aligned} \quad (3.117)$$

The first pair of second-order moments in Equation 3.117 are given by

$$E[X^*(\beta)X^*(f - \beta)] = S_{xx}(\beta)\delta_1(f) \quad (3.118)$$

$$E[X(\alpha)X(f - \alpha)] = S_{xx}(\alpha)\delta_1(f) \quad (3.119)$$

where $S_{xx}(\alpha)$ and $S_{xx}(\beta)$ are two-sided autospectral density functions of $x(t)$ and where $\delta_1(f)$ is the finite delta function defined by

$$\begin{aligned} \delta_1(f) &= \delta_1(-f) = T & (-1/2T) \leq f \leq (1/2T) \\ &= 0 & \text{otherwise} \end{aligned} \quad (3.120)$$

$$\int_{-\infty}^{\infty} \delta_1(f) df = \int_{(-1/2T)}^{(1/2T)} \delta_1(f) df = 1 \quad (3.121)$$

The first pair gives a contribution to $S_{uu}(f)$ of Equation 3.116 only at $f = 0$ since

$$\frac{1}{T} \int_{-\infty}^{\infty} \int S_{xx}(\alpha) S_{xx}(\beta) \sigma_1^2(f) d\alpha d\beta = \sigma_x^4 \delta_1(f) \quad (3.122)$$

Here

$$\sigma_x^2 = \int_{-\infty}^{\infty} S_{xx}(\alpha) d\alpha = \int_{-\infty}^{\infty} S_{xx}(\beta) d\beta \quad (3.123)$$

The second pair of second-order moments in Equation 3.117 are given by

$$E[X^*(\beta)X(\alpha)] = S_{xx}(\beta)\delta_1(\alpha - \beta) \quad (3.124)$$

$$E[X^*(f - \beta)X(f - \alpha)] = S_{xx}(f - \beta)\delta_1(\alpha - \beta) \quad (3.125)$$

This second pair gives a contribution to $S_{uu}(f)$ of Equation 3.116 represented by

$$\frac{1}{T} \int_{-\infty}^{\infty} \int S_{xx}(\beta) S_{xx}(f - \beta) \delta_1^2(\alpha - \beta) d\beta d\alpha = \int_{-\infty}^{\infty} S_{xx}(\alpha) S_{xx}(f - \alpha) d\alpha \quad (3.126)$$

The third-pair of second-order moments in Equation 3.117 are given by

$$E[X^*(f)X(f - \alpha)] = S_{xx}(\beta)\delta_1(f - \alpha - \beta) \quad (3.127)$$

$$E[X^*(f - \beta)X(\alpha)] = S_{xx}(f - \beta)\delta_1(f - \alpha - \beta) \quad (3.128)$$

This third pair gives a contribution to $S_{uu}(f)$ of Equation 3.116 represented by

$$\frac{1}{T} \int_{-\infty}^{\infty} \int S_{xx}(\beta) S_{xx}(f - \beta) \delta_1^2(f - \alpha - \beta) d\beta d\alpha = \int_{-\infty}^{\infty} S_{xx}(f - \alpha) S_{xx}(\alpha) d\alpha \quad (3.129)$$

Equation 3.129 is exactly the same as Equation 3.126.

Equations 3.117 to 3.129 prove for $f \neq 0$ that

$$\frac{1}{T} \int_{-\infty}^{\infty} \int E[X^*(\beta)X^*(f - \beta)X(\alpha)X(f - \alpha)] d\alpha d\beta = 2 \int_{-\infty}^{\infty} S_{xx}(\alpha) S_{xx}(f - \alpha) d\alpha \quad (3.130)$$

Similarly, one can prove for $f \neq 0$ that the other fourth-order moments in Equation 3.116 lead to the results

$$\frac{1}{T} \int_{-\infty}^{\infty} \int E[\tilde{X}^*(\beta)\tilde{X}^*(f - \beta)\tilde{X}(\alpha)\tilde{X}(f - \alpha)] d\beta d\alpha = 2 \int_{-\infty}^{\infty} S_{xx}(\alpha) S_{xx}(f - \alpha) d\alpha \quad (3.131)$$

$$\frac{1}{T} \int_{-\infty}^{\infty} \int E[X^*(\beta)X^*(f - \beta)\tilde{X}(\alpha)\tilde{X}(f - \alpha)] d\beta d\alpha = 2 \int_{-\infty}^{\infty} \tilde{S}_{xx}(\alpha) \tilde{S}_{xx}(f - \alpha) d\alpha \quad (3.132)$$

$$\frac{1}{T} \int_{-\infty}^{\infty} E[\tilde{X}^*(\beta) \tilde{X}^*(f - \beta) X(\alpha) X(f - \alpha)] d\beta d\alpha = 2 \int \tilde{S}_{xx}(\alpha) \tilde{S}_{xx}(f - \alpha) d\alpha \quad (3.133)$$

The derivation of Equations 3.131 to 3.133 requires formulas from Table 13.2 of Reference [2]. In particular

$$\tilde{S}_{xx}(\alpha) = S_{\tilde{xx}}(\alpha) = -S_{\tilde{xx}}(\alpha) \quad (3.134)$$

where $\tilde{S}_{xx}(\alpha)$ is the Fourier transform of $\tilde{R}_{xx}(\tau)$, and $\tilde{R}_{xx}(\tau)$ is the Hilbert transform of the autocorrelation function $R_{xx}(\tau)$. Hence

$$\tilde{S}_{xx}(\alpha) = B(\alpha) S_{xx}(\alpha) \quad (3.135)$$

where $B(\alpha)$ satisfies Equation 3.29.

Substitution of Equation 3.117 into Equation 3.116 followed by substitutions from Equations 3.130 to 3.133 now proves the theoretical formulas that for any $f \neq 0$,

$$S_{uu}(f) = 4 \int_{-\infty}^{\infty} [S_{xx}(\alpha) S_{xx}(f - \alpha) + \tilde{S}_{xx}(\alpha) \tilde{S}_{xx}(f - \alpha)] d\alpha \quad (3.136)$$

$$S_{uu}(f) = 4 \int_{-\infty}^{\infty} [1 + B(\alpha) B(f - \alpha)] S_{xx}(\alpha) S_{xx}(f - \alpha) d\alpha \quad (3.137)$$

These formulas show how to compute $S_{uu}(f)$ from knowledge of $S_{xx}(f)$.

The one-sided autospectral density functions $G_{uu}(f)$ and $G_{xx}(f)$ are related to the two-sided autospectral density functions $S_{uu}(f)$ and $S_{xx}(f)$ by

$$G_{uu}(f) = \begin{cases} 2S_{uu}(f) & f \geq 0 \\ 0 & f < 0 \end{cases} \quad (3.138)$$

$$G_{xx}(f) = \begin{cases} 2S_{xx}(f) & f \geq 0 \\ 0 & f < 0 \end{cases} \quad (3.139)$$

Also

$$S_{uu}(f) = S_{uu}(-f) = \frac{1}{2} G_{uu}(f) \quad (3.140)$$

$$S_{xx}(f) = S_{xx}(-f) = \frac{1}{2} S_{uu}(f) \quad (3.141)$$

Consider any value of $f > 0$ and apply Equation 3.31 to Equation 3.137. Now

$$S_{uu}(f) = 8 \int_{-\infty}^0 S_{xx}(\alpha) S_{xx}(f - \alpha) d\alpha + 8 \int_f^{\infty} S_{xx}(\alpha) S_{xx}(f - \alpha) d\alpha \quad (3.142)$$

This is the same as

$$S_{uu}(f) = 8 \int_0^{\infty} S_{xx}(-\beta) S_{xx}(f + \beta) d\beta + 8 \int_f^{\infty} S_{xx}(\alpha) S_{xx}(f - \alpha) d\alpha \quad (3.143)$$

by letting $\beta = -\alpha$ and $d\beta = -d\alpha$. Replacing β by α again and using the fact that $S_{xx}(-\alpha) = S_{xx}(\alpha)$, $S_{xx}(f - \alpha) = S_{xx}(\alpha - f)$,

$$S_{uu}(f) = 8 \int_0^{\infty} S_{xx}(\alpha) S_{xx}(f + \alpha) d\alpha + 8 \int_f^{\infty} S_{xx}(\alpha) S_{xx}(\alpha - f) d\alpha \quad (3.144)$$

For any $f > 0$, one now has the equivalent formula in terms of one-sided autospectral density functions

$$G_{uu}(f) = 4 \int_0^{\infty} G_{xx}(\alpha) G_{xx}(f + \alpha) d\alpha + 4 \int_f^{\infty} G_{xx}(\alpha) G_{xx}(\alpha - f) d\alpha \quad (3.145)$$

Equation 3.145 shows how to compute $G_{uu}(f)$ from knowledge of $G_{xx}(f)$.

3.8.2 Theoretical Formula for $G_{uy}(f)$

Another theoretical formula of interest is the cross-spectral density function between $u(t)$ and $y(t)$. The two-sided cross-spectral density function $S_{uy}(f)$ is defined by

$$S_{uy}(f) = \frac{1}{T} E[U^*(f)Y(f)] \quad (3.146)$$

where $U(f)$ and $Y(f)$ satisfy Equations 3.27 and 3.39, respectively. Hence

$$S_{uy}(f) = \frac{1}{T} \int_{-\infty}^{\infty} [1 + B^*(\alpha)B^*(f - \alpha)] E[X^*(\alpha)X^*(f - \alpha)Y(f)] d\alpha \quad (3.147)$$

For all values of α and f , one can verify that the product quantity

$$B^*(\alpha)B^*(f - \alpha) = B(\alpha)B(f - \alpha) \quad (3.148)$$

The two-sided cross-bispectrum (also called the second-order cross-spectral density function) between $x(t)$ and $y(t)$ is defined for all possible f and g by the two-dimensional function

$$S_{xxy}(f, g) = \frac{1}{T} E[X^*(f)X^*(g)Y(f + g)] \quad (3.149)$$

As a special case, when $f = \alpha$ and $g = (f - \alpha)$, one can compute

$$S_{xxy}(\alpha, f - \alpha) = \frac{1}{T} E[X^*(\alpha)X^*(f - \alpha)Y(f)] \quad (3.150)$$

This result will not be zero for the $Y(f)$ of Equation 3.39. Substitution of Equations 3.148 and 3.150 into Equation 3.147 yields the formula

$$S_{uy}(f) = \int_{-\infty}^{\infty} [1 + B(\alpha)B(f - \alpha)] S_{xxy}(\alpha, f - \alpha) d\alpha \quad (3.151)$$

This formula shows how to compute $S_{uy}(f)$ from knowledge of $S_{xxy}(\alpha, f - \alpha)$.

The one-sided cross-spectral density function $G_{uy}(f)$ is related to the two-sided cross-spectral density function $S_{uy}(f)$ by

$$G_{uy}(f) = \begin{cases} 2S_{uy}(f) & f \geq 0 \\ 0 & f < 0 \end{cases} \quad (3.152)$$

Define the one-sided cross-bispectrum $G_{xxy}(\alpha, f - \alpha)$ by

$$G_{xxy}(\alpha, f - \alpha) = \begin{cases} 2S_{xxy}(\alpha, f - \alpha) & f \geq 0 \\ 0 & f < 0 \end{cases} \quad (3.153)$$

Now, for any $f > 0$, Equation 3.151 becomes

$$G_{uy}(f) = \int_{-\infty}^{\infty} [1 + B(\alpha)B(f - \alpha)] G_{xxy}(\alpha, f - \alpha) d\alpha \quad (3.154)$$

Applying Equation 3.31 to Equation 3.154 yields

$$G_{uy}(f) = 2 \int_{-\infty}^0 G_{xxy}(\alpha, f - \alpha) d\alpha + 2 \int_f^{\infty} G_{xxy}(\alpha, f - \alpha) d\alpha \quad (3.155)$$

Also

$$G_{uy}(f) = 2 \int_0^{\infty} G_{xxy}(-\alpha, f + \alpha) d\alpha + 2 \int_f^{\infty} G_{xxy}(\alpha, f - \alpha) d\alpha \quad (3.156)$$

The cross-bispectrum functions in Equations 3.155 and 3.156 can be determined for any $f > 0$ by the computations

$$G_{xxy}(-\alpha, f + \alpha) = \frac{2}{T} E[X^*(-\alpha)X^*(f + \alpha)Y(f)] = \frac{2}{T} E[X(\alpha)X^*(f + \alpha)Y(f)] \quad (3.157)$$

$$G_{xxy}(\alpha, f - \alpha) = \frac{2}{T} E[X^*(\alpha)X^*(f - \alpha)Y(f)] = \frac{2}{T} E[X^*(\alpha)X(\alpha - f)Y(f)] \quad (3.158)$$

Equations 3.154 to 3.158 show appropriate ways to compute $G_{uy}(f)$ from knowledge of $G_{xxy}(\alpha, f - \alpha)$.

3.8.3 Identification of $H_2(f)$

A different new theoretical way to identify $H_2(f)$ is also possible from measured $x(t)$ and $y(t)$ by using Equation 3.68 together with Equations 3.137 and 3.151. In terms of two-sided spectral density functions, Equation 3.68 is

$$S_{uy}(f) = H_2(f)S_{uu}(f) \quad (3.159)$$

Substitution from Equation 3.137 now gives

$$S_{uy}(f) = 4H_2(f) \int_{-\infty}^{\infty} [1 + B(\alpha)B(f - \alpha)] S_{xx}(\alpha) S_{xx}(f - \alpha) d\alpha \quad (3.160)$$

However, Equation 3.151 states that

$$S_{uy}(f) = \int_{-\infty}^{\infty} [1 + B(\alpha)B(f - \alpha)] S_{xxy}(\alpha, f - \alpha) d\alpha \quad (3.161)$$

Hence, one obtains the useful relation

$$S_{xxy}(\alpha, f - \alpha) = 4H_2(f) S_{xx}(\alpha) S_{xx}(f - \alpha) \quad (3.162)$$

This provides an alternate way to estimate $H_2(f)$ from computation of the other quantities. Consider a change in variables where $\alpha = g$ and $f = 2g$. Then $(f - \alpha) = g$ and Equation 3.162 becomes

$$S_{xxy}(g, g) = 4H_2(2g) S_{xx}^2(g) \quad (3.163)$$

This is the same as

$$S_{xxy}(f, f) = 4H_2(2f)S_{xx}^2(f) \quad (3.164)$$

Thus $H_2(2f)$ satisfies here the simple relation

$$H_2(2f) = \frac{S_{xxy}(f, f)}{4S_{xx}^2(f)} \quad (3.165)$$

where

$$S_{xx}(f) = \frac{1}{T} E[X^*(f)X(f)] \quad (3.166)$$

$$S_{xxy}(f, f) = \frac{1}{T} E[X^*(f)X^*(f)Y(2f)] \quad (3.167)$$

with $Y(2f)$ given by Equation . Finally, Equation proves that

$$H_2(f) = \frac{S_{xxy}(f/2, f/2)}{4S_{xx}^2(f/2)} \quad (3.168)$$

This concludes Section 3.

4. NONLINEAR NONSYMMETRICAL SYSTEMS

Section 4 develops various input/output relationships when random data passes through three types of nonlinear nonsymmetrical systems: (A) Three-Slope Systems, (B) Catenary Systems and (C) Smooth-Limiter Systems. Included are formulas for input/output probability density functions, correlation functions and spectral density functions. These particular nonlinear nonsymmetrical systems are of interest for NCEL applications. Spectral formulas are stated here using two-sided spectral density functions.

4.1 THREE-SLOPE SYSTEMS

A first example of a nonlinear nonsymmetrical system is a three-slope system as sketched in Figure 4.1. Let

$$\begin{aligned}
 y = g(x) &= x & -A \leq x \leq B \\
 &= -A + a(x + A) & x \leq -A \\
 &= B + b(x - B) & x \geq B
 \end{aligned} \tag{4.1}$$

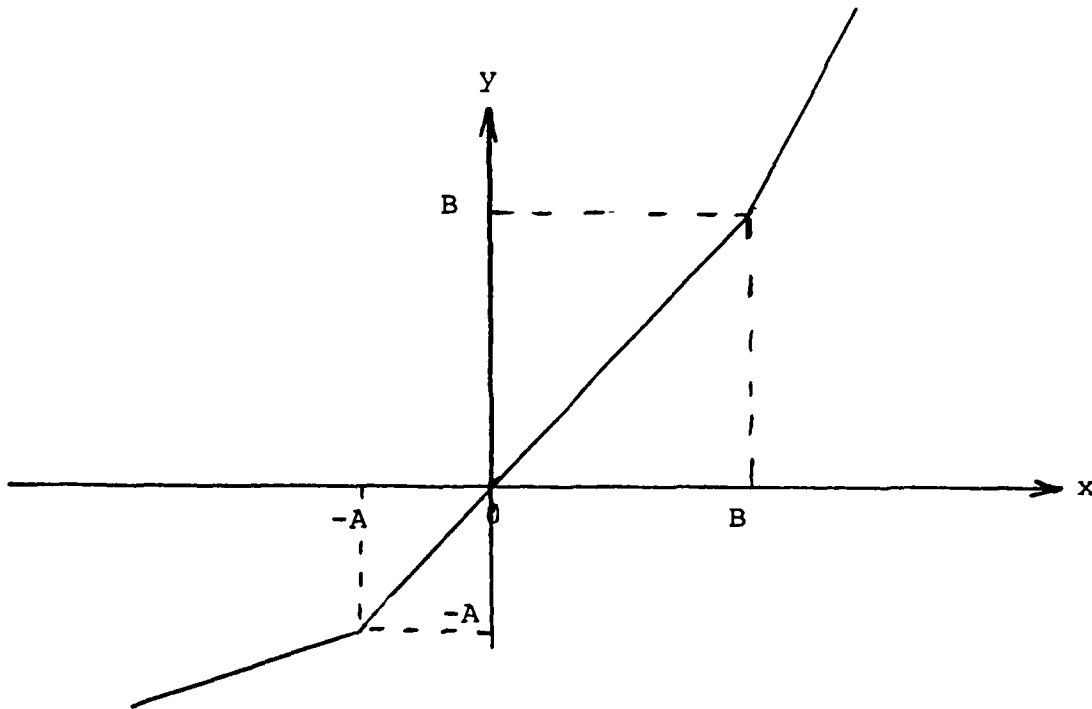


Figure 4.1 Three-slope system.

For definiteness, assume here that the constants

$$0 < A < B, \quad 0 < a < 1, \quad b > 1 \quad (4.2)$$

The inverse relations are

$$\begin{aligned} x = g^{-1}(y) &= y & -A \leq y \leq B \\ &= -A + [(y + A)/a] & y \leq -A \\ &= B + [(y - B)/b] & y \geq B \end{aligned} \quad (4.3)$$

The derivative relations are

$$\begin{aligned} \frac{dy}{dx} = g'(x) &= 1 & -A \leq x \leq B \\ &= a & x < -A \\ &= b & x > B \end{aligned} \quad (4.4)$$

Thus the derivative is discontinuous at $x = -A$ and at $x = B$.

Let $p(x)$ be the input probability density function and $p_2(y)$ be the output probability density function. For this problem, from Equation 1.5,

$$p_2(y) = \frac{p(x)}{|dy/dx|} \quad (4.5)$$

where x on the right-hand side should be replaced by its equivalent y from $x = g^{-1}(y)$. Thus

$$\begin{aligned}
 p_2(y) &= p(x) = p(y) & -A \leq y \leq B \\
 &= \frac{p(-A + [(y+A)/a])}{a} & y < -A \\
 &= \frac{p(B + [(y-B)/b])}{b} & y > B
 \end{aligned} \tag{4.6}$$

Assume the input probability density function $p(x)$ is Gaussian as sketched in Figure 4.2 with $u_x = 0$ and $\sigma_x = 1$.

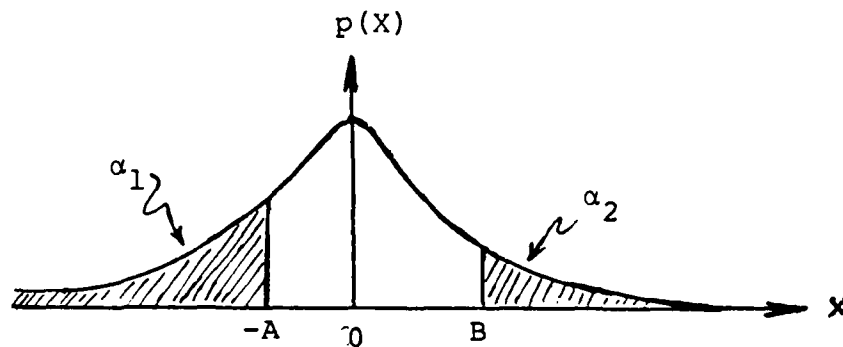


Figure 4.2 Gaussian input PDF.

Here

$$p(x) = \frac{1}{\sqrt{2\pi}} \exp(-x^2/2) \tag{4.7}$$

Let

$$\alpha_1 = \int_{-\infty}^{-A} p(x) dx = \text{Prob } [x \leq -A] \quad (4.8)$$

$$\alpha_2 = \int_B^{\infty} p(x) dx = \text{Prob } [x \geq B]$$

When $A < B$, clearly $\alpha_1 > \alpha_2$. Also

$$\text{Prob}[-A \leq x \leq B] = \int_{-A}^B p(x) dx = 1 - \alpha_1 - \alpha_2 \quad (4.9)$$

The quantities α_1 and α_2 represent for the output record

$$\alpha_1 = \int_{-\infty}^{-A} p_2(y) dy = \text{Prob } [y \leq -A] \quad (4.10)$$

$$\alpha_2 = \int_B^{\infty} p_2(y) dy = \text{Prob } [y \geq B]$$

Thus

$$1 - \alpha_1 - \alpha_2 = \int_{-A}^B p_2(y) dy = \text{Prob } [-A \leq y \leq B] \quad (4.11)$$

Note that for $A < B$, one has

$$p(-A) > p(B) \quad (4.12)$$

Consider now the shape of $p_2(y)$. As y approaches the value $-A$ from inside, $[y > -A]$,

$$p_2(-A^+) = p(-A) \quad (4.13)$$

However, as y approaches the value $-A$ from outside, $[y < -A]$,

$$p_2(-A^-) = \frac{p(-A)}{a} \quad (4.14)$$

For an assumed $a < 1$, there results

$$p_2(-A^-) > p_2(-A^+) \quad (4.15)$$

The reverse inequality would be true if $a > 1$.

Similarly, as y approaches the value B from inside, $[y < B]$,

$$p_2(B^-) = p(B) \quad (4.16)$$

while as y approaches the value B from outside $[y > B]$,

$$p_2(B^+) = \frac{p(B)}{b} \quad (4.17)$$

Here, for an assumed $b > 1$, these results

$$p_2(B^+) < p_2(B^-) \quad (4.18)$$

with a reverse inequality if $b < 1$. This treatment shows that the shape of $p_2(y)$ under the assumption that $0 < a < 1, b > 1$, must be as sketched in Figure 4.3. For the assumed values here, observe that $\alpha_1 > \alpha_2$ and

$$p_2(-A^-) > p_2(B^+) \quad (4.19)$$

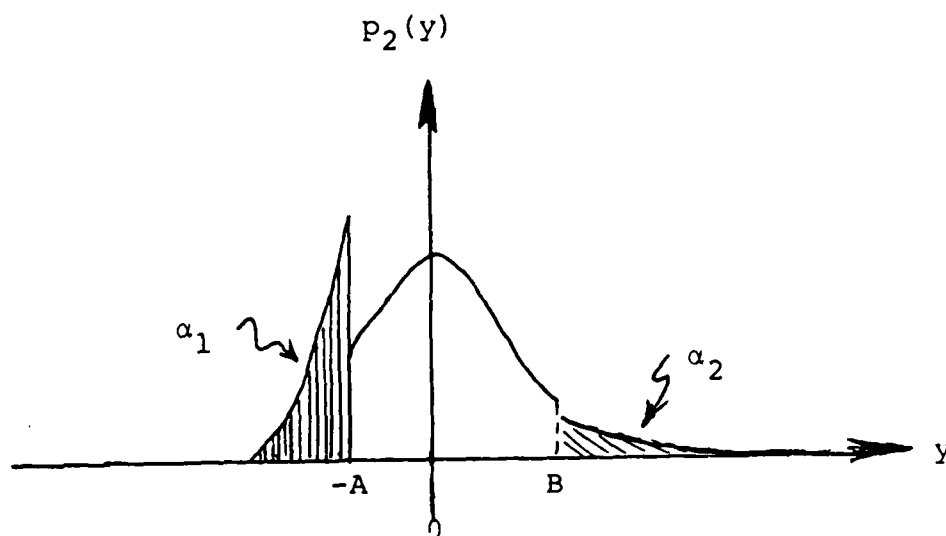


Figure 4.3 Output PDF for three-slope system.

Suppose the three-slope system is hard-limited at $x = -A$ and at $x = B$ such that

$$\begin{aligned} y = g(x) &= x & -A \leq x \leq B \\ &= -A & x \leq -A \\ &= B & x \geq B \end{aligned} \quad (4.20)$$

This nonlinear nonsymmetrical system is sketched in Figure 4.4.

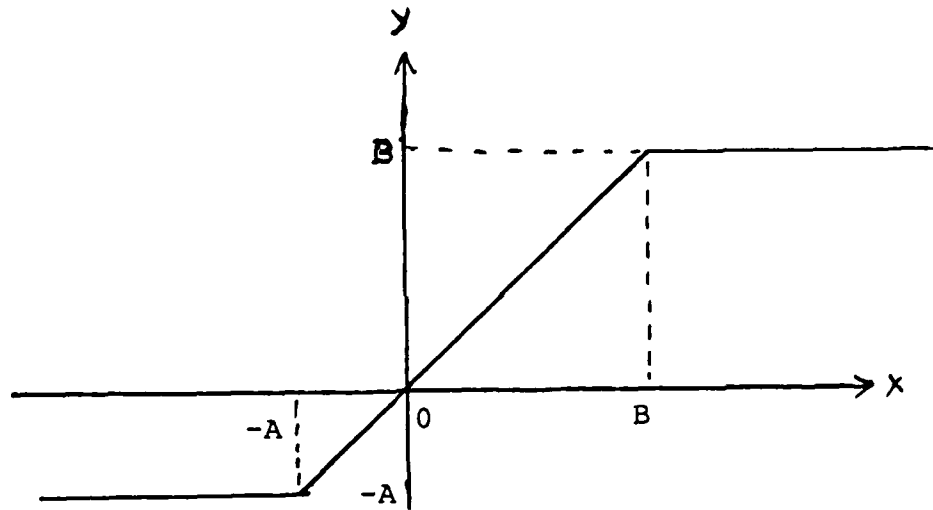


Figure 4.4 Hard-limited three-slope system.

As before, assume the input probability density function is Gaussian with $u_x = 0$ and $\sigma_x = 1$. Now

$$\alpha_1 = \text{Prob}[x \leq -A] = \text{Prob}[y = -A] \quad (4.21)$$

$$\alpha_2 = \text{Prob}[x \geq B] = \text{Prob}[y = B]$$

This gives the output probability density function

$$\begin{aligned}
 p_2(y) &= p(y) & -A \leq y \leq B \\
 &= \alpha_1 \delta(y + A) & y = -A \\
 &= \alpha_2 \delta(y - B) & y = B
 \end{aligned} \tag{4.22}$$

where $\delta(y)$ is the usual delta function. Assuming that $\alpha_1 > \alpha_2$, the shape of $p_2(y)$ is sketched in Figure 4.5.

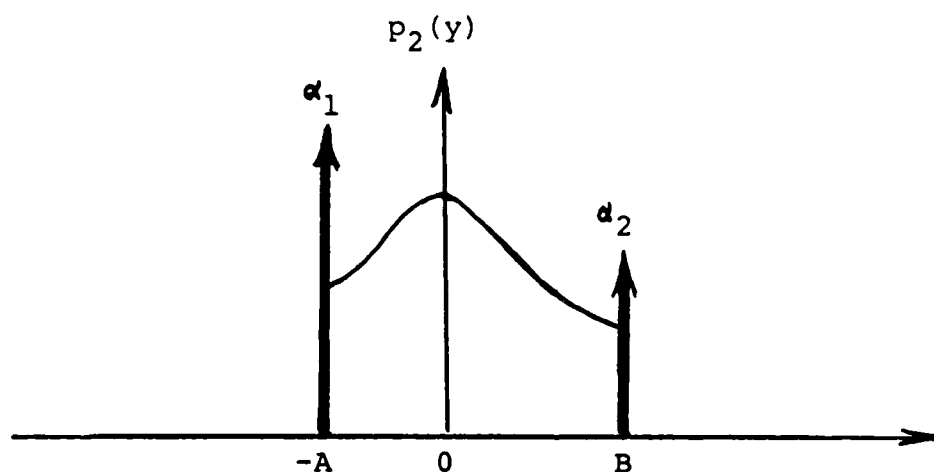


Figure 4.5 Output PDF for hard-limited three-slope system.

4.2 CATENARY SYSTEMS

A second example of a nonlinear nonsymmetrical system is a catenary system as sketched in Figure 4.6. Let

$$\begin{aligned}
 y = g(x) &= -aA^2 & x &\leq -A \\
 &= a(x^2 + 2Ax) & -A &\leq x \leq B \\
 &= a(B^2 + 2AB) & x &\geq B
 \end{aligned} \tag{4.23}$$

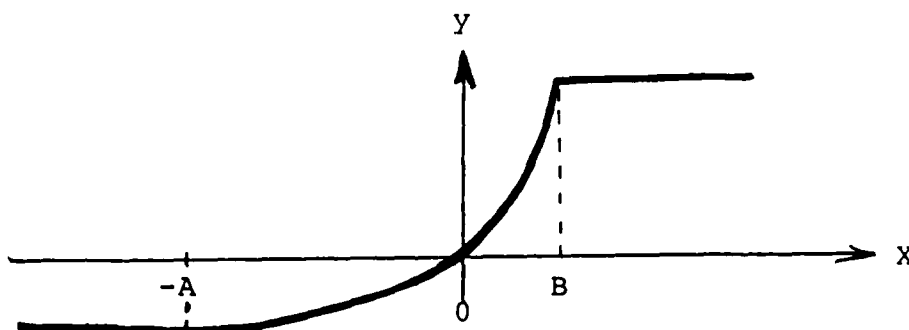


Figure 4.6 Catenary system.

For definiteness, assume here that the constants

$$A > B > 0, \quad a > 0 \tag{4.24}$$

The inverse relations are

$$\begin{aligned}
 x &= g^{-1}(y) = \text{any value of } x \leq -A \\
 &\quad \text{when } y = -aA^2 \\
 &= -A + \sqrt{A^2 + (y/a)}, \quad -aA^2 < y < a(B^2 + 2AB) \quad (4.25) \\
 &= \text{any value of } x \geq B \\
 &\quad \text{when } y = a(B^2 + 2AB)
 \end{aligned}$$

The middle range is obtained by solving the quadratic equation

$$x^2 + 2Ax - (y/a) = 0 \quad (4.26)$$

where only the positive square root operation makes sense. The derivative relations are

$$\begin{aligned}
 \frac{dy}{dx} &= g'(x) = 0 & x &\leq -A \\
 &= 2a(x + A) & -A &\leq x < B \\
 &= 0 & x &> B
 \end{aligned} \quad (4.27)$$

Thus, the derivative is discontinuous at $x = B$.

Let $p(x)$ be the input probability density function and $p_2(y)$ be the output probability density function. For this problem, from Equation 1.5,

$$p_2(y) = \frac{p(x)}{|dy/dx|} \quad (4.28)$$

only in the range where $-A < x < B$, and where the value of x in the right-hand side should be replaced by its equivalent y

from $x = g^{-1}(y)$. Thus, for y in the range $-aA^2 < y < a(B^2 + 2AB)$,

$$p_2(y) = \frac{p(x)}{2a|x+A|} = \frac{p(-A + \sqrt{A^2 + (y/a)})}{2a \sqrt{A^2 + (y/a)}} \quad (4.29)$$

This has the form of a chi-square probability density function when $p(x)$ is assumed to be Gaussian. Different relations are required for $x \leq -A$ and $x \geq B$.

Assume the input probability function $p(x)$ is Gaussian with $\mu_x = 0$ and $\sigma_x = 1$ as sketched in Figure 4.7 where

$$p(x) = \frac{1}{\sqrt{2\pi}} \exp(-x^2/2) \quad (4.30)$$

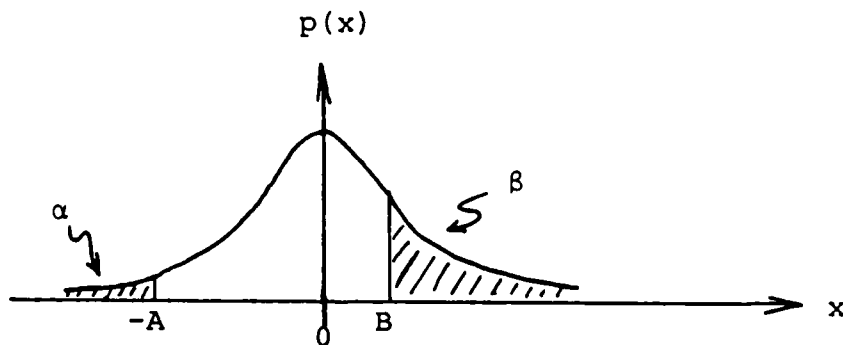


Figure 4.7 Gaussian input PDF.

The assumed values for A and B are such that $A > B > 0$. Let

$$\alpha = \int_{-\infty}^{-A} p(x) dx = \text{Prob } [x \leq -A]$$

$$\beta = \int_B^{\infty} p(x) dx = \text{Prob } [x \geq B]$$
(4.31)

Clearly,

$$\alpha < \beta$$
(4.32)

Also,

$$\text{Prob } [-A \leq x \leq B] = \int_{-A}^B p(x) dx = 1 - \alpha - \beta$$
(4.33)

All of the values of $x \leq -A$ are associated with the single value of y equal to $y = -aA^2$. Hence the output probability density function

$$p_2(y) = \alpha \delta(y + aA^2) \quad \text{at} \quad y = -aA^2$$
(4.34)

where $\delta(y)$ is the usual delta function. This gives

$$\text{Prob } [y = -aA^2] = \alpha$$
(4.35)

Similarly, all the values of $x \geq B$ are associated with the single value of $y = a(B^2 + 2AB)$. Hence the output probability density function

$$p_2(y) = \beta \delta(y - a[B^2 + 2AB]) \quad \text{at} \quad y = a(B^2 + 2AB)$$

where $\delta(y)$ is the usual delta function. This gives

$$\text{Prob} [y = a(B^2 + 2AB)] = \beta$$

There is zero probability here that $y < -aA^2$ or that $y > a(B^2 + 2AB)$. The probability that y falls inside these two bounds is

$$\text{Prob} [-aA^2 < y < a(B^2 + 2AB)] = 1 - \alpha - \beta$$

A typical shape for $p_2(y)$ is sketched in Figure 4.8.

Observe that $p_2(y)$ approaches infinity as y approaches the value $-aA^2$ from inside $[y > -aA^2]$, but $p_2(y)$ stays finite as y approaches the value $a(B^2 + 2AB)$ from inside, $[y < a(B^2 + 2AB)]$.

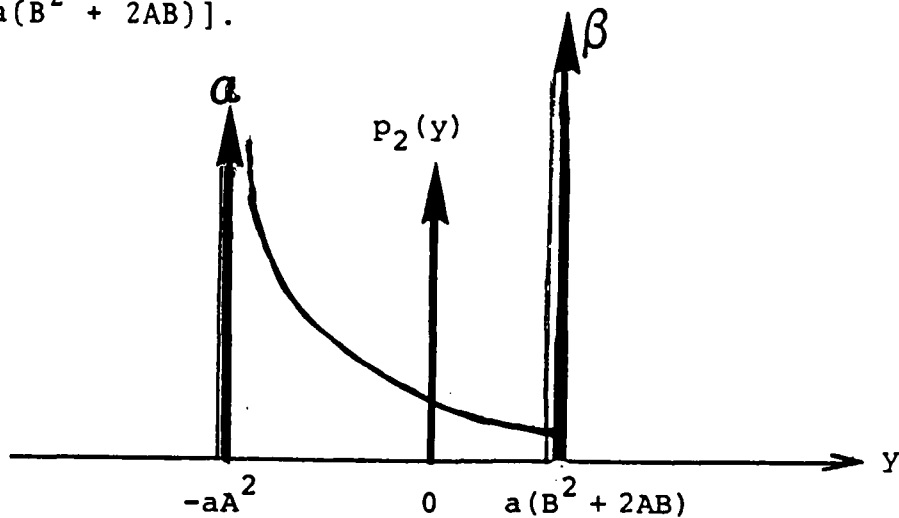


Figure 4.8 Output PDF for catenary system.

Input/Output Spectrum Relations for Catenary System

In the range from $-A \leq x \leq B$, the catenary output $y(t)$ is assumed to consist of two components:

- (1) a linear term that is proportional to $x(t)$,
- (2) a nonlinear term that is proportional to $x^2(t)$.

In terms of constants k_1 and k_2 ,

$$y(t) = k_1 x(t) + k_2 x^2(t) \quad (4.39)$$

This equation can be made to apply to more general situations as shown in Figure 4.9 by letting the catenary output be represented by

$$y(t) = y_1(t) + y_2(t) + n(t) \quad (4.40)$$

where

$y_1(t)$ = linear output due to $x(t)$

$y_2(t)$ = nonlinear output due to $v(t) = x^2(t)$

$n(t)$ = uncorrelated zero mean Gaussian output noise

In Figure 4.9 the constant parameter linear system frequency response functions $H_1(f)$ and $H_2(f)$ incorporate the constants k_1 and k_2 , respectively. Note that Figure 4.9 is a special case of Figure 1.8 that can be analyzed by formulas in Section 1.5. Figure 4.9 can be replaced by a two-input/single-output linear model with inputs $x(t)$ and $v(t)$ that will be uncorrelated when $x(t)$ is Gaussian.

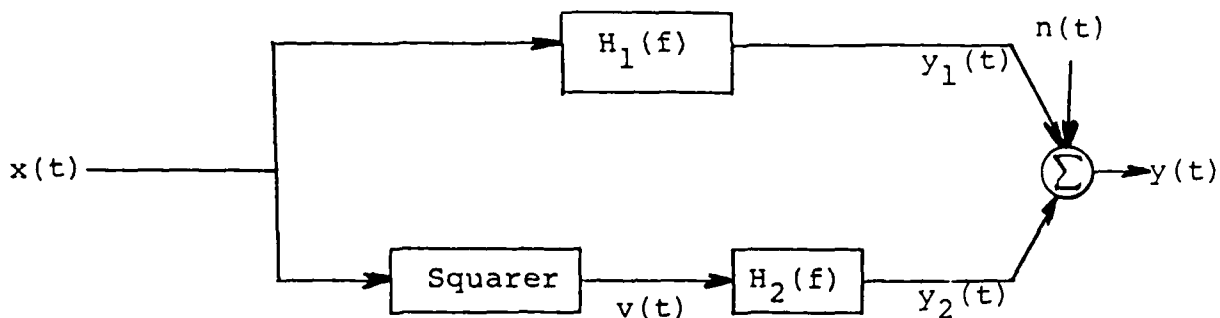


Figure 4.9 Catenary system model.

In the frequency domain, the governing relation of this catenary system model is

$$Y(f) = Y_1(f) + Y_2(f) + N(f) \quad (4.41)$$

where $Y_1(f)$, $Y_2(f)$ and $N(f)$ are Fourier transforms of $y_1(t)$, $y_2(t)$ and $n(t)$, respectively. In terms of $X(f)$ and $V(f)$, the Fourier transforms of $x(t)$ and $v(t) = x^2(t)$,

$$Y_1(f) = H_1(f)X(f) \quad (4.42)$$

$$Y_2(f) = H_2(f)V(f) \quad (4.43)$$

$$V(f) = \int_{-\infty}^{\infty} v(t) e^{-j2\pi ft} dt = \int_{-\infty}^{\infty} X(\alpha) X(f - \alpha) d\alpha \quad (4.44)$$

Note that $V(f)$ can be computed by two different methods, either directly from $v(t)$ or indirectly from $X(f)$.

For Gaussian input data $x(t)$ as assumed here, the output terms $y_1(t)$ and $y_2(t)$ will be uncorrelated. Hence, the two-sided output spectral density function $S_{yy}(f)$ satisfies the relation

$$S_{yy}(f) = S_{y_1y_1}(f) + S_{y_2y_2}(f) + S_{nn}(f) \quad (4.45)$$

In terms of $S_{xx}(f)$ and $S_{vv}(f)$, the two-sided spectral density functions of $x(t)$ and $v(t) = x^2(t)$,

$$S_{y_1y_1}(f) = |H_1(f)|^2 S_{xx}(f) \quad (4.46)$$

$$S_{y_2y_2}(f) = |H_2(f)|^2 S_{vv}(f) \quad (4.47)$$

$$S_{vv}(f) = \frac{1}{T} E[V^*(f)V(f)] \quad (4.48)$$

Also, for $f \neq 0$,

$$S_{vv}(f) = 2 \int_{-\infty}^{\infty} S_{xx}(\alpha) S_{xx}(f - \alpha) d\alpha \quad (4.49)$$

Note that $S_{vv}(f)$ can be computed by two different methods, either directly from $V(f)$ or indirectly from $S_{xx}(f)$.

Given $H_1(f)$ and $H_2(f)$, plus measurement only of $x(t)$, the above equations show how to determine the spectral properties of $y_1(t)$ and $y_2(t)$, namely, $S_{y_1y_1}(f)$ and $S_{y_2y_2}(f)$. If $y(t)$ is measured as well as $x(t)$, then one can also determine the two-sided spectral density function $S_{nn}(f)$ of the unmeasured $n(t)$ by the relation . .

$$S_{nn}(f) = S_{yy}(f) - S_{y_1y_1}(f) - S_{y_2y_2}(f) \quad (4.50)$$

A good model occurs when $S_{nn}(f)$ is small compared to $S_{yy}(f)$.

For situations where $H_1(f)$ and $H_2(f)$ are not known, optimum estimates of their properties can be obtained that minimize $S_{nn}(f)$ provided one can make simultaneous measurements of $x(t)$

and $y(t)$. This system identification problem can be solved using the relations

$$S_{xy}(f) = S_{xy_1}(f) = H_1(f)S_{xx}(f) \quad (4.51)$$

$$S_{vy}(f) = H_2(f)S_{vv}(f) \quad (4.52)$$

Thus

$$H_1(f) = \frac{S_{xy}(f)}{S_{xx}(f)} \quad (4.53)$$

$$H_2(f) = \frac{S_{vy}(f)}{S_{vv}(f)} \quad (4.54)$$

Here, $S_{xy}(f)$ is the two-sided cross-spectral density function between $x(t)$ and $y(t)$, and $S_{vy}(f)$ is the two-sided cross-spectral density function between $v(t)$ and $y(t)$. These quantities can be computed directly by

$$S_{xy}(f) = \frac{1}{T} E[X^*(f)Y(f)] \quad (4.55)$$

$$S_{vy}(f) = \frac{1}{T} E[V^*(f)Y(f)] \quad (4.56)$$

The quantity $S_{vy}(f)$ can also be computed indirectly by

$$S_{vy}(f) = \int_{-\infty}^{\infty} S_{xxy}(\alpha, f - \alpha) d\alpha \quad (4.57)$$

where $S_{xxy}(\alpha, f - \alpha)$ is the two-sided cross-bispectrum (also called the second-order cross-spectral density function) defined for all f and g by the two-dimensional function

$$S_{xxy}(f, g) = \frac{1}{T} E[X^*(f) X^*(g) Y(f+g)] \quad (4.58)$$

The integrand

$$S_{xxy}(\alpha, f - \alpha) = \frac{1}{T} E[X^*(\alpha) X^*(f - \alpha) Y(f)] \quad (4.59)$$

is a special case of $S_{xxy}(f, g)$ when $f = \alpha$ and $g = (f - \alpha)$.

For $f \neq 0$, one can also compute $S_{vy}(f)$ from Equations 4.49 and 4.52 by the relation

$$S_{vy}(f) = 2H_2(f) \int_{-\infty}^{\infty} S_{xx}(\alpha) S_{xx}(f - \alpha) d\alpha \quad (4.60)$$

Hence, for $f \neq 0$, the two-sided cross-bispectrum satisfies

$$S_{xxy}(\alpha, f - \alpha) = 2H_2(f) S_{xx}(\alpha) S_{xx}(f - \alpha) \quad (4.61)$$

This provides an alternate way to determine $H_2(f)$ from computation of the other quantities. Consider a change in variables where $\alpha = g$ and $f = 2g$. Then $(f - \alpha) = g$ so that one obtains

$$S_{xxy}(g, g) = 2H_2(2g) S_{xx}^2(g) \quad (4.62)$$

Now, replacing g by f gives

$$S_{xxy}(f, f) = 2H_2(2f) S_{xx}^2(f) \quad (4.63)$$

Solving for $H_2(2f)$ shows

$$H_2(2f) = \frac{S_{xxy}(f, f)}{2S_{xx}^2(f)} \quad (4.64)$$

Finally, replacing f by $(f/2)$ proves

$$H_2(f) = \frac{S_{xy}(f/2, f/2)}{2S_{xx}^2(f/2)} \quad (4.65)$$

This concludes the material on system identification and on input/output spectrum relations for the catenary system.

4.3 SMOOTH-LIMITER SYSTEMS

Consider the nonlinear nonsymmetric smooth-limiter system sketched in Figure 4.10 where

$$\begin{aligned} y = g(x) &= \sqrt{\frac{2}{\pi}} \int_0^x \exp(-t^2/2) dt & x \geq 0 \\ &= 0 & x < 0 \end{aligned} \quad (4.66)$$

Equation 4.66 is the equation for the normal probability integral.

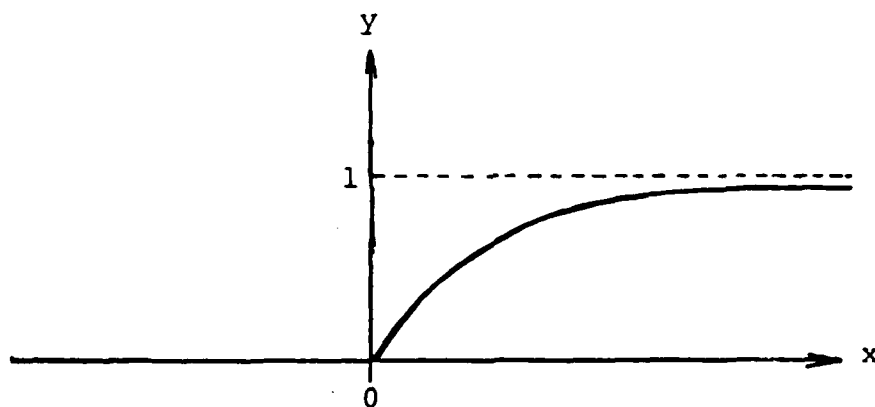


Figure 4.10 Smooth-limiter system.

For this nonlinear transformation, special values are

$$\begin{aligned} g(0) &= 0 \\ g(1) &= 0.683 \\ g(2) &= 0.954 \\ g(3) &= 0.997 \\ g(\infty) &= 1.000 \end{aligned} \quad (4.67)$$

Tables are available that give $g(x)$ as a function of x , and that can also be used to find x for any $g(x)$ in range $0 < g(x) < 1$.

The inverse relations are

$$\begin{aligned} x = g^{-1}(y) &= \text{any value of } x \leq 0 \quad \text{for } y = 0 \\ &= \text{unique value of } x \text{ in range } 0 < x < \infty \quad \text{for } 0 < y < 1 \\ &= \text{no value of } x \quad \text{for } y < 0 \text{ or } \text{for } y > 1 \end{aligned}$$

The derivative relations are

$$\begin{aligned} \frac{dy}{dx} = g'(x) &= \sqrt{\frac{2}{\pi}} \exp(-x^2/2) & x > 0 \\ &= 0 & x < 0 \end{aligned} \quad (4.68)$$

Here the derivative is discontinuous at $x = 0$.

Assume that $p(x)$, the input probability density function, is Gaussian with mean zero and standard deviation σ where

$$p(x) = \frac{1}{\sigma\sqrt{2\pi}} \exp(-x^2/2\sigma^2) \quad (4.69)$$

All of the values of $x \leq 0$ are associated with the single value of $y = 0$. Hence $p_2(y)$, the output probability density function, is such that

$$p_2(y) = \frac{1}{2} \delta(y) \quad \text{at } y = 0 \quad (4.70)$$

where the factor $(1/2)$ occurs because the probability is $(1/2)$ that $x \leq 0$. There are no values of x where $y < 0$ or $y > 1$. Hence

$$p_2(y) = 0 \quad \text{for } y < 0 \text{ or } y > 1 \quad (4.71)$$

In the range where $0 < y < 1$, from Equation 1.5, the result is

$$p_2(y) = \frac{p(x)}{|dy/dx|} = \sqrt{\frac{\pi}{2}} \left[\frac{p(x)}{\exp(-x^2/2)} \right] \quad (4.72)$$

where the value of x on the right-hand side should be replaced by its equivalent y from $x = g^{-1}(y)$. As y approaches the value 0 from the inside where $y > 0$, the value of x also approaches zero so that

$$p_2(0^+) = \sqrt{\frac{\pi}{2}} \left[\frac{p(0)}{1} \right] = \frac{1}{2\sigma} \quad (4.73)$$

As y approaches the value 1 from the inside where $y < 1$, the value of x approaches infinity so that

$$p_2(1^-) = \infty \quad (4.74)$$

A typical shape for $p_2(y)$ is sketched in Figure 4.11.

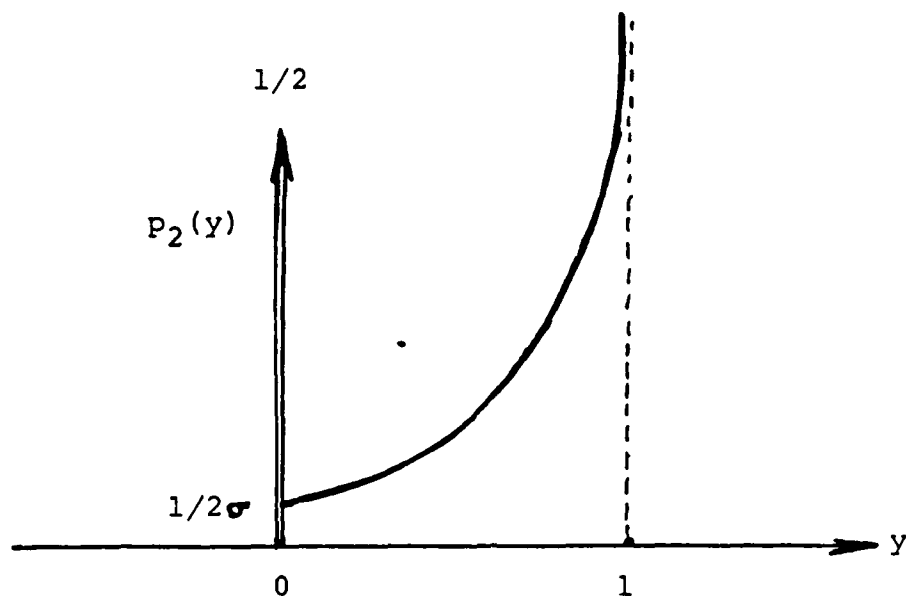


Figure 4.11 Output PDF for smooth-limiter system.

It is of interest to be able to determine the output autocorrelation function and the input/output cross-correlation function for Gaussian input data through this smooth-limiter system. Such formulas can be found using Price's Theorem of Equation 1.6 and Busgang's Theorem of Equation 1.7.

Output Autocorrelation Function for Smooth-Limiter System

By Price's Theorem, the output autocorrelation function $R_{YY}(\tau)$ and input autocorrelation $R_{XX}(\tau)$ for Gaussian input data satisfies the equation

$$\begin{aligned}\frac{\partial R_{YY}(\tau)}{\partial R_{XX}(\tau)} &= E[g'(x_1)g'(x_2)] \\ &= \int_0^\infty \int_0^\infty g'(x_1)g'(x_2)p(x_1, x_2)dx_1dx_2\end{aligned}\quad (4.75)$$

where

$$\begin{aligned}x_1 &= x(t) & y_1 &= y(t) \\ x_2 &= x(t + \tau) & y_2 &= y(t + \tau)\end{aligned}\quad (4.76)$$

The correlation functions

$$R_{XX}(\tau) = E[x_1x_2] \quad R_{YY}(\tau) = E[y_1y_2] \quad (4.77)$$

Derivative values from Equation 4.68 are

$$\begin{aligned}g'(x_1) &= \sqrt{\frac{2}{\pi}} \exp(-x_1^2/2) \quad \text{for } x > 0, \quad \text{otherwise zero} \\ g'(x_2) &= \sqrt{\frac{2}{\pi}} \exp(-x_2^2/2) \quad \text{for } x > 0, \quad \text{otherwise zero}\end{aligned}\quad (4.78)$$

The joint probability density function

$$p(x_1, x_2) = \frac{1}{2\pi\sigma^2\sqrt{1-\rho^2}} \exp \left[\frac{-(x_1^2 + x_2^2 - 2\rho x_1x_2)}{2\sigma^2(1-\rho^2)} \right] \quad (4.79)$$

Thus

$$\frac{\partial R_{yy}(\tau)}{\partial R_{xx}(\tau)} = \frac{1}{\pi^2 \sigma^2 \sqrt{1 - \rho^2}} \int_0^\infty \int \exp \left[\frac{-(x_1^2 + x_2^2 - 2\rho x_1 x_2)}{2\sigma^2(1 - \rho^2)} - \frac{(x_1^2 + x_2^2)}{2} \right] dx_1 dx_2 \quad (4.80)$$

The bracketed quantity contains

$$\begin{aligned} \frac{(x_1^2 + x_2^2 - 2\rho x_1 x_2)}{2\sigma^2(1 - \rho^2)} + \frac{(x_1^2 + x_2^2)}{2} &= \frac{(x_1^2 + x_2^2)[1 + \sigma^2(1 - \rho^2)] - 2\rho x_1 x_2}{2\sigma^2(1 - \rho^2)} \\ &= \frac{x_1^2 + x_2^2 - 2\rho x_1 x_2 / [1 + \sigma^2(1 - \rho^2)]}{2\sigma^2(1 - \rho^2) / [1 + \sigma^2(1 - \rho^2)]} \\ &= \frac{x_1^2 + x_2^2 - 2\rho_0 x_1 x_2}{2\sigma^2(1 - \rho^2) / [1 + \sigma^2(1 - \rho^2)]} = \frac{x_1^2 + x_2^2 - 2\rho_0 x_1 x_2}{2\sigma_0^2(1 - \rho_0^2)} \end{aligned} \quad (4.81)$$

where ρ_0 and σ_0^2 are defined by

$$\rho_0 = \frac{\rho}{[1 + \sigma^2(1 - \rho^2)]} \quad \text{with} \quad \rho = \rho_{xx}(\tau) = \frac{R_{xx}(\tau)}{\sigma^2} \quad (4.82)$$

$$\sigma_0^2(1 - \rho_0^2) = \sigma^2(1 - \rho^2) / [1 + \sigma^2(1 - \rho^2)] = \sigma^2(1 - \rho^2)(\rho_0 / \rho)$$

$$\sigma_0^2 = \sigma^2 \left[\frac{\rho_0(1 - \rho^2)}{\rho(1 - \rho_0^2)} \right] \quad (4.83)$$

By these substitutions,

$$\frac{\partial R_{YY}(\tau)}{\partial R_{XX}(\tau)} = \frac{1}{\pi^2 \sigma^2 \sqrt{1 - \rho^2}} \int_0^\infty \int \exp \left[\frac{-(x_1^2 + x_2^2 - 2\rho_0 x_1 x_2)}{2\sigma_0^2(1 - \rho_0^2)} \right] dx_1 dx_2 \quad (4.84)$$

The integral is now in the form of a joint Gaussian probability density function over one quadrant where

$$\int_0^\infty \int \frac{1}{2\pi\sigma_0^2 \sqrt{1 - \rho_0^2}} \exp \left[\frac{-(x_1^2 + x_2^2 - 2\rho_0 x_1 x_2)}{2\sigma_0^2(1 - \rho_0^2)} \right] dx_1 dx_2 = \frac{1}{4} \quad (4.85)$$

Hence

$$\frac{\partial R_{YY}(\tau)}{\partial R_{XX}(\tau)} = \left(\frac{1}{2\pi} \right) \frac{\sigma_0^2 \sqrt{1 - \rho_0^2}}{\sigma^2 \sqrt{1 - \rho^2}} = \left(\frac{1}{2\pi} \right) \frac{\rho_0 \sqrt{1 - \rho^2}}{\rho \sqrt{1 - \rho_0^2}} \quad (4.86)$$

But

$$\rho_0^2 = \frac{\rho^2}{[1 + \sigma^2(1 - \rho^2)]^2} \quad (4.87)$$

and

$$\begin{aligned} 1 - \rho_0^2 &= \frac{[1 + \sigma^2(1 - \rho^2)]^2 - \rho^2}{[1 + \sigma^2(1 - \rho^2)]^2} = \frac{1 + 2\sigma^2(1 - \rho^2) + \sigma^4(1 - \rho^2)^2 - \rho^2}{(\rho/\rho_0)^2} \\ &= (\rho_0/\rho)^2 (1 - \rho^2) [(1 + \sigma^2)^2 - \sigma^4 \rho^2] \end{aligned} \quad (4.88)$$

This gives

$$\begin{aligned} \frac{\rho_o^2(1 - \rho_o^2)}{\rho^2(1 - \rho_o^2)} &= \frac{1}{[(1 + \sigma^2)^2 - \sigma^4 \rho^2]} \\ &= \frac{1}{[(1 + \sigma^2)^2 - R_{xx}^2(\tau)]} \end{aligned} \quad (4.89)$$

Now

$$\frac{\partial R_{yy}(\tau)}{\partial R_{xx}(\tau)} = \frac{1}{2\pi[(1 + \sigma^2)^2 - R_{xx}^2(\tau)]^{1/2}} \quad (4.90)$$

Thus

$$R_{yy}(\tau) = \left(\frac{1}{2\pi}\right) \sin^{-1} \left[\frac{R_{xx}(\tau)}{1 + \sigma^2} \right] + C \quad (4.91)$$

Using the fact that the indefinite integral

$$\int \frac{dx}{\sqrt{a^2 - x^2}} = \sin^{-1} \left(\frac{x}{|a|} \right) + C \quad (4.92)$$

where C is a constant of integration. At $\tau = 0$,

$$R_{yy}(0) = \psi_y^2 = \left(\frac{1}{2\pi}\right) \sin^{-1} \left[\frac{\sigma^2}{1 + \sigma^2} \right] + C \quad (4.93)$$

from which C can be determined.

Input/Output Cross-Correlation Function for Smooth-Limiter System

By Busgang's Theorem, the input/output cross-correlation function $R_{xy}(\tau)$ for Gaussian input data satisfies the equation

$$R_{xy}(\tau) = \frac{R_{xx}(\tau)}{\sigma^2} \int_0^{\infty} xg(x)p(x)dx \quad (4.94)$$

where

$$g(x) = \sqrt{\frac{2}{\pi}} \int_0^x \exp(-t^2/2) dt \quad x \geq 0 \quad (4.95)$$

$$p(x) = \frac{1}{\sigma\sqrt{2\pi}} \exp(-x^2/2\sigma^2) \quad (4.96)$$

Integration by parts formula gives

$$\int u dv = uv - \int v du \quad (4.97)$$

Let

$$u = g(x) \quad \text{and} \quad dv = xp(x)dx \quad (4.98)$$

Then

$$du = g'(x)dx = \sqrt{\frac{2}{\pi}} \exp(-x^2/2) dx \quad (4.99)$$

$$v = -\sigma^2 p(x) \quad (4.100)$$

At $x = 0$ and at $x = \infty$, the product $uv = 0$. Hence

$$\begin{aligned} \int_0^{\infty} x g(x) p(x) dx &= \sigma^2 \int_0^{\infty} p(x) g'(x) dx \\ &= \frac{\sigma}{\pi} \int_0^{\infty} \exp \left[\frac{-x^2}{2\sigma^2} - \frac{x^2}{2} \right] dx = \frac{\sigma}{\pi} \int_0^{\infty} \exp \left[\frac{-x^2}{2\sigma_1^2} \right] dx \end{aligned} \quad (4.101)$$

where σ_1^2 is defined by

$$\sigma_1^2 = \frac{\sigma^2}{1 + \sigma^2} \quad (4.102)$$

The integrand is now in the form of a first-order Gaussian probability density function for $x \geq 0$ satisfying

$$\frac{1}{\sigma_1 \sqrt{2\pi}} \int_0^{\infty} \exp \left[\frac{-x^2}{2\sigma_1^2} \right] dx = \frac{1}{2} \quad (4.103)$$

Hence

$$\int_0^{\infty} x g(x) p(x) dx = \frac{\sigma \sigma_1}{\sqrt{2\pi}} = \frac{\sigma^2}{\sqrt{2\pi(1 + \sigma^2)}} \quad (4.104)$$

and

$$R_{xy}(\tau) = \frac{R_{xx}(\tau)}{\sqrt{2\pi(1 + \sigma^2)}} \quad (4.105)$$

This concludes Section 4.

REFERENCES

1. Bendat, J. S., Nonlinear System Analysis and Identification from Random Data, Wiley-Interscience, New York, 1990.
2. Bendat, J. S., Nonlinear System Dynamic Analysis Using Random Data, CR 85.006, Naval Civil Engineering Laboratory, Port Hueneme, California, March 1985.
3. Bendat, J. S., and Piersol, A. G., Random Data: Analysis and Measurement Procedures, 2nd Edition, Wiley-Interscience, New York, 1986.
4. Bendat, J. S., and Piersol, A. G., Engineering Applications of Correlation and Spectral Analysis, Wiley-Interscience, New York, 1980.
5. Bendat, J. S., and Piersol, A. G., "Spectral analysis of nonlinear systems involving square-law operations," Journal of Sound and Vibration, 81(2), 199 (1982).
6. Bendat, J. S., "Statistical errors for nonlinear system measurements involving square-law operations," Journal of Sound and Vibration, 90(2), 275 (1983).
7. Bendat, J. S., and Piersol, A. G., "Decomposition of wave forces into linear and nonlinear components," Journal of Sound and Vibration, 106(3), 391 (1986).
8. Rice, H. J., and Fitzpatrick, J. A., "A generalized technique for spectral analysis of nonlinear systems," Mechanical Systems and Signal Processing, 2(2), 195 (1988).

9. Morison, J. R., et al, "The forces exerted by surface waves on piles," Journal of Petroleum Techniques, American Institute of Mining Engineers, 189, 149 (1950).
10. Sarpkaya, T., and Isaacson, M., Mechanics of Wave Forces on Offshore Structures, Van Nostrand Reinhold Company, New York, 1981.
11. Vugts, J. H., and Bouquet, A. G., "A nonlinear frequency domain description of wave forces on an element of a vertical pile," Proceedings, Behavior of Offshore Structures, BOSS '85, Delft, Netherlands, 1985.
12. Dalzell, J. F., "Cross-bispectral analysis: application to ship resistance in waves," Journal of Ship Research, 18, 62 (1974).
13. Kim, C. H., and Breslin, J. P., "Prediction of slow drift oscillations of a moored ship in head seas," Proceedings, Behavior of Offshore Structures, BOSS '76, Trondheim, Norway, 1976.
14. Roberts, J. B., "Nonlinear analysis of slow drift oscillations of moored vessels in random seas," Journal of Ship Research, 25, 130 (1981).
15. Broch, J. T., Nonlinear Systems and Random Vibration, Bruel & Kjaer, Naerum, Denmark, 1975.
16. Crandall, S. H., and Mark, W. D., Random Vibration in Mechanical Systems, Academic Press, New York, 1963.